# Chapter 1: Overview of Partial Differential Equations of Relevance to Science and Engineering

## 1.1) Introduction

Scientists, engineers and applied mathematicians have always seen the value of obtaining precise solutions to the problems that they work on. Because of the deterministic nature of physical laws, the solution of many of these problems is governed by *partial differential equations*. While there is still great value attached to an exact, analytical solution to a problem in engineering or science, it is well-recognized that only a limited number of problems are amenable to analytical solution. The easy availability of high performance computers has made it attractive to obtain numerical solutions to the plethora of problems for which analytic solutions are too difficult to arrive at. Matching this explosion in computer power, the last few decades have also seen the emergence of applied and computational mathematics as disciplines unto themselves. This has resulted in the advent of stable, reliable numerical methods for solving the problems that scientists and engineers usually have to confront. These methods enable us to solve problems with increasing complexity in the physics they represent or in solving problems with complex geometric configurations. In this book we focus on the most frequently occurring partial differential equations (PDEs) that engineers or scientists might have to solve numerically in the course of their work. The emphasis throughout this book will not be on mathematical rigor but rather on intuitive understanding that is later supported by several detailed examples that help one develop a practical knowledge of the solution techniques. In this chapter we introduce some of the partial differential equations, understand how they arise and show that they fall into certain familiar categories. By the end of this book, the reader will have mastered several powerful solution techniques for numerically solving the PDEs of interest. Since part of the emphasis in this book is on the broad *algorithmic ideas* that apply to general classes of PDEs, the knowledge acquired here will stand the reader in good stead when tackling newer classes of PDEs that may not even be contained in this book.

Computational scientists have always placed equal emphasis on theory and technique. As a result, the text comes with an associated website. The website contains several codes that relate to the computational exercises that are contained at the end of each chapter. By the end of the book, the reader who has done the analytical problems as well as the computational exercises should develop a very sophisticated understanding of how big simulation codes are assembled and the algorithms that make them work.

The PDEs that interest us can be divided into some simple classes that go under interesting names such as: *hyperbolic, parabolic and elliptic*. We quickly explain these new names with some pedestrian definitions and familiar examples. A more sophisticated understanding will be built up as this chapter progresses. Hyperbolic PDEs are those that enable information to propagate as waves. For example, the propagation of sound waves in a fluid, water waves, oscillations in a solid structure and electromagnetic radiation all take place due to the existence of hyperbolic terms in certain PDEs that govern those processes. Parabolic PDEs, on the other hand, permit information to travel through a diffusive process. Thus the flow of heat in solids, the propagation of water or pollutants in porous media such as sand beds and the propagation of photons deep within the sun's interior are all represented by parabolic terms in PDEs. Elliptic PDEs that we normally encounter do not have temporal propagation and yet they convey the effects of one object on others around it. Examples include Newtonian gravity which we all experience on earth and various examples from electrostatics and magnetostatics. The *Poisson equation*, which appears in self-gravitating problems as well as problems in electrostatics, is a very prominent example of an elliptic equation. In practice, one or more of these types of terms could be present in the PDEs that we wish to solve. Understanding the operation of these terms in isolation will eventually enable us to assemble methods for several classes of PDEs. The contents of this chapter will show us how to identify the various terms in a PDE and classify them as hyperbolic, parabolic or elliptic. In subsequent chapters we will develop powerful solution methods for these PDEs.

It is worth mentioning that not all classes of PDEs that are of interest to engineers and scientists can be neatly divided into the above classification, yet many of them can be

viewed as such. Furthermore, not all research problems may be amenable to treatment via PDEs. There is a vast literature on particle methods and also on hybrid methods that combine particle methods with PDE methods. A full discussion of all such methods would be out of scope for this book.

When embarking on a study of PDE techniques one needs a set of equations that might serve as a touchstone with which to motivate further examples. We prefer to use the Navier Stokes equations as our motivating example because it is a PDE system of great practical value to large numbers of engineers, space scientists, geophysicists, meteorologists, astronomers and applied mathematicians. For that reason, the next section demonstrates how the fluid equations arise from an underlying model which assumes that atoms are in frequent collision – the fluid approximation. Sections 1.3 and 1.4 deal with the Euler and Navier-Stokes equations respectively. Section 1.5 shows us how to classify PDEs and is rather important to the later chapters in the book. The remaining sections of this chapter introduce various PDEs that are important to engineers and scientists. Solution methods will be developed for them during the course of the book. The reader can read the sections according to need and interest. Sections 1.6 and 1.7 introduce the equations for incompressible flow and the shallow water equations. Sections 1.8 and 1.9 introduce Maxwell's equations and the magnetohydrodynamic equations respectively. Section 1.10 discusses the equations of flux limited diffusion radiation hydrodynamics. Section 1.11 does the same for the radiative transfer equation. Section 1.12 introduces the equations of linear elasticity. Section 1.13 discusses relativistic hydrodynamics and magnetohydrodynamics. Section 1.14 underscores the importance of scientific visualization in computational problems.

## 1.2) Derivation of the Fluid Equations

This section is divided into several sub-sections. In Sub-section 1.2.1 we start by explaining the importance of frequent collisions between particles in obtaining a fluid approximation. Sub-sections 1.2.2 and 1.2.3 explain how the continuum description of a fluid can be derived by averaging over the collisional *Boltzmann equation*. Sub-sections

1.2.4, 1.2.5 and 1.2.6 then derive the mass, momentum and energy conservation equations that govern the dynamics of fluids. This section enables us to relate the PDEs that arise on the macroscopic scales to the dynamics of atoms and molecules on the microscopic scales, yielding insights that are valuable throughout the book. However, the reader who wants to avoid this level of detail can skip directly to Section 1.3.

### 1.2.1) The Role of Collisions

Our daily experience gives us an intuitive knowledge that fluids are made up of things that flow from one place to another. Air and water are good examples of fluids. We are interested in the dynamical equations that govern their motion. The air in a typical sized room consists of about $10^{28}$ molecules, each having a position vector $\mathbf{x}$ and a momentum vector $\mathbf{p}$. The six-dimensional space formed by the vectors $\mathbf{x}$ and $\mathbf{p}$ forms the *phase space*. For any finite temperature, the air molecules will have a certain random velocity with respect to each other. While air is a mixture of molecules, we simplify the problem by considering a fluid with a single type of molecule. It could in principle be specified by a *distribution function* $f(\mathbf{x},\mathbf{p},t)$ so that $f(\mathbf{x},\mathbf{p},t)\, d^3x\, d^3p$ gives us the number of molecules within a six-dimensional infinitesimal volume in phase space, $d^3x\, d^3p$, centered about $(\mathbf{x},\mathbf{p})$ at a time *t*. If these molecules were to coast freely without interactions with one another, one would indeed have to solve the dynamical equations for each of them, resulting in a very difficult problem in a six-dimensional phase space. Fortunately, in most systems of interest, collisions occur quite readily between the molecules, atoms or ions that make up the system. These collisions, along with the laws of statistical mechanics and thermodynamics, enable us to make an immense simplification.

Let us focus on collisions first. All interacting particles present a certain collisional *cross section,* $\sigma$, to other particles. This cross section can be crudely thought of as the amount of area presented by the particle in question to another particle that is headed towards it. For the very simple example of identical interacting particles that are

modeled as hard spheres, the cross section is simply the area of a disk having a radius that is twice as large as the radius of the spheres in question. Fig. 1.1 provides a schematic representation of such a collision. For more complicated inter-particle interactions, the cross section depends on the inner structure of the particles as well as the details of their relative momenta. The details of the interactions are not as important to us as the fact that the interactions are indeed frequent. One way of characterizing the frequency of interactions is to say that each particle travels but a short distance, $l$, before it has another interaction. Thus if the number density of particles is given by $n$, we can assert that the *mean free path* is given by $l \sim 1/(n\sigma)$. Furthermore, if all the particles in a parcel of gas have a characteristic relative speed given by $w^T$ with respect to one another, we can assert that the mean time between collisions is given by $\tau \sim l/w^T$. A *fluid approximation* is then said to prevail if we want to understand the dynamics of the different parcels of gas on characteristic length scales $L$ that are much larger than the collision length $l$ and, furthermore, if we only wish to track the dynamics over a characteristic time scale $T$ that is much larger than the *collision time* $\tau$.

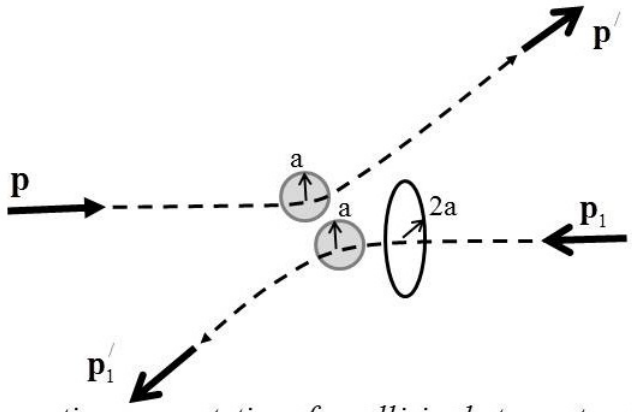


*Fig. 1.1 shows a schematic representation of a collision between two hard spheres of radius "a". The diskwith a radius "2a" shows the collision cross section. The area of the disk gives the collision cross section* $\sigma=\pi(2a)^2$. *The initial and final momenta of the incident particle (unsubscripted) and target particle (subscript 1) are also shown.*

Fortunately, a fluid approximation is easy to justify in several systems. For example, consider the air in the room you are sitting in. It has $n \sim 10^{19}$ particles/cm$^3$, $\sigma \sim 10^{-15}$ cm$^2$ and $w^T \sim 3\times10^4$ cm/sec, which gives us $l \sim 10^{-4}$ cm and $\tau \sim 3\times10^{-9}$ sec. Thus over length and time scales larger than $10^{-4}$ cm and $3\times10^{-9}$ sec respectively the air in the room can be modeled very nicely as a fluid. The fluid approximation also applies

quite well to some of the largest systems that we might wish to model. For example, the gas that permeates our Galaxy has $n \sim 1$ particles/cm$^3$ and $w^T \sim 8 \times 10^5$ cm/sec, yielding $l \sim 10^{15}$ cm and $\tau \sim 1.3 \times 10^9$ sec $\sim 42$ years. These might seem like colossal distances and times at first blush, except for the fact that astronomers are only interested in Galactic phenomena that take place on length scales and time scales that are significantly larger than the ones quoted above. Thus a fluid approximation is again justified for Galactic scale gas dynamics. We have simplified our example about Galactic gas dynamics by assuming that the cross section is the same as the one we used for our terrestrial example. However, the gas that makes up the Galaxy is a partially ionized plasma. The ions and electrons that make up such a plasma can have long range, screened Coulombic interactions, resulting in increased cross sections. Particles can also be scattered in plasmas due to collective effects, i.e. via interactions with collective oscillations that occur in the plasma. The latter examples in this paragraph are, therefore, meant to reinforce the viewpoint that a fluid approximation, while often readily justified in many systems of interest, should indeed be carefully examined. Astrophysicists and space physicists will find further discussions along these lines in the texts by Spitzer (1978) and Shu (1992).

It is worth noting that a fluid approximation is not justified in certain situations. Prominent examples include the study of plasmas in certain terrestrial fusion experiments, the earth's magnetosphere, the sun's corona and the magnetospheres of compact stars. The interaction of radiation with matter presents another interesting case study. When radiation causes the electrons in an atom to undergo transitions across energy levels, the matter usually presents a large cross section to the radiation. However, any patch of matter, even if it is electrically neutral, will always have electrons. The Thompson scattering of a photon with an electron yields a cross section of $0.67 \times 10^{-24}$ cm$^2$ . Thus a photon gas will always have some interaction with the matter that surrounds it. However, comparing the Thompson cross section to the cross section between molecules that we quoted in the previous paragraph we realize that the former is substantially smaller by several orders of magnitude. As a result, photon mean free paths can be substantially larger than molecular and atomic mean free paths. Even so, equations

for radiation hydrodynamics, i.e. a fluid-like approximation for the radiation field, can be built (Mihalas & Weibel-Mihalas 1999, Castor 2004). However the validity of that approximation has to be examined more carefully on a case by case basis.

Having understood the role of collisions, let us now focus on what *statistical mechanics* tells us about systems that have frequent collisions. The fundamental postulate of statistical mechanics then tells us that any isolated system in equilibrium will populate all its accessible microstates with equal probability (Reif 2008, Huang 1963). The collisions perfectly scramble any initial velocity distribution in a fluid and this equilibrating process takes place within a few collision times. Once equilibrium is established, and we have seen that it is established rapidly, all configurations of phase space that are energetically permitted are accessed with equal probability. Thus for a parcel of gas at rest, statistical mechanics tells us that there is a single number, the temperature of the gas, that specifies the entire velocity distribution of particles in that parcel. If the particles in a gas can be treated classically, their velocities will follow a *Maxwell-Boltzmann distribution*. If quantum mechanical effects need to be included, fermions and bosons will acquire a Fermi-Dirac or Bose-Einstein velocity distribution respectively. Thus if a parcel of gas is viewed from its local rest frame, the velocity distribution of the particles is indeed simple. This simplicity can always be exploited to relate the *thermodynamic variables* of a gas. For example, the *pressure* of the gas "P" can be related to its *temperature* "T" and *density* $\rho$, giving rise to one possible *equation of state*. Similarly, the random motions of the molecules or atoms that make up a parcel of gas at any finite temperature endow the parcel with a certain *internal energy density* "e". This internal energy density can again be related to the pressure and density of the gas, yielding another possible equation of state. In principle, statistical mechanics makes it possible for us to obtain such equations of state though, in practice, the derivation might be very involved. To take but a simple example for a thermally *ideal gas*, one can write

$$\mathrm{P} = \frac{R\rho\mathrm{T}}{\bar{\mu}} \tag{1.1}$$

where $R$ is the gas constant and $\bar{\mu}$ is the reduced mass of the gas being considered. Similarly, for a calorically ideal gas one has

$$\mathrm{e} = \frac{\mathrm{P}}{\Gamma - 1} \tag{1.2}$$

where "e" is the internal energy density and $\Gamma$ is the *polytropic index* of the gas being considered.

Our eventual goal is to describe the dynamics of parcels of fluid. The previous paragraph has shown that the velocity distribution of a parcel of fluid is indeed quite simple when viewed in its rest frame. Furthermore, if the local thermodynamic properties of that parcel of fluid can be specified then the local velocity distribution of molecules, viewed in the parcel's own rest frame, is indeed specified. This suggests that instead of a six-dimensional space in which the distribution $f(\mathbf{x},\mathbf{p},t)$ is specified, one might indeed be able to specify the problem in a three dimensional space given by the position vector $\mathbf{x}$. For example, it is intuitively obvious that the local density of the fluid, as measured in gm/cm$^3$ or Kg/m$^3$ , can be determined by integrating over the space of all possible particle momenta. Thus we have

$$\rho(\mathbf{x},t) \equiv \int m\, f(\mathbf{x},\mathbf{p},t)\, d^3p \tag{1.3}$$

where $m$ is the mass of the fluid particles, all of which are assumed to have identical masses for the sake of simplicity. As the fluid flows, $\rho(\mathbf{x},t)$ changes from one location to another. Thus we wish to obtain an evolutionary equation for $\rho(\mathbf{x},t)$. We are helped in this endeavor by the fact that the number of particles is a conserved quantity, at least when a gas is not undergoing ionization or nuclear reactions.

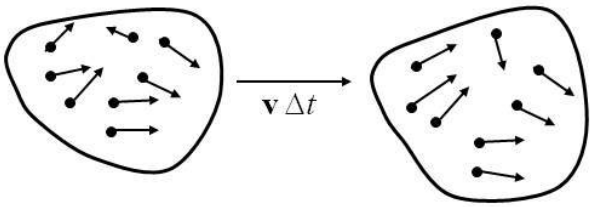


*Fig. 1.2 shows the translation of a fluid element with a mean velocity* $\mathbf{v}$ *over a time* $\Delta t$*. A parcel of fluid along with the molecules/atoms it contains is depicted. Frequent scatterings between the particles change the fluctuating parts of their velocities,* $\mathbf{w}$*. However, the very small mean free path between collisions also permits the fluid element to be identified a short time later as containing the same particles. The fluid element does, however, deform in response to the collisions.*

To obtain the dynamics of individual particles as well as assemblages of particles one needs to apply Newton's second law to them. Recall though that Newton's second law needs to be applied to the same set of particles. If the particles could stream freely without copious collisions, we would not be in a position to keep the same set of particles physically contiguous from one time to a slightly later time. However, the fluid approximation, with its implicit assumption of plentiful collisions, ensures that a particle that is part of a parcel of particles does not get too far away from the parcel a very short time later. I.e., as shown in Fig. 1.2, the fluid element may deform as it moves, but the particles that make up the fluid element can be identified a short time later. This permits us to specify a mean *fluid velocity*, $\mathbf{v} = \mathbf{v}(\mathbf{x},t)$, with which the fluid element moves. Because the fluid has a finite temperature, every particle also has a certain random velocity, $\mathbf{w}$, with respect to the mean motion of the fluid element. Thus the velocity of any particle can be specified as $\mathbf{u} = \mathbf{v} + \mathbf{w}$, i.e. it is comprised of a mean velocity and a random fluctuation about the mean. We can then write the *momentum density* as

$$\rho(\mathbf{x},t)\,\mathbf{v}(\mathbf{x},t) \equiv \int \mathbf{p}\, f\,(\mathbf{x},\mathbf{p},t)\, d^3p \tag{1.4}$$

We will presently see that the evolutionary equation for the velocity field $\mathbf{v}(\mathbf{x},t)$ is an exact expression of Newton's second law as applied to a parcel of fluid.

Energy conservation is another very important principle of physics. A fluid can contain internal thermal energy due to the random motion of its molecules. It can also have bulk energy due to the overall motion of the fluid element. Thus we can define the *total energy density* of a fluid as

$$\mathcal{E}(\mathbf{x},t) \equiv \int \frac{\mathbf{p}^2}{2m} f(\mathbf{x},\mathbf{p},t)\, d^3p \tag{1.5}$$

Based on our intuition, we would expect the total energy density $\mathcal{E}(\mathbf{x},t)$ to consist of a bulk kinetic energy when the fluid is in motion as well as an internal (thermal) energy density. The bulk kinetic energy should evolve in conformance with Newton's second law. If there are no internal or external sources of heat acting upon the fluid, the first law of thermodynamics dictates that the internal energy of a parcel of fluid should change in response to the mechanical work done by the external pressure as the parcel is compressed or as it expands. We will presently see that the evolutionary equation for $\mathcal{E}(\mathbf{x},t)$ can be shown to express the first law of thermodynamics. It should also be noted that the internal energy of real fluids can change in response to ionization, recombination or chemical and nuclear reactions. External sources of radiation and thermal conduction from a boundary can also change the internal energy of a fluid.

A simple example drawn from the above three paragraphs can now be provided. Consider a monoatomic, ideal gas where the particles satisfy a Maxwell-Boltzmann velocity distribution in the fluid's rest frame. As before, the atoms have a mass $m$ so that the local number density can be written as $\rho(\mathbf{x},t)/m$. The fluid has a local velocity given by $\mathbf{v}(\mathbf{x},t)$ and a local temperature $\mathrm{T}(\mathbf{x},t)$. Notice from eqns. (1.1) and (1.2) that the temperature is related to the internal energy density of the fluid. Furthermore, the fluctuating part of each particle's momentum, i.e. the part that does not contribute to the mean momentum density, is then given by $\left(\mathbf{p} - m\,\mathbf{v}(\mathbf{x},t)\right)$. Since the Maxwell-Boltzmann velocity distribution is specified with respect to the fluid's rest frame, it can

be written in terms of the fluctuating part of each particle's momentum. We can then write the distribution function as

$$f\left(\mathbf{x},\mathbf{p},t\right)=\frac{\rho\left(\mathbf{x},t\right)}{m}\;\frac{1}{\left(2\,\pi\,m\,k\,\mathrm{T}\left(\mathbf{x},t\right)\right)^{3/2}}\;\mathrm{e}^{-\frac{\left(\mathbf{p}\,-\,m\,\mathbf{v}\left(\mathbf{x},t\right)\right)^{2}}{2\,m\,k\,\mathrm{T}\left(\mathbf{x},t\right)}} \tag{1.6}$$

where *k* is the *Boltzmann constant*. It is very easy to show that the distribution function from eqn. (1.6) satisfies eqn. (1.3). It is only a slight bit more involved to show that the above distribution function satisfies eqn. (1.4). Substituting eqn. (1.6) in eqn. (1.5) eventually allows us to show that

$$\mathcal{E}\left(\mathbf{x},t\right)\;=\;\frac{\mathrm{P}\left(\mathbf{x},t\right)}{\Gamma-1}\;+\;\frac{1}{2}\,\rho\left(\mathbf{x},t\right)\,\mathbf{v}\left(\mathbf{x},t\right)^{2} \tag{1.7}$$

where $\Gamma=5/3$ in the above equation and $\mathrm{P}\left(\mathbf{x},t\right)$ is the local pressure in the fluid. Notice that $\mathrm{P}\left(\mathbf{x},t\right)/\left(\Gamma-1\right)$ can be identified as the internal energy density while $\rho\left(\mathbf{x},t\right)\,\mathbf{v}\left(\mathbf{x},t\right)^{2}/2$ can be identified as the kinetic energy density. These identifications can be strengthened if one draws on relations from statistical mechanics that allow us to identify the pressure $\mathrm{P}\left(\mathbf{x},t\right)$ and thermal energy density $\mathrm{e}\left(\mathbf{x},t\right)$ as

$$\begin{aligned}\mathrm{P}\left(\mathbf{x},t\right)\;&\equiv\;\frac{1}{3}\int\frac{\left(\mathbf{p}\,-\,m\,\mathbf{v}\left(\mathbf{x},t\right)\right)^{2}}{m}\,f\left(\mathbf{x},\mathbf{p},t\right)\,d^{3}p\;;\\ \mathrm{e}\left(\mathbf{x},t\right)\;&\equiv\;\int\frac{\left(\mathbf{p}\,-\,m\,\mathbf{v}\left(\mathbf{x},t\right)\right)^{2}}{2m}\,f\left(\mathbf{x},\mathbf{p},t\right)\,d^{3}p\end{aligned} \tag{1.8}$$

Notice that the pressure and thermal energy density are defined in terms of the fluctuating part of the velocity. Eqn. (1.8) also enables us to identify $\Gamma=5/3$ for a monoatomic ideal gas. It is also worth noting that eqn. (1.6) is only valid at the lowest order of approximation. It would not, for example, enable us to deduce the existence of viscous

terms in the flow. In general, one can envision a sequence of higher order corrections to eqn. (1.6), see Chapman and Cowling (1961).

### 1.2.2) The Boltzmann Equation

When collisions are absent, *Liouville's theorem* tells us that a distribution of particles preserves the six-dimensional volume of phase space that it occupies. The particles can in fact respond to external body forces. For the sake of simplicity, let us call those forces $\mathbf{F}$ in this sub-section. Examples of such body forces include gravity or forces produced by electric and magnetic fields. We then have an evolutionary equation for the distribution function $f(\mathbf{x},\mathbf{p},t)$ given by

$$\frac{df}{dt} = 0 = \frac{\partial f}{\partial t} + \frac{d\mathbf{x}}{dt} \bullet \frac{\partial f}{\partial \mathbf{x}} + \frac{d\mathbf{p}}{dt} \bullet \frac{\partial f}{\partial \mathbf{p}} \Rightarrow$$
$$\frac{\partial f}{\partial t} + \frac{\mathbf{p}}{m} \bullet \frac{\partial f}{\partial \mathbf{x}} + \mathbf{F} \bullet \frac{\partial f}{\partial \mathbf{p}} = 0 \qquad (1.9)$$

The reader might find it instructive to write the above equation out in component form to see that it simply causes the particles to evolve in phase space. Introducing collisions makes the above equation much more interesting. When collisions are present, and when the duration of the interparticle scattering is much shorter than the mean interval between scatterings, we can think of the scattering as providing a non-zero right hand side in eqn. (1.9). Thus one gets

$$\frac{\partial f}{\partial t} + \frac{\mathbf{p}}{m} \bullet \frac{\partial f}{\partial \mathbf{x}} + \mathbf{F} \bullet \frac{\partial f}{\partial \mathbf{p}} = \left(\frac{\delta f}{\delta t}\right)_c \qquad (1.10)$$

where the right hand side in eqn. (1.10) represents the effect of collisions.

Collisions can change the particles' momentum transferring the particles from one part of phase space to the other. Thus consider an incident particle with momentum $\mathbf{p}$

that is entering into an elastic collision with a target particle with momentum $\mathbf{p}_1$. After the collision, the incident particle has momentum $\mathbf{p}'$ while the target particle has momentum $\mathbf{p}_1'$, see Fig. 1.1. As a result of collisions, new particles may get scattered into a part of phase space around $(\mathbf{x},\mathbf{p})$ resulting in an increase in the local distribution function $f(\mathbf{x},\mathbf{p},t)$. Likewise, particles that originally had a momentum $\mathbf{p}$ at the location $\mathbf{x}$ might get scattered by collisions so as to have a different momentum, thereby resulting in a decrease in the local distribution function $f(\mathbf{x},\mathbf{p},t)$. Momentum and energy conservation still hold so that we have

$$\mathbf{p} + \mathbf{p}_1 = \mathbf{p}' + \mathbf{p}_1' \quad ; \quad \frac{(\mathbf{p})^2}{2m} + \frac{(\mathbf{p}_1)^2}{2m} = \frac{(\mathbf{p}')^2}{2m} + \frac{(\mathbf{p}_1')^2}{2m} \tag{1.11}$$

The above equations provide four constraints on the outgoing momenta, $\mathbf{p}'$ and $\mathbf{p}_1'$. This leaves two degrees of freedom, and those are mediated by the details of the interaction. The actual scattering cross section depends on the physics of the interaction. We will not study the details of such interactions here. We just quote the result that the collisional cross section for the interaction $(\mathbf{p},\mathbf{p}_1) \to (\mathbf{p}',\mathbf{p}_1')$ is given by $\sigma(\mathbf{p},\mathbf{p}_1 \,|\, \mathbf{p}',\mathbf{p}_1')$. Roughly speaking, the collision cross section gives us the probability of a certain pair of output momenta $(\mathbf{p}',\mathbf{p}_1')$ being favored in the collision for a given pair of input momenta $(\mathbf{p},\mathbf{p}_1)$. All pairs of output momenta also have to satisfy the momentum and energy constraints in eqn. (1.11). The number of particles scattering out of the distribution function $f(\mathbf{x},\mathbf{p},t)$ within a unit spatial volume per unit of time is given by

$$\int \left(\frac{\delta f}{\delta t}\right)_{\text{c; sink}} \mathrm{d}^3\mathrm{p} = \int \frac{|\mathbf{p}-\mathbf{p}_1|}{m} f(\mathbf{x},\mathbf{p}_1,t)\ \mathrm{d}^3\mathrm{p}_1\ \sigma(\mathbf{p},\mathbf{p}_1 \,|\, \mathbf{p}',\mathbf{p}_1')\ \mathrm{d}\Omega\, f(\mathbf{x},\mathbf{p},t)\ \mathrm{d}^3\mathrm{p} \tag{1.12}$$

where $\mathrm{d}\Omega$ represents the infinitesimal solid angle into which the incident particle is scattered. Eqn. (1.12) can be thought of as a collisional sink term. The reader can check

that eqn. (1.12) is dimensionally correct. There will also be particles scattering into the region of phase space being considered, yielding a source term from collisions. The source term is given by

$$\int \left( \frac{\delta f}{\delta t} \right)_{\text{c; source}} \mathrm{d}^3\mathrm{p} = \int \frac{\left| \mathbf{p}' - \mathbf{p}_1' \right|}{m} f\left(\mathbf{x}, \mathbf{p}_1', t\right) \, \mathrm{d}^3\mathrm{p}_1' \, \sigma\left(\mathbf{p}', \mathbf{p}_1' \mid \mathbf{p}, \mathbf{p}_1\right) \, \mathrm{d}\Omega \, f\left(\mathbf{x}, \mathbf{p}', t\right) \, \mathrm{d}^3\mathrm{p}' \quad (1.13)$$

The total number of particles being scattered within a unit spatial volume per unit of time is then the source terms from eqn. (1.13) with the sink terms from eqn. (1.12) subtracted from them.

There are indeed some further constraints on the interaction terms. For our purposes it suffices to state that the interaction should be time-reversible so that

$$\sigma\left(\mathbf{p}', \mathbf{p}_1' \mid \mathbf{p}, \mathbf{p}_1\right) = \sigma\left(\mathbf{p}, \mathbf{p}_1 \mid \mathbf{p}', \mathbf{p}_1'\right) \quad (1.14)$$

Similarly, it can be shown that the collision should preserve volume in momentum phase space so that we have

$$\mathrm{d}^3\mathrm{p}' \, \mathrm{d}^3\mathrm{p}_1' = \mathrm{d}^3\mathrm{p} \, \mathrm{d}^3\mathrm{p}_1 \quad (1.15)$$

Utilizing eqns. (1.14) and (1.15) enables us to write the net effect of collisional sources and sinks as

$$\int \left( \frac{\delta f}{\delta t} \right)_{\text{c}} \mathrm{d}^3\mathrm{p} = \int \frac{\left| \mathbf{p} - \mathbf{p}_1 \right|}{m} \, \sigma\left(\mathbf{p}, \mathbf{p}_1 \mid \mathbf{p}', \mathbf{p}_1'\right) \left[ f\left(\mathbf{x}, \mathbf{p}_1', t\right) f\left(\mathbf{x}, \mathbf{p}', t\right) - f\left(\mathbf{x}, \mathbf{p}_1, t\right) f\left(\mathbf{x}, \mathbf{p}, t\right) \right] \mathrm{d}\Omega \, \mathrm{d}^3\mathrm{p}_1 \quad (1.16)$$

Eqn. (1.10) along with the collisional terms in eqn. (1.16) constitute the *Boltzmann equation*. More rigorous derivations of the Boltzmann equation have been presented in Uhlenbeck and Ford (1963) for fluids and in Montgomery and Tidman (1964) for

plasmas. Eqn. (1.10) gives us the evolutionary equation for all the particles that make up a fluid in a six-dimensional phase space. We seldom need that level of detail and eqns. (1.3) to (1.5) already suggest to us that the fluid variables and their time-evolution might be obtained via suitable moments of the Boltzmann equation. We study that next.

### 1.2.3) Moments of the Boltzmann Equation

Using our intuition and a few insights from statistical mechanics, we have seen how eqns. (1.3), (1.4) and (1.5) connect the intuitively obvious density, momentum density and total energy density variables for a fluid to the distribution function. Notice that eqns. (1.3), (1.4) and (1.5) indeed represent successively higher moments of the distribution function with respect to the particle momentum $\mathbf{p}$. Eqn. (1.10) is an evolutionary equation for the distribution function. Comparing eqn. (1.10) to the definitions in eqns. (1.3) to (1.5), we realize that taking the first three moments of eqn. (1.10) would give us evolutionary equations for the fluid density, momentum density and energy density. Thus define $\psi(\mathbf{p})$ to be a function of particle momentum which can be convolved with eqn. (1.10) to obtain the evolutionary equations for the fluid variables. We then choose

$$\psi(\mathbf{p}) = m \quad ; \quad \psi(\mathbf{p}) = \mathbf{p} \quad ; \quad \psi(\mathbf{p}) = \frac{\mathbf{p}^2}{2m} \tag{1.17}$$

Eqn. (1.11) along with mass conservation shows that $\psi(\mathbf{p})$ is conserved in collisions. Speaking intuitively, we are just stating that collisions conserve mass, momentum and energy. Multiplying our evolutionary eqn. (1.10) with $\psi(\mathbf{p})$ and integrating over the range of permitted momenta then yields

$$\int \left( \psi(\mathbf{p}) \frac{\partial f}{\partial t} + \psi(\mathbf{p}) \frac{\mathbf{p}}{m} \bullet \frac{\partial f}{\partial \mathbf{x}} + \psi(\mathbf{p}) \mathbf{F} \bullet \frac{\partial f}{\partial \mathbf{p}} \right) d^3p = \int \psi(\mathbf{p}) \left( \frac{\delta f}{\delta t} \right)_c d^3p \tag{1.18}$$

A problem at the end of this chapter enables one to show that the right hand side of eqn. (1.18) integrates to zero. The physical reason for this stems from the fact that collisions do not contribute to the time rate of change of a conserved quantity. This simplifies our treatment of eqn. (1.18).

To make further progress we define momentum-averaged quantities as

$$\langle \psi \rangle \equiv \frac{1}{n} \int \psi(\mathbf{p})\ f(\mathbf{x},\mathbf{p},t)\, d^3p \quad ; \quad n \equiv \int f(\mathbf{x},\mathbf{p},t)\, d^3p \tag{1.19}$$

Here $n$ is the local number density of fluid particles. Recall that $f(\mathbf{x},\mathbf{p},t)d^3p$ has units of a number density, so the division by $n$ makes the previous equation dimensionally consistent. We would like to write eqn. (1.18) in a form where its structure as a PDE becomes readily apparent. Realize from eqn. (1.18) that the first two terms on the left hand side are easily manipulated so as to move the partial derivatives outside the integrals. Quite simply, the terms $\psi(\mathbf{p})$ and $\psi(\mathbf{p})\mathbf{p}/m$ in eqn. (1.18) do not depend on $t$ or on $\mathbf{x}$ with the result that the partial derivatives slip out of the integral. Manipulating the third term on the left hand side of eqn. (1.18) requires us to carry out an integration by parts. Thus we have

$$\begin{aligned} \int \psi(\mathbf{p})\ \mathbf{F} \bullet \frac{\partial f}{\partial \mathbf{p}}\, d^3p &= \int \nabla_{\mathbf{p}} \bullet \left(\psi(\mathbf{p})\ \mathbf{F}\, f\right) d^3p \ - \ \int f\ \nabla_{\mathbf{p}} \bullet \left(\psi(\mathbf{p})\ \mathbf{F}\right) d^3p \\ &= - \ \frac{\rho(\mathbf{x},t)}{m}\ \left\langle \mathbf{F} \bullet \nabla_{\mathbf{p}} \psi(\mathbf{p}) \right\rangle \end{aligned} \tag{1.20}$$

Notice that $\nabla_{\mathbf{p}}$ denotes a gradient over the momentum vector. Gauss's Law can be used in momentum space to show that the first integral on the right hand side of the first line in eqn. (1.20) is zero. This is ensured as long as the distribution function tends to zero as the momentum approaches infinity. Obtaining the second line in eqn. (1.20) requires us to assume that the $i^{\text{th}}$ component of the force $\mathbf{F}$ does not depend on the $i^{\text{th}}$ component of the momentum $\mathbf{p}$. (Notice that the Lorentz force, which has a special type of velocity-

dependence, satisfies this requirement.) Eqn. (1.19) can now be written in a form that makes its structure as a PDE evident as follows

$$\frac{\partial}{\partial t}\left(n\langle\psi\rangle\right) + \nabla \bullet \left(n\left\langle\frac{\mathbf{p}}{m}\psi\right\rangle\right) - n\,\mathbf{F} \bullet \left\langle\nabla_{\mathbf{p}}\psi(\mathbf{p})\right\rangle = 0 \tag{1.21}$$

In deriving eqn. (1.21) we have had to further assume that $\mathbf{F}$ is, in general, not a velocity-dependent body force. In the next three sub-sections we will make a detailed study of eqn. (1.21).

The theory that we have presented in this sub-section goes under the name of *Chapman-Enskog theory* for fluids. The hierarchy of moments that we have considered here is often referred to as the *BBGKY hierarchy* where each letter in the nomenclature stands for one of the contributors (Bogoliubov 1947, Born & Green 1946, Kirkwood 1947, Yvon 1935). Notice that in this section we have only taken the first three moments of the Boltzmann equation. Furthermore, the second moment was built using the scalar $\mathbf{p}^2$ because the cross-correlation in the local particle velocities is zero up to leading order. It is very reasonable to ask whether the first three moments will suffice. It turns out that for dense enough fluids, with a high collision rate between particles, the answer is in the affirmative. It also turns out that in dilute magnetized plasmas where the electron gyroradius around the magnetic field is small enough, one can make a similar approximation. It is, however, important to be forewarned that for dilute gases the first three moments are insufficient. In such gases, the local velocity distribution can display a substantial departure from the Maxwell-Boltzmann distribution with the result that higher moments need to be retained. Such examples arise frequently when studying the fluid dynamics around space reentry vehicles and in certain kinds of tenuous space plasmas.

### 1.2.4) The Continuity Equation

Setting $\psi(\mathbf{p}) = m$ in eqn. (1.21) and then using the eqns. (1.3), (1.4) and (1.19) gives us the *continuity equation*

$$\frac{\partial \rho}{\partial t} + \frac{\partial}{\partial x_i}\left(\rho \, \mathrm{v}_i\right) = 0 \quad \Leftrightarrow \quad \frac{\partial \rho}{\partial t} + \nabla \bullet \left(\rho \, \mathbf{v}\right) = 0 \tag{1.22}$$

In keeping with the Einstein summation convention, a repeated index implicitly denotes summation over that index. The above equation is an expression of mass conservation in a simple non-reacting fluid. For a reacting fluid, we would have similar equations for the mass fractions of each of the reactants along with *source terms* on the right hand sides. The source terms on the right hand side would then specify how one species reacts to form another species. I.e., the molecules in the fluid undergo chemical reactions to form other molecules and the mass fractions keep track of how the reactions are progressing. With or without source terms, eqn. (1.22) shows that the density changes in response to local variations in the flow variables, a property shared by all hyperbolic PDEs. Variations in the flow variables that take place far away from the point of interest do not affect the density at the point of interest instantaneously fast. The conservative nature of eqn. (1.22) will be discussed in great depth in the next section.

Eqn. (1.22) can also be written in the form

$$\frac{\partial \rho}{\partial t} + \mathbf{v} \bullet \nabla \rho = -\rho \, \nabla \bullet \mathbf{v} \tag{1.23}$$

It shows that without any compression or rarefaction in the flow (i.e. when $\nabla \bullet \mathbf{v} = 0$), the density is constant along the *streamlines* traced out by the velocity. See Fig. 1.3 for a pictorial depiction of streamlines around a (highly idealized) mountain range as well as a strategy for obtaining streamlines from a given velocity field. Compressions in the flow, denoted by $\nabla \bullet \mathbf{v} < 0$, can cause an increase in the local density. Rarefactions in the flow, denoted by $\nabla \bullet \mathbf{v} > 0$, can cause an decrease in the local density. The differential terms

$$\frac{D}{Dt} \equiv \frac{\partial}{\partial t} + \mathbf{v} \bullet \nabla \tag{1.24}$$

occurring on the left hand side have a special structure that recurs very often in fluid dynamics. As a result, it carries a special name, the *Lagrangian derivative* or the *material derivative*. It measures the variation in a flow variable as measured in a local frame of reference that moves with the instantaneous velocity of the fluid, i.e. along the streamlines shown in Fig. 1.3. In physics, such a frame is referred to as a Lagrangian frame of reference, hence the name. To develop an intuitive understanding of fluid dynamics, the reader is urged to view the beautiful images in Van Dyke (1982).

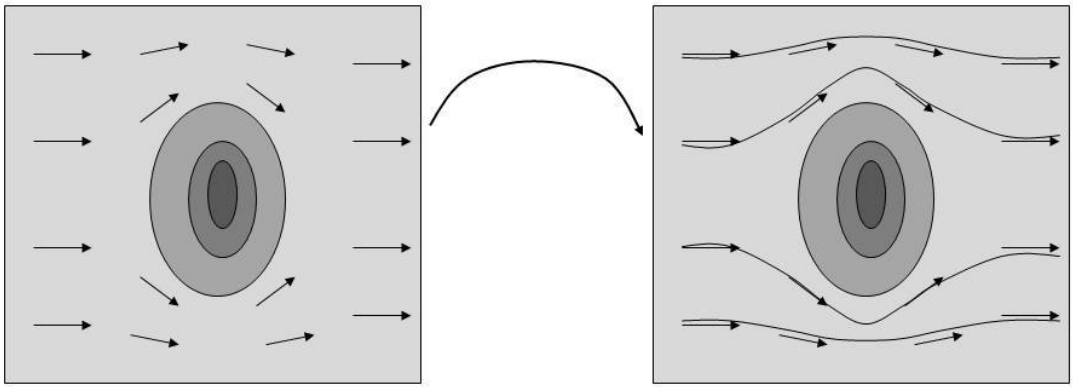

*Fig. 1.3 shows the wind flow around a mountain range (shown with darker shading). The left panel shows wind velocity vectors. By connecting the velocity vectors, one obtains the streamlines, as shown in the right panel. The Lagrangian derivative at each location is measured along the local streamline.*

### 1.2.5) The Momentum Equation

Setting $\psi(\mathbf{p}) = \mathbf{p} = m(\mathbf{v} + \mathbf{w})$ in eqn. (1.21) gives us the *momentum equation* for a fluid. Recall that the vector $\mathbf{v}$ denotes the mean velocity of the flow whereas the vector $\mathbf{w}$ denotes the fluctuation in the velocity relative to the mean; consequently the momentum equation has three components. Thus for the $i^{\text{th}}$ component we get

$$\frac{\partial}{\partial t}(\rho \mathrm{v}_i) + \frac{\partial}{\partial x_j}\left(\rho\left\langle(\mathrm{v}_i + \mathrm{w}_i)(\mathrm{v}_j + \mathrm{w}_j)\right\rangle\right) = \rho\, \mathrm{a}_i \qquad (1.25)$$

where $\mathbf{a} = \mathbf{F}/m$ is the acceleration due to external body forces.

We realize that we might achieve considerable simplification if we could relate $\left\langle \left(\mathrm{v}_i + \mathrm{w}_i\right)\left(\mathrm{v}_j + \mathrm{w}_j\right)\right\rangle$ to well-known quantities. To that end, we write

$$\left\langle \left(\mathrm{v}_i + \mathrm{w}_i\right)\left(\mathrm{v}_j + \mathrm{w}_j\right)\right\rangle = \mathrm{v}_i\mathrm{v}_j + \left\langle \mathrm{w}_i\mathrm{w}_j \right\rangle \tag{1.26}$$

The fluctuating part of one component of a particle's velocity is unlikely to have much of a correlation with the fluctuating part of another of its components. As a result, we would expect only the diagonal part of the tensor $\left\langle \mathrm{w}_i\mathrm{w}_j \right\rangle$ to be dominant. Furthermore, due to the random and isotropic nature of the collisions, we would expect all the diagonal elements of $\left\langle \mathrm{w}_i\mathrm{w}_j \right\rangle$ to have almost the same value. This allows us to extract the dominant parts of $\left\langle \mathrm{w}_i\mathrm{w}_j \right\rangle$ and write the sub-dominant part as $\pi_{ij}$. The dominant part reveals itself to be the isotropic fluid pressure. Thus we get

$$\rho\left\langle \mathrm{w}_i\mathrm{w}_j \right\rangle = \mathrm{P}\,\delta_{ij} - \pi_{ij} \quad ; \quad \mathrm{P} \equiv \frac{1}{3}\rho\left\langle \mathbf{w}^2 \right\rangle \quad ; \quad \pi_{ij} \equiv \rho\left\langle \frac{1}{3}\mathbf{w}^2\,\delta_{ij} - \mathrm{w}_i\mathrm{w}_j \right\rangle \tag{1.27}$$

where $\delta_{ij}$ is the Kronecker delta. For general enough flows we would expect the tensor $\pi_{ij}$ to have some non-zero contribution. We refer to it as the *viscous tensor*. The final form of the momentum equation can now be written as

$$\frac{\partial}{\partial t}\left(\rho\mathrm{v}_i\right) + \frac{\partial}{\partial x_j}\left(\rho\mathrm{v}_i\mathrm{v}_j + \mathrm{P}\,\delta_{ij} - \pi_{ij}\right) = \rho\,\mathrm{a}_i \tag{1.28}$$

We see that the momentum density, $\rho\mathrm{v}_i$, responds to variations in the advective stresses, $\rho\mathrm{v}_i\mathrm{v}_j$, the pressure stresses, $\mathrm{P}\,\delta_{ij}$, and the viscous stresses, $\pi_{ij}$. It also responds to the body forces. The three stresses taken together give us the momentum fluxes. The viscous terms can sometimes be negligible. The above equations without the viscous terms are

referred to as the *Euler equations*. With the viscous terms, they yield the *Navier-Stokes equations*. As with the continuity equation, eqn. (1.28) displays a *conservation form* which is very valuable for numerical solution.

It is also useful to rewrite eqn. (1.28) in another format, especially because it enables us to make contact with Newton's laws. Using eqn. (1.22) in eqn. (1.28) one can write the previous equation as

$$\rho \frac{D\, \mathrm{v}_i}{D\, t} = - \frac{\partial\, \mathrm{P}}{\partial\, x_i} + \rho\, \mathrm{a}_i + \frac{\partial}{\partial\, x_j} \pi_{ij} \tag{1.29}$$

Notice that $D\, \mathrm{v}_i / D\, t$ is the acceleration of the fluid as measured in its own Lagrangian frame of reference. Thus the left hand side of eqn. (1.29) measures the time rate of change of momentum in a fluid element that tracks the same underlying fluid particles. The right hand side of eqn. (1.29) just sums up the contribution from the pressure forces, the body forces and the viscous forces. Consequently, eqn. (1.29) is an expression of Newton's second law for a fluid element. Eqn. (1.29) is often referred to as the *primitive form* of the momentum equation and it shows itself to be very useful for analytical work with the fluid equations.

**1.2.6) The Energy Equation**

Using eqns. (1.5), (1.7) and (1.2) we can write a general expression for the total energy density of a fluid as

$$\mathcal{E} = \mathrm{e} + \frac{1}{2}\, \rho\, \mathbf{v}^2 \tag{1.30}$$

Setting $\psi(\mathbf{p}) = \mathbf{p}^2 / (2m) = m(\mathbf{v} + \mathbf{w})^2 / 2$ in eqn. (1.21) gives us the *energy equation* for a fluid, which is an evolutionary equation for the total energy density $\mathcal{E}$. We get

$$\frac{\partial \mathcal{E}}{\partial t} + \frac{\partial}{\partial x_i}\left(\frac{\rho}{2}\left\langle \left(\mathrm{v}_i + \mathrm{w}_i\right)\left(\mathbf{v} + \mathbf{w}\right)^2 \right\rangle\right) = \rho\, \mathrm{v}_i\, \mathrm{a}_i \tag{1.31}$$

Notice that the right hand side of eqn. (1.31) is effectively the dot product of a force and a velocity. Thus the right hand side gives us the amount of power provided by the external body forces per unit volume as the fluid moves.

As with the momentum equation, we undertake a careful examination of the second term on the left hand side of eqn. (1.31). Thus we have

$$\frac{\rho}{2}\left\langle \left(\mathrm{v}_i + \mathrm{w}_i\right)\left(\mathbf{v} + \mathbf{w}\right)^2 \right\rangle = \frac{\rho}{2}\,\mathbf{v}^2\,\mathrm{v}_i + \rho\left\langle \frac{1}{2}\,\mathbf{w}^2 \right\rangle \mathrm{v}_i + \rho\left\langle \mathrm{w}_i\,\mathrm{w}_j \right\rangle \mathrm{v}_j + \rho\left\langle \mathrm{w}_i\,\frac{1}{2}\,\mathbf{w}^2 \right\rangle \tag{1.32}$$

Each of the terms in the above equation has an interesting physical interpretation. Recall that $\rho\,\mathbf{v}^2/2$ and $\rho\left\langle \mathbf{w}^2/2 \right\rangle$ can be identified as the kinetic and internal energy densities of the fluid. Thus the first two terms on the right hand side of eqn. (1.32) can be interpreted as a flux of those energy densities. The $\left\langle \mathrm{w}_i\,\mathrm{w}_j \right\rangle$ part in the third term on the right hand side of eqn. (1.32) intimates to us that we should use eqn. (1.27) to write it as the sum of a pressure and a viscous stress term. Only the last term, $\rho\left\langle \mathrm{w}_i\,\mathbf{w}^2/2 \right\rangle$, in eqn. (1.32) is new to us. But notice that $\mathbf{w}^2/2$ within the angular brackets indicates that we are dealing with a particle thermal energy while the $\mathrm{w}_i$ term within the angular brackets indicates that this thermal energy is being propagated via random motions. This is exactly what heat transport does – it causes thermal energy to flow through a material due to the random walk of the energy-bearing particles. Thus we identify the *conduction heat flux* as

$$\mathrm{F}_i^{cond} \equiv \rho\left\langle \mathrm{w}_i\,\frac{1}{2}\,\mathbf{w}^2 \right\rangle \tag{1.33}$$

We can now write our total energy equation using terms that have physical meaning as

$$\frac{\partial\, \mathcal{E}}{\partial\, t} + \frac{\partial}{\partial\, x_i}\left(\left(\mathcal{E} + \mathrm{P}\right) \mathrm{v}_i - \mathrm{v}_j\, \pi_{ji} + \mathrm{F}_i^{cond}\right) = \rho\, \mathrm{v}_i\, \mathrm{a}_i \tag{1.34}$$

The viscous and thermal conduction terms are often referred to as *non-ideal terms*. We will see in the next couple of sections that their inclusion changes the character of the equations from hyperbolic to parabolic. Without the non-ideal terms eqn. (1.34) is part of the Euler equations; with the non-ideal terms it makes up the equation set that is referred to as the Navier-Stokes equations. As with the mass and momentum conservation equations, eqn. (1.34) has a conservation form that is very useful for numerical codes.

Just as the momentum equation was shown to be consistent with Newton's laws, we can also demonstrate that the energy equation is consistent with the first law of thermodynamics. After multiplying eqn. (1.28) with the velocity $\mathrm{v}_i$ and using eqn. (1.22) we get the *work equation*

$$\frac{\partial}{\partial\, t}\left(\frac{\rho}{2}\, \mathbf{v}^2\right) + \frac{\partial}{\partial\, x_i}\left(\frac{\rho}{2}\, \mathbf{v}^2\, \mathrm{v}_i\right) = \rho\, \mathrm{v}_i\, \mathrm{a}_i - \mathrm{v}_i \frac{\partial\, \mathrm{P}}{\partial\, x_i} + \mathrm{v}_i \frac{\partial\, \pi_{ij}}{\partial\, x_j} \tag{1.35}$$

Subtracting the above equation from eqn. (1.34) gives us an equation for the evolution of the internal (thermal) energy density as

$$\frac{\partial\, \mathrm{e}}{\partial\, t} + \frac{\partial}{\partial\, x_i}\left(\mathrm{e}\, \mathrm{v}_i\right) = -\, \mathrm{P} \frac{\partial\, \mathrm{v}_i}{\partial\, x_i} - \frac{\partial\, \mathrm{F}_i^{cond}}{\partial\, x_i} + \pi_{ij} \frac{\partial\, \mathrm{v}_i}{\partial\, x_j} \tag{1.36}$$

Just as we would expect, we see that the internal energy density does not change due to external body forces. Compression or rarefaction of the fluid can change its energy density as shown by the first term on the right hand side in eqn. (1.36). Similarly, the existence of thermal conduction or viscosity can change the energy density. Since the first law of thermodynamics is most easily recognized in terms of specific variables, i.e. variables that are defined per unit mass, we obtain an equation for the specific energy from the above equation as

$$\frac{\mathrm{D}}{\mathrm{D}\,t}\left(\frac{\mathrm{e}}{\rho}\right) = -\frac{\mathrm{P}}{\rho}\,\nabla \bullet \mathbf{v} - \frac{1}{\rho}\,\nabla \bullet \mathbf{F}^{cond} + \frac{1}{\rho}\,\pi_{ij}\frac{\partial\,\mathrm{v}_i}{\partial\,x_j} \tag{1.37}$$

Since the continuity equation gives us $\nabla \bullet \mathbf{v}/\rho = D\left(\rho^{-1}\right)\Big/Dt$ , we realize that $\nabla \bullet \mathbf{v}/\rho$ is just the rate of change of volume occupied by a unit mass. Thus eqn. (1.37) tells us that the rate of change of specific energy is given by the $\mathrm{P\,dV}$ work done on the fluid element when the non-ideal terms associated with thermal conduction and viscosity are neglected. Thus we see that eqn. (1.37) is an expression of the first law of thermodynamics.

We can also establish an interesting connection with the second law of thermodynamics. Using eqn. (1.2) in eqn. (1.37) we can also show that

$$\rho\,\mathrm{T}\,\frac{D\mathrm{s}}{Dt} = -\nabla \bullet \mathbf{F}^{cond} + \pi_{ij}\frac{\partial\,\mathrm{v}_i}{\partial\,x_j} \tag{1.38}$$

Here "s" is the specific entropy so that we realize that the entropy remains constant along each individual Lagrangian fluid element when the non-ideal terms are ignored. We should, however, note that the entropy is not constant when a fluid element goes through a *shock* because the rapid variation in velocity across a shock implicitly causes an increase in the viscous terms in the vicinity of the shock. It can also be shown that the contribution of the viscous terms on the right hand sides of eqns. (1.37) and (1.38) is always positive. Consequently, whenever viscosity is present, it will always cause an increase in the internal energy as well as the entropy. This gives us our first glimpse of the fact that the presence of shocks always introduces an irreversible process in the fluid dynamics.

**1.3) The Euler Equations**

While all real fluids do have a certain amount of viscosity and heat conduction, a very useful idealization arises when the viscous and heat conduction terms are ignored in eqns. (1.28) and (1.34). The complete set of equations then becomes

$$\begin{aligned} &\frac{\partial \rho}{\partial t} + \frac{\partial}{\partial x_i}\left(\rho \, \mathrm{v}_i\right) = 0 \\ &\frac{\partial}{\partial t}\left(\rho \mathrm{v}_i\right) + \frac{\partial}{\partial x_j}\left(\rho \mathrm{v}_i \mathrm{v}_j + \mathrm{P}\, \delta_{ij}\right) = 0 \\ &\frac{\partial \mathcal{E}}{\partial t} + \frac{\partial}{\partial x_i}\left(\left(\mathcal{E} + \mathrm{P}\right) \mathrm{v}_i\right) = 0 \end{aligned} \tag{1.39}$$

where $\mathcal{E} = \mathrm{e} + \rho \, \mathbf{v}^2/2$ and the body forces have been dropped. As stated, eqn. (1.39) is a system of five PDEs with six unknowns. In order to be able to solve the system we need an extra relationship, one that relates the internal energy "e" to the density $\rho$ and pressure "P". As discussed in sub-section 1.2.1, such a *constitutive relationship* comes from thermodynamics, or alternatively statistical mechanics, and goes under the name of an equation of state. For an ideal gas, eqn. (1.2) constitutes such an equation of state.

Notice that the system in eqn. (1.39) has a very interesting structure. It says that the flow variables change in time by responding to local, spatial variations in the flow variables themselves. By focusing on the continuity equation, we see that the mass density $\rho$ changes in response to the flux of mass given by $\rho \, \mathbf{v}$. A *flux* is formed by multiplying a density with a velocity. The flux of any quantity has dimensions of that quantity times a speed. This concept extends to momentum and energy densities and their fluxes. We also see that the momentum density and total energy densities change in response to fluxes of momentum and energy respectively.

Eqn. (1.39) is in conservation form. Let us study the consequences of having a conservation form. Consider a small three-dimensional cuboidal volume "V" and say that we integrate the continuity equation over that volume. See Fig. 1.4 where we denote the

upper and lower x-faces by $A_1$ and $A_2$ , the upper and lower y-faces by $A_3$ and $A_4$ and the upper and lower z-faces by $A_5$ and $A_6$ . Fig. 1.4 only labels the visible faces. We have

$$\iiint_V \left( \frac{\partial \rho}{\partial t} + \frac{\partial (\rho \, v_x)}{\partial x} + \frac{\partial (\rho \, v_y)}{\partial y} + \frac{\partial (\rho \, v_z)}{\partial z} \right) dx \, dy \, dz = 0 \tag{1.40}$$

Integrating the above equation by parts or, equivalently, by using Gauss's Law, we get

$$\frac{\partial}{\partial t} \iiint_V \rho \, dx \, dy \, dz + \iint_{A_1} \rho \, v_x \, dy \, dz - \iint_{A_2} \rho \, v_x \, dy \, dz + \iint_{A_3} \rho \, v_y \, dx \, dz - \iint_{A_4} \rho \, v_y \, dx \, dz + \iint_{A_5} \rho \, v_z \, dx \, dy - \iint_{A_6} \rho \, v_z \, dx \, dy = 0 \tag{1.41}$$

Eqn. (1.41) makes it evident that the density integrated over the volume "V" is only changed by fluxes flowing in through the boundaries. Such a form for representing a PDE is called the *flux form* or the *conservation form* for the PDE. Similar conservative forms can be written for the momentum and energy equations. In the course of this book we will study hyperbolic PDEs, like the Euler equations above, that can admit discontinuous solutions. When such discontinuities develop, we lose our ability to precisely predict the structure of the flow within a volume that is being overrun by the discontinuity. In those situations, the conservation form of the equations, as shown by eqn. (1.39) and discretized by eqn. (1.41), continues to remain valid. As a result, if a conservative form is available for a PDE, there is a strong motivation to retain a discrete version of the conservation form in our numerical algorithms.

*Fig. 1.4 illustrates a small cuboidal volume "V" over which we integrate the continuity equation. The mass inside the volume only changes in response to the mass flux flowing through the boundaries.*

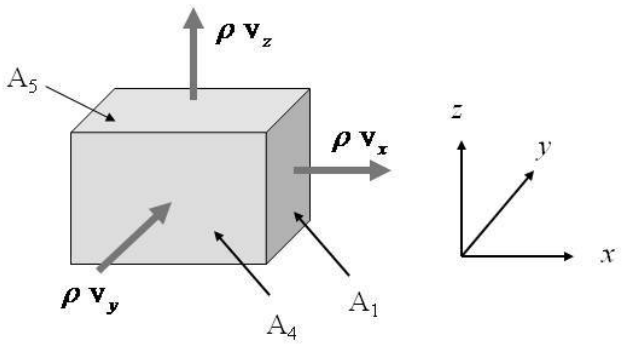

We see that the density, velocities and pressure (or, alternatively, the internal energy density) are the physically meaningful variables for the Euler equations. We call these the *primitive variables*. The Euler equations assume their simplest form when they are written in primitive variables. Analytic manipulations of the Euler equations are almost always performed in primitive variables. Using eqns. (1.22), (1.29) and (1.36) we obtain evolutionary equations for these variables as

$$\begin{aligned} \frac{D\rho}{Dt} &= -\rho \nabla \bullet \mathbf{v} \\ \rho \frac{D\, \mathrm{v}_i}{D\, t} &+ \frac{\partial\, \mathrm{P}}{\partial\, x_i} = 0 \\ \frac{\mathrm{D\, e}}{\mathrm{D}\, t} &= -\left(\mathrm{e} + \mathrm{P}\right) \nabla \bullet \mathbf{v} \end{aligned} \tag{1.42}$$

As with eqn. (1.39), eqn. (1.42) can be written in a tensor notation which makes it possible to write the Euler equations in any geometry, see Aris (1989). Excellent introductions to fluid mechanics are available in texts by Landau and Lifshitz (2000), Batchelor (2000) and Clarke and McChesney (1976). The text by Courant and Friedrichs (1948) is a classic on the physics of supersonic flow and shock waves.

The Euler equations form a hyperbolic system and indeed that demonstration will be furnished later in this chapter. The primitive variables prove very useful when making that demonstration. We will show that eqns. (1.39), or equivalently (1.42), permit several families of waves to propagate. Some of those waves propagate with the fluid velocity whereas others propagate with the speed of sound relative to the local flow velocity. It is important to realize that these waves constitute features that propagate in the flow. We will see that the Euler equations can be discretized and evolved in time on a one, two or three-dimensional lattice of cuboidal cells as was done in eqn. (1.41). Such a lattice of cells is called a *mesh* or a *grid*. The individual cells are referred to as the *zones* of the computational mesh. It is important to realize that none of the significant flow features should propagate from one zone of the mesh to another in less than a *timestep*. A timestep is the discrete unit of time over which the solution that is present on the computational

mesh is evolved. To ensure the retention of all the significant information on the mesh, it makes intuitive sense that a flow feature should not propagate by more than one zone size in one timestep. This concept will be further developed in the next chapter.

### 1.4) The Navier-Stokes Equations

The Navier-Stokes equations result from retaining the viscous and/or heat conduction terms. In conservation form they are obtained by drawing on eqns. (1.22), (1.28) and (1.34) to get

$$\begin{aligned}
&\frac{\partial \rho}{\partial t} + \frac{\partial}{\partial x_i}\left(\rho \, \mathrm{v}_i\right) = 0 \\
&\frac{\partial}{\partial t}\left(\rho \mathrm{v}_i\right) + \frac{\partial}{\partial x_j}\left(\rho \mathrm{v}_i \mathrm{v}_j + \mathrm{P}\, \delta_{ij} - \pi_{ij}\right) = 0 \\
&\frac{\partial \mathcal{E}}{\partial t} + \frac{\partial}{\partial x_i}\left(\left(\mathcal{E} + \mathrm{P}\right) \mathrm{v}_i - \mathrm{v}_j \, \pi_{ji} + \mathrm{F}_i^{cond}\right) = 0
\end{aligned} \tag{1.43}$$

where $\mathcal{E} = \mathrm{e} + \rho \, \mathbf{v}^2/2$ and the body forces have been dropped. As with the Euler equations, the equation of state helps close the system. The above equations can be written in primitive form by using eqns. (1.22), (1.29) and (1.34) to obtain

$$\begin{aligned}
&\frac{D\rho}{Dt} = -\rho \, \nabla \bullet \mathbf{v} \\
&\rho \frac{D \, \mathrm{v}_i}{D \, t} + \frac{\partial \, \mathrm{P}}{\partial \, x_i} - \frac{\partial}{\partial \, x_j}\pi_{ij} = 0 \\
&\frac{\mathrm{D} \, \mathrm{e}}{\mathrm{D} \, t} = -\left(\mathrm{e} + \mathrm{P}\right) \nabla \bullet \mathbf{v} - \nabla \bullet \mathbf{F}^{cond} + \pi_{ij} \frac{\partial \, \mathrm{v}_i}{\partial \, x_j}
\end{aligned} \tag{1.44}$$

Comparing eqns. (1.43) and (1.44) to eqns. (1.39) and (1.42) we realize that the Navier-Stokes equations retain all the same hyperbolic terms that were present in the Euler equations. However, they do have additional terms which change their character. The viscous and conduction terms have the property that they diffuse any crisp flow profile

that develops. In other words, they are represented by parabolic operators. As a result, the Navier-Stokes equations have hyperbolic and parabolic terms. Since the parabolic terms have the highest spatial derivatives, we say that the overall character of the Navier Stokes equations is parabolic.

Examination of eqns. (1.27) and (1.33) suggests that it ought to be possible to derive the viscous and heat conduction operators from first principles by using gas kinetic theory. In practice, the structure of these operators as well as the coefficients that go into defining them are determined by a combination of theory and experiment. The viscous tensor $\pi_{ij}$ is taken to be proportional to the *deformation rate tensor* in a fluid, denoted by $D_{ij}$. The latter measures the extent to which local shearing motions are present in the flow. Thus we have

$$\pi_{ij} \equiv \mu\, D_{ij} \qquad ; \qquad D_{ij} \equiv \frac{\partial \mathrm{v}_i}{\partial x_j} + \frac{\partial \mathrm{v}_j}{\partial x_i} - \frac{2}{3} \left(\nabla \bullet \mathbf{v}\right) \delta_{ij} \tag{1.45}$$

Here $\mu$ is the *coefficient of shear viscosity* and is usually determined experimentally though its value can be estimated from gas kinetic theory. Notice that $D_{ij}$ is a traceless, symmetric tensor. An exercise at the end of the chapter shows that such a structure for $D_{ij}$ is sufficient to ensure that the viscous terms always cause the internal energy and entropy to increase. Eqn. (1.45) is valid for a monoatomic gas where we do not expect isotropic compressions or rarefactions to contribute to the viscosity. In practical situations one needs an extra bulk viscosity term so that the viscous stress tensor is given by

$$\pi_{ij} \equiv \mu \left( \frac{\partial \mathrm{v}_i}{\partial x_j} + \frac{\partial \mathrm{v}_j}{\partial x_i} \right) + \left( \mu_b - \frac{2}{3}\, \mu \right) \left(\nabla \bullet \mathbf{v}\right) \delta_{ij} \tag{1.46}$$

where $\mu_b$ is the *coefficient of bulk viscosity*. The thermal conduction vector $\mathbf{F}^{cond}$ is taken to be proportional to the gradient of the temperature. We therefore have

$$\mathbf{F}^{cond} \equiv -\kappa \nabla \mathrm{T} \tag{1.47}$$

Here $\kappa$ is the *coefficient of thermal conductivity*. The parabolic nature of the thermal conduction operator is easily seen by inserting eqn. (1.47) in eqn. (1.44) and realizing that for static fluids it yields a heat conduction equation for the temperature. The parabolic nature of the viscous term can is also revealed by inserting eqn. (1.45) in eqn. (1.44) and simplifying the resulting expressions.

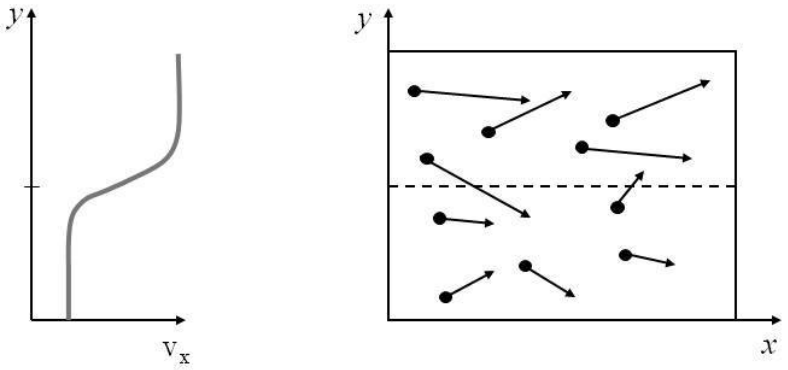


*Fig. 1.5 shows a shearing flow in a section of a channel. The x-velocity profile of the flow is shown on the left. It has a variation in the y-direction. The channel along with the particles and their velocities are shown in an idealized sense to the right. The fluid moves faster on the top and slower at the bottom of the channel. The middle of the channel is shown by the dashed line.*

It is possible to make the transport coefficients intuitively obvious. Fig. 1.5 shows a shearing flow in a section of a channel. The x-velocity profile of the flow is shown on the left. We see that $v_x$ has a steep variation in the y-direction at the location of the shear, with the result that $\partial^2 v_x / \partial y^2$ is large. The momentum equation in eqn. (1.44) shows that this results in viscous stresses being applied to the x-velocity in the vicinity of the shear. The channel, along with the particles and their velocities, is shown in an idealized sense to the right. The fluid moves faster on the top and slower at the bottom of the channel. The middle of the channel is shown by the dashed line. We assume that the upper and lower walls of the channel are moving with the local velocity of the fluid. When a faster moving particle crosses over into the lower half of the channel and a slower moving particle crosses over into the upper half of the channel, as shown in Fig. 1.5, x-momentum is exchanged across the dashed surface resulting in viscous momentum

transfer. The upper fluid loses a little bit of its x-momentum while the lower fluid gains some x-momentum. Substituting eqn. (1.45) in eqn. (1.44) we see that the viscous coefficient $\mu$ should have units of density times a square of the length divided by time. Since the viscosity-driven momentum transfer is mediated by particle collisions, the only physical length and time scales that govern this process are given by the mean free path $l$ and the collision time $\tau$. Thus $\mu$ must scale as $\rho\, l^2/\tau$. Using our study of the fluid approximation in Sub-section 1.2.1 we see that $\mu/\rho$ scales as $w^T l$ . Any classical fluid must, therefore, have some viscosity.

A shock, by the same token, can be envisioned as a faster moving stream of particles colliding with a slower moving set of particles as shown in Fig. 1.6. The x-velocity varies along the x-direction and is shown in the plot on the top of that figure. At the location of the shock we have strongly compressive motion, i.e. $\partial \mathrm{v_x}/\partial x$ assumes a large negative value. (The divergence of the velocity is often used in numerical codes as a diagnostic for the existence of a shock.) The one-dimensional channel along which the planar shock moves, known as a *shock tube*, is shown at the bottom. The dashed line shows the location of the shock. At the point of their interaction the streams interpenetrate over a short distance, of the order of a few mean free paths. This produces large viscous stresses at the location of the shock, resulting in substantial energy being imparted by the faster moving particles to the slower moving particles. From the upper panel in Fig. 1.6 we see that $\mathrm{v_x}$ has a steep variation in the x-direction at the location of the shock, with the result that $\partial^2 \mathrm{v_x}/\partial x^2$ is large. The momentum equation in eqn. (1.44) shows that this results in large viscous stresses being applied to the x-velocity in the vicinity of the shock, which is how the unshocked gas is slowed down at the shock. The pile up of molecules at the shock, just like the pile up of cars in a car crash, causes the density and internal energy of the shocked molecules to be higher than the corresponding variables of the unshocked molecules.

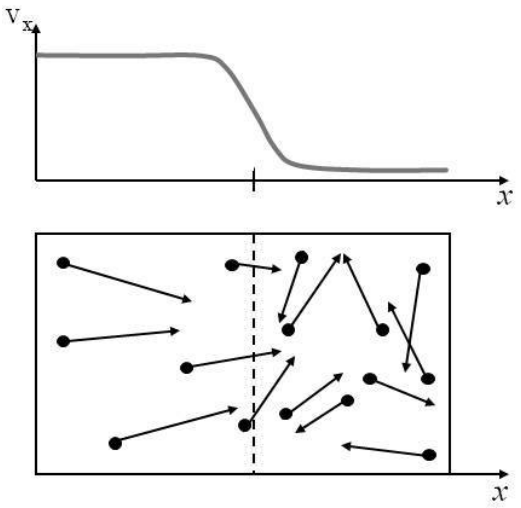


*Fig. 1.6 provides a schematic of the processes that occur in a one-dimensional planar shock. The upper plot shows the variation in the x-velocity as a function of position along the x-axis. The lower diagram shows a schematic of the high-speed stream coming in from the left. The dashed line shows the location of the shock. The shocked gas is to the right of the dashed line. The gas to the right is denser and has larger random motions, showing that it is hotter, i.e. it has larger internal energy.*

The above two paragraphs have shown us that any shear layer or shock will have a finite thickness due to the operation of the non-ideal parabolic terms in the Navier Stokes equations. The Euler equations ignore these parabolic terms. Consequently, they can in principle support discontinuous solutions that have infinitely thin shear layers or shocks. The discussion above has shown, however, that any interpretation of these discontinuities that arise from the Euler equations has to rely on the conceptual underpinning provided by the Navier Stokes equations.

Similar considerations from the kinetic theory of gases also allow us to claim that $\kappa \sim C_v \mu$ where $C_v$ is the *specific heat at constant volume* for the gas. An exercise at the end of the chapter illustrates this concept.

### 1.5) Classifying and Understanding PDEs

The previous two sections have shown us that PDEs can take various forms which influence their function. It is, therefore, interesting to understand how a PDE can be analyzed with a view to understanding what it does. We do that in the next three Sub-sections. The first Sub-section motivates our study. The second Sub-section formalizes our understanding by introducing us to the eigenmodal analysis of the Euler equations. The second Sub-section also introduces us to the concept of domain of dependence and range of influence for hyperbolic PDEs. The third Sub-section generalizes these ideas so that they may be applied to any hyperbolic PDE.

### 1.5.1) Motivation

Let us motivate our study by understanding the behavior of simple, model PDEs. These can be thought of as arising from smaller portions of the PDEs that we have studied. For example, consider the following scalar PDE

$$\frac{\partial \rho}{\partial t} + \mathrm{a}\,\frac{\partial \rho}{\partial x} + \mathrm{b}\,\frac{\partial \rho}{\partial y} = 0 \tag{1.48}$$

which can be thought of as a special case of the continuity equation, eqn. (1.22), when the velocity is constant. Since the left hand side of eqn. (1.48) can be interpreted as a Lagrangian derivative, it is easy to realize that the above equation tells us that density features are being propagated, i.e. *advected*, with speeds "a" and "b" in the x and y-directions respectively. We therefore do not need any further mathematical analysis to realize that eqn. (1.48) is hyperbolic. However, it is useful to find a formal way of demonstrating that this PDE is hyperbolic, with the hope that the process can be generalized to more complicated PDEs. Let us, therefore, try the formal solution

$$\rho(x,y,t) = \rho_0 + \rho_1\, \mathrm{e}^{i\left(k_x x + k_y y - \omega t\right)} \tag{1.49}$$

which consists of a constant part with a wave-like fluctuation. In other words, we improve our chance of proving that eqn. (1.48) is hyperbolic by positing a solution that has a wave-like character. Substituting eqn. (1.49) in eqn. (1.48) then gives us

$$\omega = k_x\,\mathrm{a} + k_y\,\mathrm{b} \quad ; \quad \rho(x,y,t) = \rho_0 + \rho_1\, \mathrm{e}^{i\left[k_x(x - \mathrm{a}\,t) + k_y(y - \mathrm{b}\,t)\right]} \tag{1.50}$$

The traveling wave nature of the solution is readily apparent. We see that only certain real values of "$\omega$" were allowed. Thus the PDE serves to restrict the wave-speeds of the wave-like solution that we substituted into it as our initial conjecture. The acceptable

solutions that arise when a harmonic ansatz, like that in eqn. (1.49), is made are called the *eigenmodes* of the PDE. Thus in eqn. (1.50) the coefficient of $\rho_1$ is the eigenmode of the hyperbolic PDE. The acceptable values of the wave-speeds are called the *eigenvalues* of the hyperbolic PDE.

Now consider the temperature variation in a static, thermally conducting, two-dimensional medium. From the last equation in eqn. (1.44) we realize that the evolutionary equation for the temperature is parabolic and is written as

$$\frac{\partial \, \mathrm{T}}{\partial \, t} = \kappa \left( \frac{\partial^2 \, \mathrm{T}}{\partial \, x^2} + \frac{\partial^2 \, \mathrm{T}}{\partial \, y^2} \right) \tag{1.51}$$

If we now pattern a conjectured solution for the temperature after eqn. (1.49) we get

$$\mathrm{T}\left(x, y, t\right) = \mathrm{T}_0 + \mathrm{T}_1 \, \mathrm{e}^{i \left( k_x x + k_y y - \omega \, t \right)} \tag{1.52}$$

Substituting eqn. (1.52) into eqn. (1.51) then yields

$$\omega = -i \, \kappa \, \left( k_x^2 + k_y^2 \right) \quad ; \quad \mathrm{T}\left(x, y, t\right) = \mathrm{T}_0 + \mathrm{T}_1 \, \mathrm{e}^{i \left( k_x x + k_y y \right) - \kappa \left( k_x^2 + k_y^2 \right) t} \tag{1.53}$$

We see that the PDE restricts "$\omega$" to imaginary values. Furthermore, eqn. (1.53) shows that the harmonic initial conditions decay as a function of time without any wave-like propagation. Thus eqn. (1.51) is parabolic with the coefficient of $\mathrm{T}_1$ in eqn. (1.53) being the *eigenmode* of the parabolic PDE.

Having studied eqns. (1.48) and (1.51) in isolation it is now possible to see how they might be combined together to yield a scalar *advection-diffusion equation* as follows

$$\frac{\partial \rho}{\partial t} + \mathrm{a}\,\frac{\partial \rho}{\partial x} + \mathrm{b}\,\frac{\partial \rho}{\partial y} = \kappa \left( \frac{\partial^2 \rho}{\partial x^2} + \frac{\partial^2 \rho}{\partial y^2} \right) \tag{1.54}$$

Systems of such equations are often used in computational biology to model the transport of chemicals in tissues. The chemicals might react with one another resulting in the inclusion of stiff source terms on the right hand side of eqn. (1.54) and yielding systems of *advection-diffusion-reaction equations*. Such equations play a very important role in *chemo-taxis* problems from mathematical biology. In such problems, the evolution of chemical concentrations at any location in a biological system depends on their values and their spatial gradients.

### 1.5.2) Characteristic Analysis of the Euler Equations

We can now generalize the ideas that were developed in the previous Sub-section. The generalization in the case of hyperbolic PDEs is especially interesting. Thus let us consider the Euler equations. We suppress variation in the other two directions and only consider variations in the x-direction. To further simplify the analysis, let us restrict attention to variations in the density, x-velocity and pressure. Eqn. (1.42) can then be written in an elegant matrix notation as

$$\frac{\partial}{\partial t}\begin{pmatrix} \rho \\ \mathrm{v_x} \\ \mathrm{P} \end{pmatrix} + \begin{pmatrix} \mathrm{v_x} & \rho & 0 \\ 0 & \mathrm{v_x} & \dfrac{1}{\rho} \\ 0 & \Gamma\,\mathrm{P} & \mathrm{v_x} \end{pmatrix} \frac{\partial}{\partial x}\begin{pmatrix} \rho \\ \mathrm{v_x} \\ \mathrm{P} \end{pmatrix} = 0 \tag{1.55}$$

The 3×3 matrix in the above system is referred to as the *characteristic matrix* and the above system is often referred to as a 3×3 system.

It turns out that several of the wave-propagation properties of eqn. (1.55) can be understood by understanding the *eigenvalues* and *eigenvectors* of the characteristic

matrix. The eigenvalues of a characteristic matrix are also called its *characteristic values*. To that end, let us parody eqn. (1.50) for systems of equations by writing

$$\begin{pmatrix} \rho(x,t) \\ \mathrm{v_x}(x,t) \\ \mathrm{P}(x,t) \end{pmatrix} = \begin{pmatrix} \rho_0 \\ \mathrm{v_{x0}} \\ \mathrm{P}_0 \end{pmatrix} + \begin{pmatrix} \rho_1 \\ \mathrm{v_{x1}} \\ \mathrm{P}_1 \end{pmatrix} \mathrm{e}^{\,i\,(\mathrm{k\,x} - \omega\,\mathrm{t})} \tag{1.56}$$

To understand eqn. (1.56) first realize that the characteristic matrix in eqn. (1.55) is not a constant but rather depends on the solution. Eqn. (1.56) then tells us that the variables that have been subscripted with a "1" make a small fluctuation about the original, physically realizable, constant state. This constant state has variables that are subscripted with a "0". (To be physically realizable, the constant state should at least have positive values for density and pressure.) Consequently, the time derivative as well as the spatial derivative in eqn. (1.55) will be proportional to the vector $\left(\rho_1, \mathrm{v_{x1}}, \mathrm{P}_1\right)^T$. However, the terms in the 3×3 matrix in eqn. (1.55) will, for the most part, depend on the constant state given by the vector $\left(\rho_0, \mathrm{v_{x0}}, \mathrm{P}_0\right)^T$. Thus disregarding the small fluctuations, we can use the constant state to approximate the terms in the 3×3 matrix. In technical terms, we have *linearized* the hyperbolic system that was originally non-linear. Putting eqn. (1.56) in the linearized version of eqn. (1.55) gives us

$$-\,i\,\omega \begin{pmatrix} \rho_1 \\ \mathrm{v_{x1}} \\ \mathrm{P}_1 \end{pmatrix} + i\,\mathrm{k} \begin{pmatrix} \mathrm{v_{x0}} & \rho_0 & 0 \\ 0 & \mathrm{v_{x0}} & \dfrac{1}{\rho_0} \\ 0 & \Gamma\,\mathrm{P}_0 & \mathrm{v_{x0}} \end{pmatrix} \begin{pmatrix} \rho_1 \\ \mathrm{v_{x1}} \\ \mathrm{P}_1 \end{pmatrix} = 0 \tag{1.57}$$

Defining $\lambda \equiv \omega/k$ and realizing that it has units of speed allows us to write the following eigenvalue problem.

$$\begin{pmatrix} v_{x0}-\lambda & \rho_0 & 0 \\ 0 & v_{x0}-\lambda & \dfrac{1}{\rho_0} \\ 0 & \Gamma\, P_0 & v_{x0}-\lambda \end{pmatrix} \begin{pmatrix} \rho_1 \\ v_{x1} \\ P_1 \end{pmatrix} = 0 \qquad (1.58)$$

The determinant of the above *characteristic matrix* yields the *characteristic equation* which can in turn be solved for the eigenvalues. For the Euler system we see that the three permitted eigenvalues form an ordered set given by

$$\lambda^1 = v_{x0} - c_0 \quad ; \quad \lambda^2 = v_{x0} \quad ; \quad \lambda^3 = v_{x0} + c_0 \quad ; \quad c_0 \equiv \sqrt{\frac{\Gamma\, P_0}{\rho_0}} \qquad (1.59)$$

Here $c_0$ is the sound speed in the gas, $\lambda^1$ is the eigenvalue corresponding to the left-going *sound wave,* $\lambda^2$ is the eigenvalue corresponding to the *entropy wave* and $\lambda^3$ is the eigenvalue corresponding to the right-going sound wave. Fig. 1.7 traces out these three waves and their propagation in a space-time diagram for the case where $v_{x0}$ is positive and smaller than the sound speed $c_0$ , i.e. for *subsonic flow*. (When $|v_{x0}| > c_0$ we call the flow *supersonic*.) Because we only consider small fluctuations about a constant state, the waves propagate as straight lines in space-time. The curves that trace out the propagation of waves in space-time are called *characteristic curves*. In a more general situation, i.e. if the non-linearity inherent in the hyperbolic system is reintroduced, the characteristic curves need not be straight lines.

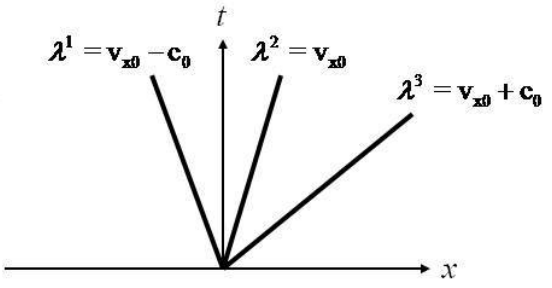


*Fig. 1.7 shows a space-time diagram for the 3×3 Euler system. The characteristic curves in space-time showing the left-going sound wave, entropy wave and right-going sound wave are also shown. The three waves form an ordered set with the result that the characteristic curves for this 3×3 system do not overlap.*

Corresponding to each of the three eigenvalues in eqn. (1.59), the matrix in eqn. (1.58) admits three linearly independent *right eigenvectors* and a corresponding number of *left eigenvectors*. We can write out the right eigenvectors explicitly as

$$r^1 = \begin{pmatrix} \rho_0 \\ -\,c_0 \\ \rho_0\, c_0^2 \end{pmatrix} \quad ; \quad r^2 = \begin{pmatrix} 1 \\ 0 \\ 0 \end{pmatrix} \quad ; \quad r^3 = \begin{pmatrix} \rho_0 \\ c_0 \\ \rho_0\, c_0^2 \end{pmatrix} \tag{1.60}$$

The right eigenvectors give us some very useful information about the waves that are supported in the fluid. We see that for a right-going sound wave, which corresponds to the eigenvector $r^3$ in eqn. (1.60), the ratios between the fluctuations in the density, x-velocity and pressure must be given by $\rho_1 : v_{x1} : P_1 = \rho_0 : c_0 : \rho_0\, c_0^2$ . We see, therefore, that an increase in the x-velocity in a right-going sound wave also causes a simultaneous increase in the density and the pressure. Thus sound waves are *compressive waves*, i.e. they propagate by introducing a sequence of alternating compressions and rarefactions in the gas, see Fig. 1.8. It is this fluctuating pressure that gives our ears the sensation of sound. Compressive waves are also referred to as *longitudinal waves*. In such waves the material motion is in the direction of wave propagation. Such waves should be contrasted with the *transverse waves* that propagate, say for instance, on a taut string. In transverse waves the material motion is orthogonal to the direction of propagation. Fluids do not have any tensional force between molecules. Consequently, they cannot support the propagation of transverse waves, though we will soon see examples of systems that can sustain transverse waves. By examining the second eigenvector in eqn. (1.60) we also see that the entropy wave only generates fluctuations in the density without causing changes in the x-velocity or pressure. In doing so, it causes a change in the entropy of the gas, hence its name. The entropy wave is also called a *contact discontinuity* because it can result in a jump in the density variable without having a jump in the pressure or the normal velocity. The reader can analyze the remaining, i.e. first, eigenvector in eqn. (1.60) to see that it is also a sound wave.

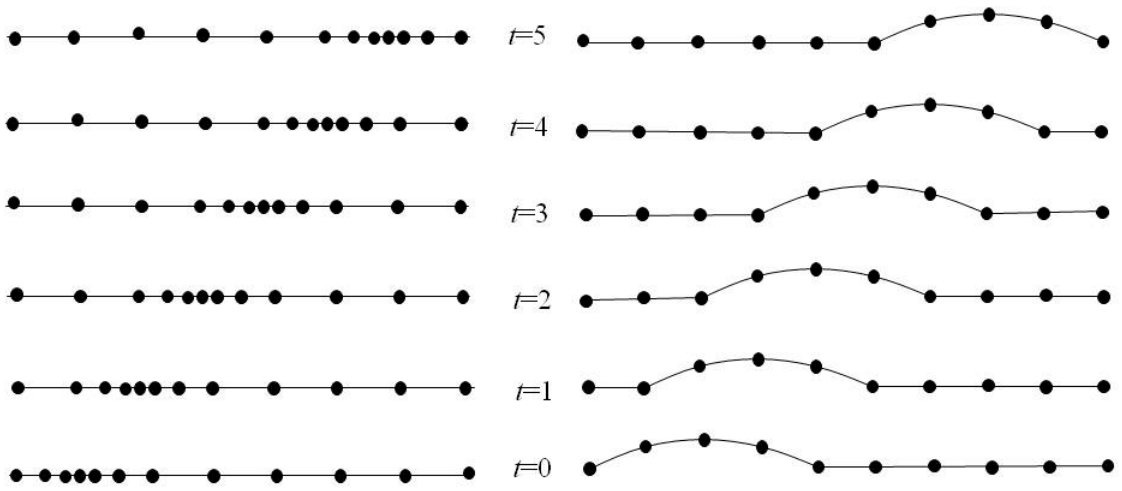


*Fig. 1.8 illustrates the difference in propagation of a longitudinal and transverse wave. In both instances the wave propagates to the right. The panel to the left shows a sequence of snapshots of the propagation of a longitudinal wave, an example of this being the propagation of a right-going sound wave. The material motion is along the direction of propagation. The panel to the right shows the propagation of a transverse wave pulse, an example being the plucking of a taut string. The material motion is transverse to the direction of propagation. Time runs upward in both the panels so that the reader can get a sense of the wave propagating in space and time.*

The linear independence of the right eigenvectors is a very useful property because it ensures that any general, small fluctuation around any constant initial state of the fluid can be projected into the space of right eigenvectors, i.e. the eigenspace of the characteristic matrix is *complete*. To instantiate this using Fig. 1.7, if a small perturbation of any sort is introduced at $(x,t)=(0,0)$ then that perturbation can be viewed as a linear combination of right and left-going sound waves as well as an entropy wave. For $t>0$ the waves propagate away from the origin in Fig. 1.7 with amplitudes that are set by the initial perturbation and speeds that are given by eqn. (1.59). This is a very useful property and we will see later on that this property is very helpful in designing some very elegant schemes. When projecting variables into the right eigenspace of any matrix, it is very advantageous to have an *orthonormal* set of left eigenvectors. For the 3×3 Euler system, the orthonormalized left eigenvectors are given by

$$l^1=\begin{pmatrix}0 & \dfrac{-1}{2\,\mathrm{c}_0} & \dfrac{1}{2\,\rho_0\,\mathrm{c}_0^2}\end{pmatrix}\;;\;\; l^2=\begin{pmatrix}1 & 0 & -\dfrac{1}{\mathrm{c}_0^2}\end{pmatrix}\;;\;\; l^3=\begin{pmatrix}0 & \dfrac{1}{2\,\mathrm{c}_0} & \dfrac{1}{2\,\rho_0\,\mathrm{c}_0^2}\end{pmatrix} \qquad (1.61)$$

This completes our introduction of the eigensystem for the 3×3 Euler equations.

Let us now demonstrate exactly how a small perturbation propagates. Thus imagine an initial condition that is made up of a constant state plus a small Gaussian fluctuation as follows

$$\begin{pmatrix} \rho(x,t=0) \\ \mathrm{v_x}(x,t=0) \\ \mathrm{P}(x,t=0) \end{pmatrix} = \begin{pmatrix} \rho_0 \\ \mathrm{v_{x0}} \\ \mathrm{P_0} \end{pmatrix} + \begin{pmatrix} \rho_1 \\ \mathrm{v_{x1}} \\ \mathrm{P_1} \end{pmatrix} \mathrm{e}^{-x^2} = \mathrm{V_0} + \mathrm{V_1}\ \mathrm{e}^{-x^2} \tag{1.62}$$

Thus $\mathrm{V_0}$ in the above equation denotes the constant state and $\mathrm{V_1}$ is the amplitude of the small Gaussian fluctuation. Notice that $\rho_1$, $\mathrm{v_{x1}}$ and $\mathrm{P_1}$ can have any reasonably small values one desires and their ratios are not constrained. We can now project this initial state into the space of right eigenvectors by first obtaining the *eigenweights*. In other words, we wish to write $\mathrm{V_1} = \alpha^1 r^1 + \alpha^2 r^2 + \alpha^3 r^3$, which we can do if we can find $\alpha^1$, $\alpha^2$, and $\alpha^3$. The physical motivation for making this projection is that we know the dynamics of the eigenvectors, i.e. based on the Euler equations we know that each of the eigenvectors has a simple wave-like evolution in time. Thus the eigenweights are obtained by using the left eigenvectors as follows

$$\alpha^1 = \left(l^1 \bullet \mathrm{V_1}\right);\ \alpha^2 = \left(l^2 \bullet \mathrm{V_1}\right);\ \alpha^3 = \left(l^3 \bullet \mathrm{V_1}\right) \text{ which gives us } \mathrm{V_1} = \alpha^1 r^1 + \alpha^2 r^2 + \alpha^3 r^3 \tag{1.63}$$

The time evolution of the initial state in eqn. (1.62) can now be specified as follows

$$\begin{pmatrix} \rho(x,t) \\ \mathrm{v_x}(x,t) \\ \mathrm{P}(x,t) \end{pmatrix} = \begin{pmatrix} \rho_0 \\ \mathrm{v_{x0}} \\ \mathrm{P_0} \end{pmatrix} + \alpha^1 \begin{pmatrix} \rho_0 \\ -\mathrm{c_0} \\ \rho_0\ \mathrm{c_0^2} \end{pmatrix} \mathrm{e}^{-(x-\lambda_1 t)^2} + \alpha^2 \begin{pmatrix} 1 \\ 0 \\ 0 \end{pmatrix} \mathrm{e}^{-(x-\lambda_2 t)^2} + \alpha^3 \begin{pmatrix} \rho_0 \\ \mathrm{c_0} \\ \rho_0\ \mathrm{c_0^2} \end{pmatrix} \mathrm{e}^{-(x-\lambda_3 t)^2} \tag{1.64}$$

I.e. the initial Gaussian pulse propagates away as three Gaussian pulses with amplitudes given by the eigenweights and speeds given by the eigenvalues. (Our assumed linearization ensures that the waves propagate in a non-dispersive fashion. In other words, the group velocity is equal to the phase velocity, ensuring that the width of the Gaussian in this example is preserved as time evolves.) We see that eqn. (1.64) will remain valid as long as our linearization in eqn. (1.55) remains valid and the fluctuations remain small and smoothly varying. The situation is depicted in Fig. 1.9 where the left panel shows the propagation of the Gaussians when the flow is subsonic. The right panel shows the same thing as a space-time diagram. It tells us that a small fluctuation introduced at the origin only influences the shaded region that is bounded by the characteristic curves associated with the two extremal eigenvalues $\lambda^1$ and $\lambda^3$ . Such a shaded region is called the *range of influence*. It tells us that a perturbation introduced at a certain location can only influence that portion of space-time that lies within the range of influence associated with that location.

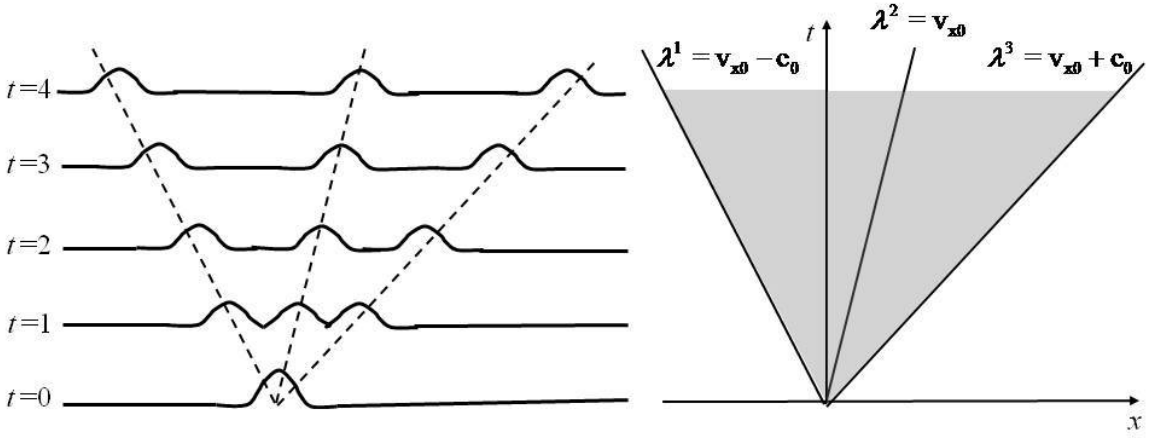


*Fig. 1.9 illustrates the concept of a range of influence. A small fluctuation that is initially Gaussian is prepared at the origin. This initial condition evolves into three smaller Gaussians that propagate away from each other. The left panel shows the propagation of the Gaussians with time increasing to the top. The right panel shows the same thing as a space-time diagram. It tells us that a small fluctuation introduced at the origin only influences the shaded region that is bounded by the two extremal characteristic curves. The shaded region is called the range of influence.*

The Euler equations are strongly non-linear. However, as long as we accept the linearization in eqn. (1.55) and only consider very small fluctuations about a constant

state, we can gain yet another very interesting insight. Fig. 1.9 has shown us that each small localized fluctuation only influences a restricted region of space-time. Thus if there are small fluctuations seeded along the x-axis then we may well ask how much of the original information along the x-axis influences a given space-time point at some future time? Consider the point $(x,t)$ with $t>0$ in Fig. 1.10. Realize that information only travels at a finite speed in a hyperbolic system. As a result, only points along the x-axis that can send information to the point of interest can influence the dynamics at that point. We see, therefore, that we have to propagate the characteristics backward in time from the point of interest to find the domain along the x-axis that influences it. This domain, which is bounded by the two extremal characteristic curves, is called the *domain of dependence*. Within the context of our linearization, the characteristic curves are straight lines and so this is easy to do. The shaded region in Fig. 1.10 identifies the domain of dependence for the point $(x,t)$ when the flow is subsonic. We see that the leftmost point in the domain of dependence for the point $(x,t)$ is obtained by tracing the fastest characteristic curve back in time. Likewise, the rightmost point in the domain of dependence for the point $(x,t)$ is obtained by tracing the slowest characteristic curve back in time.

*Fig. 1.10 illustrates the concept of a domain of dependence. We focus on the point (x,t) in the space-time diagram. Only points along the x-axis that can send information to the point of interest can influence the dynamics at that point. The shaded region, which is bounded by the two extremal characteristic curves, identifies the domain of dependence for the point (x,t).*

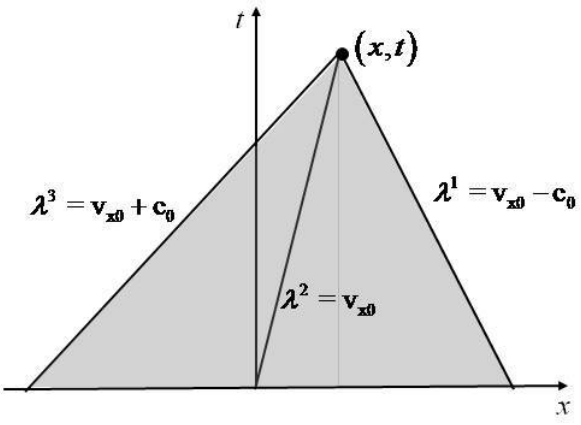


### 1.5.3) Generalized Definition of a Hyperbolic PDE

In this text we will take the Euler system as a prototypical hyperbolic system. The previous Sub-section has shown us that a study of the characteristic matrix of the Euler

system yields rich insights into its workings. It is, therefore, interesting to generalize those insights so that we may be in a good position to understand any hyperbolic system.

Several, although not all, hyperbolic systems can be written as an "*M*" component vector of conserved variables whose time-evolution is governed by similar vectors for the fluxes. Thus we can write any general *system of conservation laws* in a formal notation that will come handy later on as

$$\mathrm{U}_t + \mathrm{F}(\mathrm{U})_x + \mathrm{G}(\mathrm{U})_y + \mathrm{H}(\mathrm{U})_z = \mathrm{S}(\mathrm{U}) \tag{1.65}$$

Where "U" is the vector of conserved variables, "F", "G" and "H" are flux vectors in the x, y and z-directions and "S" is the vector of source terms. For any such system we can always derive characteristic matrices "A", "B" and "C" in the conserved variables so that we may write the above system as

$$\begin{aligned} &\mathrm{U}_t + \mathrm{A(U)}\,\mathrm{U}_x + \mathrm{B(U)}\,\mathrm{U}_y + \mathrm{C(U)}\,\mathrm{U}_z = \mathrm{S}(\mathrm{U}) \\ &\text{with} \quad \mathrm{A(U)} \equiv \frac{\partial \mathrm{F}(\mathrm{U})}{\partial \mathrm{U}} \quad ; \quad \mathrm{B(U)} \equiv \frac{\partial \mathrm{G}(\mathrm{U})}{\partial \mathrm{U}} \quad ; \quad \mathrm{C(U)} \equiv \frac{\partial \mathrm{H}(\mathrm{U})}{\partial \mathrm{U}} \end{aligned} \tag{1.66}$$

To provide an example, the *(i,j)*th element of the matrix $\mathrm{A(U)}$ is given by $\partial \mathrm{F}_i(\mathrm{U}) / \partial \mathrm{U}_j$ where $\mathrm{F}_i(\mathrm{U})$ is the *i*th component of the flux and $\mathrm{U}_j$ is the *j*th component of the vector of conserved variables. As we will see presently, the hyperbolic property can be formulated in terms of the eigenvalues and eigenvectors of characteristic matrices defined above. Note though that a PDE can be hyperbolic even if it cannot be expressed in conservation form.

As with the Euler equations it often so happens that there is another set of "*M*" variables, called the primitive variables "V", which help simplify the system of PDEs. When that happens, there exists an invertible Jacobian matrix $\partial \mathrm{U} / \partial \mathrm{V}$ which can be used

to relate any fluctuation $\delta \mathrm{U}$ to a fluctuation in the primitive variables $\delta \mathrm{V}$ . Thus we have

$$\delta \mathrm{U} = \left( \frac{\partial \mathrm{U}}{\partial \mathrm{V}} \right) \delta \mathrm{V} \quad ; \quad \delta \mathrm{V} = \left( \frac{\partial \mathrm{V}}{\partial \mathrm{U}} \right) \delta \mathrm{U} \tag{1.67}$$

The characteristic matrices and source terms in eqn. (1.66) can now be written in terms of the primitive variables as

$$\begin{aligned} &\mathrm{A(V)} \equiv \left( \frac{\partial \mathrm{V}}{\partial \mathrm{U}} \right) \frac{\partial \mathrm{F(U)}}{\partial \mathrm{U}} \left( \frac{\partial \mathrm{U}}{\partial \mathrm{V}} \right) \; ; \quad \mathrm{B(V)} \equiv \left( \frac{\partial \mathrm{V}}{\partial \mathrm{U}} \right) \frac{\partial \mathrm{G(U)}}{\partial \mathrm{U}} \left( \frac{\partial \mathrm{U}}{\partial \mathrm{V}} \right) \; ; \\ &\mathrm{C(V)} \equiv \left( \frac{\partial \mathrm{V}}{\partial \mathrm{U}} \right) \frac{\partial \mathrm{H(U)}}{\partial \mathrm{U}} \left( \frac{\partial \mathrm{U}}{\partial \mathrm{V}} \right) \; ; \quad \mathrm{S(V)} \equiv \left( \frac{\partial \mathrm{V}}{\partial \mathrm{U}} \right) \mathrm{S(U)} \end{aligned} \tag{1.68}$$

so that the hyperbolic system can be written in primitive form as

$$\mathrm{V}_t + \mathrm{A(V)}\, \mathrm{V}_x + \mathrm{B(V)}\, \mathrm{V}_y + \mathrm{C(V)}\, \mathrm{V}_z = \mathrm{S(V)} \tag{1.69}$$

The system in eqn. (1.65) can usually be analyzed more easily if it is formulated in primitive variables.

Even when a conservation form is not available for a hyperbolic system, it can always be written in a form given by eqn. (1.69). The vector "V" has "*M*" components, making eqn. (1.69) an "*M*×*M*" system. We then say that eqn. (1.69) is a *hyperbolic system* if each of its characteristic matrices "A", "B" and "C" admits "*M*" real eigenvalues and a complete set of "*M*" right eigenvectors. Furthermore, we require that all linear combinations of "A", "B" and "C" with real coefficients should also have "*M*" real eigenvalues and a complete set of "*M*" right eigenvectors. The latter property ensures that waves can propagate in any direction, not just along the directions that are aligned with the *x, y* and *z*-coordinates. The fact that a complete set of "*M*" right eigenvectors is available ensures that an orthonormal set of left eigenvectors is also available. As in the

example with the Euler system in the previous Sub-section, this ensures that any one-dimensional fluctuation can be projected into the space of right eigenvectors. Consequently, our mathematical definition ensures the important physical property that small fluctuations can at least be evolved forward for a short time in a dynamically consistent, wave-like fashion.

The previous Sub-section provided us with an extensive example drawn from the one-dimensional Euler system. It is interesting to make the connection between the Euler system and a general one-dimensional hyperbolic system. Ignoring the source term in eqn. (1.69), and retaining only the variations in the x-direction, we then have

$$\mathrm{V}_t + \mathrm{A}\,\mathrm{V}_x = 0 \tag{1.70}$$

where "A" in the above equation can be solution-dependent but is taken to be frozen at some physically realizable constant state $\mathrm{V}_0$ so that we have $\mathrm{A} \equiv \mathrm{A}(\mathrm{V}_0)$. This process of freezing the characteristic matrix can be carried out for any hyperbolic system even if it is initially non-linear and is referred to as *linearizing the hyperbolic system*. Eqn. (1.70) is analogous to eqn. (1.55). We then consider fluctuations about that constant state. The eigenvalues of the characteristic matrix can be written as an ordered sequence so that we have

$$\lambda^1 \le \lambda^2 \le \ldots \le \lambda^M \tag{1.71}$$

These eigenvalues are analogous to eqn. (1.59) for the Euler case. Analogously to eqns. (1.60) and (1.61) we can now find the right and left eigenvectors of "A". Consequently, we have the $m^{\text{th}}$ right eigenvector of "A" which satisfies $\mathrm{A}\,r^m = \lambda^m\, r^m$ and the $m^{\text{th}}$ left eigenvector of "A" which satisfies $l^m\ \mathrm{A} = l^m \lambda^m$ for all $m = 1,..,M$. The definition of the next three matrices is purely formal but yields a very useful notation that is routinely used in the study of hyperbolic systems. Fig. 1.11 schematically illustrates the structure of these three matrices. First, let "*R*" be a matrix of right eigenvectors whose $m^{\text{th}}$ column is

given by $r^m$. Because of the hyperbolic condition, "*R*" is invertible. Thus let "*L*" be the matrix of left eigenvectors whose $m^{\text{th}}$ row is given by $l^m$. Second, let the left eigenvectors be orthonormalized with respect to the right eigenvectors so that we have $L\,R = I$ where "*I*" is the identity matrix. ( If the eigenvalues are degenerate, we can always resort to Gram-Schmidt orthogonalization.) By defining our third matrix to be $\Lambda \equiv \text{diag}\left\{\lambda^1, \lambda^2, ..., \lambda^M\right\}$ we have

$$\text{A}\,R = R\,\Lambda \quad ; \quad L\,\text{A} = \Lambda\,L \quad ; \quad L\,\text{A}\,R = \Lambda \quad ; \quad \text{A} = R\,\Lambda\,L \tag{1.72}$$

The first equation in eqn. (1.72) is usually hardest for the student to comprehend and we urge the reader to verify it explicitly for each eigenvector in the matrix "*R*". I.e., go ahead and explicitly verify that the first column in $\text{A}\,R$ is just $\text{A}\,r_1$ ; then verify that the first column of $R\,\Lambda$ is just $\lambda_1\,r_1$ . Do the same for the remaining columns. It is an expression of the fact that the columns of "*R*" consist of an ordered set of right eigenvectors of "A" where the ordering is consistent with eqn. (1.71), see Fig. 1.11. The second equation in eqn. (1.72) follows from a similar consideration of the left eigenvectors, also see Fig. 1.11. The remaining two equations in eqn. (1.72) follow from the first two and the orthonormality of the left eigenvectors.

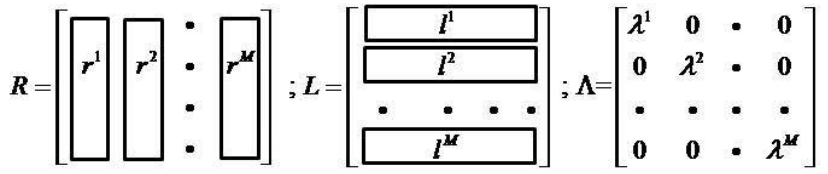


*Fig. 1.11 schematically shows the structure of the matrices R, L and Λ .*

The dynamics, i.e. the time-dependent evolution, of the hyperbolic system in eqn. (1.70) is obtained by first assuming a constant state $\text{V}_0$ along with small fluctuations $\text{V}_1$ about the constant state. The constant state satisfies eqn. (1.70) trivially by virtue of its constancy; eqn. (1.70) for the fluctuations becomes $\left(\text{V}_1\right)_t + \text{A}\left(\text{V}_1\right)_x = 0$. Consider the vector of eigenweights defined by $W \equiv L\,\text{V}_1$ and take the matrix *L* to be a constant, consistent with our assumption of linearization. It is easiest to find a time-evolutionary

equation for the vector of eigenweights "*W*" and then relate it to the time evolution of $\mathrm{V}_1$. Toward that goal, left multiply eqn. (1.70) by "*L*" to get

$$L\ \frac{\partial \mathrm{V}_1}{\partial t} + \left(L\ \mathrm{A}\ R\right)\ L\ \frac{\partial \mathrm{V}_1}{\partial x} = 0 \qquad \Rightarrow \qquad W_t + \Lambda\ W_x = 0 \tag{1.73}$$

Because $\Lambda$ is diagonal, each component of $W_t + \Lambda\ W_x = 0$ evolves independently of the other. Thus denoting the $m^{\text{th}}$ component of "*W*" by $w^m$, we get an evolutionary equation for the $m^{\text{th}}$ eigenweight that is given by

$$w_t^m + \lambda^m w_x^m = 0 \quad \text{for } m = 1,...,M \tag{1.74}$$

The above equation gives us the useful insight that the eigenweight associated with each wave family propagates with the corresponding eigenvalue.

Say that we are given initial conditions at $t = 0$ that are specified by a general position-dependent vector $\mathrm{V}_0 + \mathrm{V}_1\left(x\right)$, where $\mathrm{V}_1\left(x\right)$ is a very small fluctuation about the constant state $\mathrm{V}_0$. We can define the spatial variation of its $m^{\text{th}}$ eigenweight at $t = 0$ by $w^m\left(x\right) \equiv l^m \bullet \mathrm{V}_1\left(x\right)$. These eigenweights are analogous to eqn. (1.63). The $m^{\text{th}}$ eigenweight evolves according to eqn. (1.74) so that at a slightly later time $t > 0$ it is given by $w^m\left(x - \lambda^m t\right)$. The entire time-dependent solution at a slightly later time can now be written as

$$\mathrm{V}\left(x,t\right) = \mathrm{V}_0 + \sum_{m=1}^{M} w^m\left(x - \lambda^m t\right)\ r^m \tag{1.75}$$

The above equation should be compared to eqn. (1.64). In fact, this Sub-section closely mirrors the previous one, casting the development in general terms for any hyperbolic problem. Please note that in writing eqn. (1.75) we have implicitly assumed that the

system is not dispersive, i.e. the wave speed $\lambda^m$ does not vary with the wavelength of the impressed fluctuations. For a non-linear hyperbolic PDE we have to assume a linearization around a constant state to obtain this non-dispersive property. When non-linearities are included, eqn. (1.75) only holds for an infinitesimally short time after $t = 0$ and we additionally have to assume that $\mathrm{V}_1(x)$ is a smooth function. The theory leading up to eqn. (1.75) is important though because it is a very useful building block in many numerical schemes for solving hyperbolic PDEs.

As in the previous Sub-section, the extremal eigenvalues can be used to define the range of influence and domain of dependence for the PDE in space-time. The next several sections will give us numerous examples of PDEs, many of which have predominantly hyperbolic terms.

### 1.5.4) Analysis of the Navier Stokes Equations

Section 1.5.2 showed us how the wave modes of the Euler equations can be analyzed. We have seen that the Navier Stokes equations have non-ideal terms which make them parabolic. The non-ideal terms, like the viscosity and thermal conduction operators, have second derivatives in space, which changes their character. For a general PDE, the character of the eigenmodes that it will support has to be analyzed on a case-by-case basis. In this section we show how the eigenvalues and eigenvectors can be used to reveal the parabolic nature of the Navier Stokes equations.

As before, we restrict our focus to one dimension. We also assume that the coefficients of viscosity and thermal conduction are constant. A polytropic gas is also assumed, see eqn. (1.2). The density and x-velocity are our first two primitive variables and are governed by one-dimensional specializations of eqns. (1.22) and (1.29). The viscous tensor is given by eqn. (1.46) with the bulk viscosity set to zero. Because the flux of thermal conduction is written in terms of the temperature in eqn. (1.47), we prefer to use the temperature as our third primitive variable. Eqn. (1.37) gives us the evolution of

the temperature. The resulting one-dimensional equations for the evolution of density, x-velocity and temperature then become:

$$\begin{aligned}
&\frac{\partial \rho}{\partial t} + \mathrm{v_x}\frac{\partial \rho}{\partial x} + \rho\frac{\partial \mathrm{v_x}}{\partial x} = 0 \\
&\frac{\partial \mathrm{v_x}}{\partial t} + \mathrm{v_x}\frac{\partial \mathrm{v_x}}{\partial x} + \frac{R\,\mathrm{T}}{\bar{\mu}\,\rho}\frac{\partial \rho}{\partial x} + \frac{R}{\bar{\mu}}\frac{\partial \mathrm{T}}{\partial x} - \frac{4\mu}{3\rho}\frac{\partial^2 \mathrm{v_x}}{\partial x^2} = 0 \\
&\frac{\partial \mathrm{T}}{\partial t} + \mathrm{v_x}\frac{\partial \mathrm{T}}{\partial x} + (\Gamma - 1)\,\mathrm{T}\frac{\partial \mathrm{v_x}}{\partial x} - \frac{4(\Gamma-1)\bar{\mu}\,\mu}{3\,R}\left(\frac{\partial \mathrm{v_x}}{\partial x}\right)^2 - \frac{(\Gamma-1)\kappa\,\bar{\mu}}{R}\frac{\partial^2 \mathrm{T}}{\partial x^2} = 0
\end{aligned} \tag{1.76}$$

Analogous to eqn. (1.56), we linearize the above system about a constant state as follows

$$\begin{pmatrix} \rho(x,t) \\ \mathrm{v_x}(x,t) \\ \mathrm{T}(x,t) \end{pmatrix} = \begin{pmatrix} \rho_0 \\ \mathrm{v_{x0}} \\ \mathrm{T_0} \end{pmatrix} + \begin{pmatrix} \rho_1 \\ \mathrm{v_{x1}} \\ \mathrm{T_1} \end{pmatrix} \mathrm{e}^{\,i\,(\mathrm{k\,x} - \omega\,\mathrm{t})} \tag{1.77}$$

Notice that the viscosity is quadratic in the velocity gradient for the third equation in eqn. (1.76). Consequently, after linearization, the viscosity does not contribute to that equation. As before, we define $\lambda \equiv \omega/k$. When eqn. (1.77) is substituted in eqn. (1.76) the linearized system becomes

$$\begin{pmatrix} \mathrm{v_{x0}} - \lambda & \rho_0 & 0 \\ \dfrac{R\mathrm{T_0}}{\bar{\mu}\rho_0} & \mathrm{v_{x0}} - \lambda - i\,\mathrm{k}\dfrac{4\mu}{3\rho_0} & \dfrac{R}{\bar{\mu}} \\ 0 & (\Gamma-1)\mathrm{T_0} & \mathrm{v_{x0}} - \lambda - i\,\mathrm{k}\dfrac{(\Gamma-1)\kappa\bar{\mu}}{R} \end{pmatrix} \begin{pmatrix} \rho_1 \\ \mathrm{v_{x1}} \\ \mathrm{T_1} \end{pmatrix} = 0 \tag{1.78}$$

As before, setting the determinant of the previous matrix to zero gives us the eigenvalues of the system. We see though that when the viscosity and conductivity are both non-zero, the equation for the eigenvalues is a cubic. While the cubic is easily solved by using a

symbolic manipulation package, we prefer to focus on the somewhat simpler case where $\kappa = 0$ because it is equally instructive. The eigenvalues are now given by

$$\lambda_1 = \mathrm{v}_{x0} - \sqrt{\mathrm{c}_0^2 - \mathrm{k}^2 \frac{4\mu^2}{9\rho_0^2}} - i\,\mathrm{k}\,\frac{2\mu}{3\rho_0} \quad ; \quad \lambda_2 = \mathrm{v}_{x0} \quad ; \quad \lambda_3 = \mathrm{v}_{x0} + \sqrt{\mathrm{c}_0^2 - \mathrm{k}^2 \frac{4\mu^2}{9\rho_0^2}} - i\,\mathrm{k}\,\frac{2\mu}{3\rho_0} \tag{1.79}$$

The above equations show us that for a real value of the wavenumber "k", the angular frequency "$\omega$" of the sound waves will have a real and imaginary part. From the real part of "$\omega$" we observe that the sound waves have become dispersive; i.e., the propagation speed depends on the wavenumber. This is a trend that we usually find when non-ideal terms are included. As the wavelength decreases, i.e. as the wavenumber increases, the viscous stresses begin to dominate. Eqn. (1.79) therefore shows that short wavelength sound waves propagate slower than long wavelength sound waves. When the wavelength becomes comparable to the mean free path of molecules in the gas, the waves stop propagating. More importantly, we observe that the above eigenvalues for the sound waves have an imaginary part. The imaginary part of "$\omega$" shows us that the waves in eqn. (1.77) decay in time due to the effect of the viscous stresses. The inclusion of parabolic terms in the system case is quite analogous to their effect in the scalar eqns. (1.51) and (1.54).

Realize from the above discussion that the fluxes for the Navier Stokes equations include gradients of the flow variables. Contrast this with the fluxes for the Euler equations which did not include such gradients. In order to generalize the idea, we can indicate that a system is parabolic by writing it as

$$\mathrm{U}_t + \mathrm{F}(\mathrm{U})_x + \mathrm{G}(\mathrm{U})_y + \mathrm{H}(\mathrm{U})_z + \mathrm{F}_{ni}(\mathrm{U},\nabla\mathrm{U})_x + \mathrm{G}_{ni}(\mathrm{U},\nabla\mathrm{U})_y + \mathrm{H}_{ni}(\mathrm{U},\nabla\mathrm{U})_z = \mathrm{S}(\mathrm{U}) \tag{1.80}$$

We see that the non-ideal fluxes $\mathrm{F}_{ni}$ , $\mathrm{G}_{ni}$ and $\mathrm{H}_{ni}$ in general depend on the vector of conserved variables and its gradients. This renders the PDE parabolic, but only if the resulting system yields temporally decaying solutions on further analysis.

In the most general situation, a PDE may have third or higher spatial derivatives of a physical variable. The dispersion and dissipation characteristics for such a system will then have to be studied on a case-by-case basis. It becomes difficult to provide general purpose numerical solution strategies for such situations.

### 1.6) Incompressible Flow Equations

In several circumstances a fluid may be almost incompressible, i.e. the density is practically constant. For example, a liquid like water is incompressible to a very good approximation. Gases can also behave as if they are incompressible when they flow at speeds that are much smaller than their sound speed. In such situations, the role of sound waves is mainly to propagate rapidly and smooth out the density fluctuations that would otherwise arise. While such problems can indeed be solved by the Euler or Navier-Stokes equations, it is not economical to do so for the following reason. The numerical method has to capture the propagation of sound waves even though the only role of these waves is to ensure the incompressible nature of the flow. For such problems, capturing fast-moving features, such as sound waves, only decreases the timestep in the computation thus making the overall computation more expensive. In such situations, it is very advantageous to resort to the *incompressible approximation* because the flow speed, and not the sound speed, limits the timestep in that approximation. We therefore formulate the equations for incompressible flow in the next paragraph.

Thus imagine a situation where the density does not vary in the Euler equations. The continuity equation then yields

$$\nabla \bullet \mathbf{v} = 0 \tag{1.81}$$

showing that we do not need an evolutionary equation for the density because the density is known. Recall that the propagation of sound waves requires density fluctuations. Consequently, when the density is set to a constant value, the sound waves cease to be

part of the wave structure that is supported by our equations. The incompressible approximation instead provides a constraint on the velocity field, see eqn. (1.81). The momentum equation becomes

$$\frac{\partial \mathbf{v}}{\partial t} + \mathbf{v} \bullet \nabla \mathbf{v} = -\frac{1}{\rho} \nabla P \tag{1.82}$$

Taking the divergence of the above equation and using the incompressibility condition from eqn. (1.81) then yields an elliptic equation for the pressure

$$\nabla^2 P = -\rho \nabla \bullet \left( \mathbf{v} \bullet \nabla \mathbf{v} \right) \tag{1.83}$$

Thus the above equation tells us that the pressure satisfies an elliptic equation whose right hand side depends on the flow velocity. The left hand side of eqn. (1.82) forms a hyperbolic system with the gradient of the pressure providing a source term. Since the density is constant and the pressure is specified from eqn. (1.82) there is no particular need to evolve the thermal energy equation if one is solving a fluid dynamics problem without any sources of heat. Note, however, that depending on the boundary conditions, eqn. (1.83) may only provide a solution for the pressure up to a constant. If the problem involves reactive flow, where chemical reactions can generate energy, the internal energy equation can be evolved in conjunction with eqn. (1.82). In the simplest form of the incompressible flow equations discussed here, the energy equation drops out of the equation set and eqns. (1.82) and (1.83) are the only equations that need to be evolved.

### 1.7) The Shallow Water Equations

The *shallow water equations* arise when treating geophysical flows in lakes and oceans. They have also been used for predicting the formation of tsunamis. The water in the oceans constitutes a thin layer of incompressible fluid on the earth's surface. Thus it can be treated as a two-dimensional problem, which we study in the xy-plane for simplicity. Fig. 1.12 shows a schematic diagram showing the flow of water waves in a

lake with a spatially varying bottom. Because the problem is incompressible, we can ignore the energy equation for the simplest version of this problem. The equations have also been formulated in coordinate systems that can be mapped to a sphere but we keep things simple here. The bottom of the ocean varies in the xy-plane so that we represent the bottom as a two-dimensional surface $z_{bottom} = -\,\mathrm{h}(x,y)$ which does not change with time. The top of the ocean's surface is of interest to us so that we want to keep track of $z_{top} = \eta(x,y,t)$ which is allowed to change with time. The details of the z-velocity are not important to us though so that one can set the Lagrangian derivative of the z-velocity to zero along with suitable considerations for the z-velocity at the upper and lower boundary. This can be intuitively understood by realizing that the ebb and flow of tides in the ocean is a slow process and does not generate an appreciable z-velocity. As a result, the z-momentum equation drops out of the set of equations being evolved. Consequently, we are only interested in evolutionary equations for the x and y-velocities. Gravity acts in the z-direction with the result that there is a gravitational potential associated with the column of fluid. In geophysics, $\phi(x,y,t) = g\left(\eta(x,y,t) + h(x,y)\right)$, which is referred to as the *geopotential*, becomes one of the variables of interest and an evolutionary equation can be derived for it. Here "*g*" is the gravitational acceleration. The details of the derivation can be found in the text by Faber (1995) and are not repeated here. The shallow water equation set can be written in flux conservative form as

$$\frac{\partial}{\partial t}\begin{bmatrix} \phi \\ \phi\ \mathrm{v_x} \\ \phi\ \mathrm{v_y} \end{bmatrix} + \frac{\partial}{\partial x}\begin{bmatrix} \phi\ \mathrm{v_x} \\ \phi\ \mathrm{v_x^2} + \phi^2/2 \\ \phi\ \mathrm{v_x}\ \mathrm{v_y} \end{bmatrix} + \frac{\partial}{\partial y}\begin{bmatrix} \phi\ \mathrm{v_y} \\ \phi\ \mathrm{v_x}\ \mathrm{v_y} \\ \phi\ \mathrm{v_y^2} + \phi^2/2 \end{bmatrix} = \begin{bmatrix} 0 \\ g\ \phi\ \partial_x h \\ g\ \phi\ \partial_y h \end{bmatrix} \tag{1.84}$$

The above equation shows that when the bottom of the lake or ocean is changing, i.e. when we have varying bathymetry, source terms are inevitable and we will have to develop methods that incorporate them.

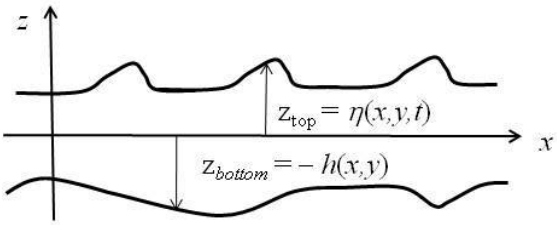


*Fig. 1.12 is a schematic diagram showing the propagating of water waves in the shallow water approximation. The top surface of the water and the bottom of the lake/ocean are shown in cross-section in the x-z plane.*

The shallow water equations can be written in primitive form as

$$\frac{\partial}{\partial t}\begin{bmatrix}\phi\\ v_x\\ v_y\end{bmatrix}+\begin{bmatrix}v_x & \phi & 0\\ 1 & v_x & 0\\ 0 & 0 & v_x\end{bmatrix}\frac{\partial}{\partial x}\begin{bmatrix}\phi\\ v_x\\ v_y\end{bmatrix}+\begin{bmatrix}v_y & 0 & \phi\\ 0 & v_y & 0\\ 1 & 0 & v_y\end{bmatrix}\frac{\partial}{\partial y}\begin{bmatrix}\phi\\ v_x\\ v_y\end{bmatrix}=\begin{bmatrix}0\\ g\,\partial_x h\\ g\,\partial_y h\end{bmatrix} \qquad (1.85)$$

The x-directional shallow water equations form a hyperbolic system with three waves. One of the waves propagates with the flow velocity $v_x$ while the other two propagate with speeds given by $v_x \pm \sqrt{\phi}$. The waves that propagate with speeds $\pm\sqrt{\phi}$ relative to the fluid velocity are called *gravity waves* because they are driven by the hydrostatic pressure resulting from gravity.

**1.8) Maxwell's Equations**

The equations of electrodynamics, also known as *Maxwell's equations,* govern the evolution of electric and magnetic fields in response to charges and currents. Their numerical solution is very useful when dealing with a diverse range of technological problems. These problems include nonlinear optics which is very useful when transmitting information over fiber optic cables. Numerical solution of Maxwell's equations is also very important in electromagnetic scattering, which is used in designing stealth aircraft. An extensive discussion of Maxwell's equations is given in the text by Jackson (1998).

In Gaussian units Maxwell's equations can be written as

$$\frac{\partial \mathbf{B}}{\partial t} + c\,\nabla \times \mathbf{E} = 0$$
$$\frac{\partial \mathbf{D}}{\partial t} - c\,\nabla \times \mathbf{H} = -4\,\pi\,\mathbf{J} \qquad (1.86)$$
$$\nabla \bullet \mathbf{D} = 4\,\pi\,\rho$$
$$\nabla \bullet \mathbf{B} = 0$$

Here "*c*" is the speed of light in vacuum. We see that the charge density $\rho$ and the vector of current density $\mathbf{J}$ provide the right hand side for these equations. As written, we see that only the first two equations for the magnetic induction vector $\mathbf{B}$ and the electric displacement vector $\mathbf{D}$ are evolutionary whereas the magnetic field vector $\mathbf{H}$ and electric field vector $\mathbf{E}$ need further specification. The first, second and third of the equations in eqn. (1.86) are popularly referred to as Faraday's law, the generalized Ampere's law and Gauss's law respectively. In vacuum we have $\mathbf{B} = \mathbf{H}$ and $\mathbf{D} = \mathbf{E}$ . In material media the three dimensional vectors $\mathbf{B}$ and $\mathbf{H}$ can be related via a 3×3 tensor which may be non-linear. Similarly, the three dimensional vectors $\mathbf{D}$ and $\mathbf{E}$ can also be related via a 3×3 tensor which may also be non-linear. In such situations Maxwell's equations can develop strong non-linearities. We restrict ourselves to simple material media where the following simple constitutive relationship holds

$$\mathbf{B} = \mu\,\mathbf{H} \quad ; \quad \mathbf{D} = \varepsilon\,\mathbf{E} \qquad (1.87)$$

where $\mu$ is the *magnetic permeability* and $\varepsilon$ is the *permittivity* and both are often assumed to be constant scalars, for the sake of simplicity. In general, $\mu$ and $\varepsilon$ can be rank two tensors.

With the previous constitutive relationships, the first two of Maxwell's equations become

$$\frac{\partial \mathbf{H}}{\partial t} + \frac{c}{\mu} \nabla \times \mathbf{E} = 0$$
$$\frac{\partial \mathbf{E}}{\partial t} - \frac{c}{\varepsilon} \nabla \times \mathbf{H} = - \frac{4 \pi}{\varepsilon} \mathbf{J} \qquad (1.88)$$

We see from eqn. (1.88) that we can now evolve these equations for the electric and magnetic fields. However, we have also to pay attention to the latter two equations in eqn. (1.86). In particular, the magnetic field evolves according to $\nabla \bullet \mathbf{B} = 0$ which means that the magnetic field starts off divergence-free and remains so forever. In other words, the components of the magnetic field are not unconstrained and, in fact, they have to satisfy a divergence-free constraint. Much attention has been devoted to satisfying this constraint in numerical codes, see Yee (1966). However, an alternative viewpoint has been to permit the divergence of the magnetic field to develop and to then sweep it out of the domain of interest using a modified form of the Maxwell's equations, see Munz *et al*. (2000).

A few other points are worth making. First, in conducting media, the current density can be related to the electric field via a constitutive relation $\mathbf{J} = \sigma \mathbf{E}$ where the *conductivity* $\sigma$ is taken to be a constant for the sake of simplicity. Second, while the electric field is a vector, the magnetic field is a pseudovector. Amongst other things, this influences the selection of boundary conditions. The boundary conditions that are used in treating Maxwell's equations can be quite different from those that are used in fluid dynamics and it is best to look up Jackson (1998) for details on boundary conditions. Lastly, when treating problems involving electromagnetic scattering it is traditional to split the waves into an incoming part, which is known, and an outgoing part, which has to be evolved. For such problems, the incoming part contributes further terms to the right hand side of eqn. (1.88), see Hesthaven and Warburton (2002).

Despite the above-mentioned complexities that one has to pay attention to, eqn. (1.88) is simple because it describes a linear system. Thus one does not need to deal with any of the difficulties associated with non-linearities. We can now study the x-directional

propagation of waves by writing eqn. (1.88) without source terms in a form that makes its characteristic matrix explicit. We have

$$\frac{\partial}{\partial t}\begin{pmatrix} E_x \\ E_y \\ E_z \\ B_x \\ B_y \\ B_z \end{pmatrix} + \begin{pmatrix} 0 & 0 & 0 & 0 & 0 & 0 \\ 0 & 0 & 0 & 0 & 0 & c/\varepsilon \\ 0 & 0 & 0 & 0 & -c/\varepsilon & 0 \\ 0 & 0 & 0 & 0 & 0 & 0 \\ 0 & 0 & -c/\mu & 0 & 0 & 0 \\ 0 & c/\mu & 0 & 0 & 0 & 0 \end{pmatrix} \frac{\partial}{\partial x}\begin{pmatrix} E_x \\ E_y \\ E_z \\ B_x \\ B_y \\ B_z \end{pmatrix} = 0 \qquad (1.89)$$

The eigenvalues reveal a set of four waves, two of which propagate to the right with speed $c/\sqrt{\varepsilon\mu}$ and the other two propagate to the left with speed $-c/\sqrt{\varepsilon\mu}$. Notice, however, that two of the eigenvectors of eqn. (1.89) cannot be constrained simply by appeal to hyperbolic systems theory. The latter two non-evolutionary equations in eqn. (1.86) have to be drawn on to constrain these terms. It is also this freedom that is exploited in modifying Maxwell's equations so that any divergence that builds up is convected away.

The propagating eigenvectors from eqn. (1.89) also have a very interesting structure. Without writing them out explicitly, it is worth mentioning that the electric and magnetic fields remain orthogonal to each other and also to the direction of propagation. I.e. electromagnetic waves are strictly transverse waves. See Fig. 1.8 for a definition of transverse waves and Fig. 1.13 for an illustration of a rightward-propagating electromagnetic wave.

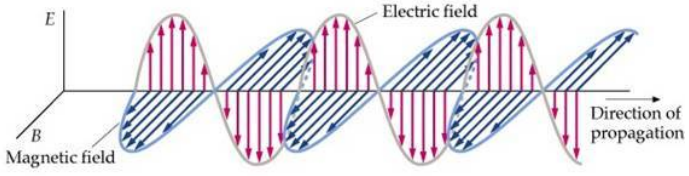


*Fig. 1.13 shows a schematic diagram of an electromagnetic wave. Notice that the electric and magnetic fields are orthogonal to each other. Furthermore, both fields are orthogonal to the direction of propagation.*

## 1.9) The Magnetohydrodynamic Equations

Gases that are heated to high enough temperatures become fully or partially ionized. Examples include terrestrial fusion experiments, the interiors or stars, the solar wind and the magnetospheres of planets and stars. In many such situations, the object is large enough and the resistivity small enough that magnetic fields can thread through the ionized plasma. The magnetic field vector, which we denote here as $\mathbf{B}$, then becomes a full participant in the fluid's dynamics. Because the charged particles spiral around the magnetic field lines, the matter and the magnetic field often become tightly coupled. Various approximations then become possible, often depending on the level of isotropy in the pressure tensor. One of the simplest and most well-studied approximations is based on assuming an isotropic pressure tensor and is called *magnetohydrodynamics* (MHD). Because the MHD equations are of such great importance in nuclear fusion research, plasma physics, solar physics, space physics and astrophysics, we will present them here. While there are several excellent texts on MHD in each of these disciplines, the text that is closest to a hyperbolic systems approach is the one by Jefferey and Taniuti (1964).

When a plasma is treated in the MHD approximation, it is still represented as a fluid. Thus it should continue to have a continuative equation, eqn. (1.22). The first law of thermodynamics also continues to hold so that the internal energy equation, at least as it is represented by eqn. (1.36), also continues to hold. Remember though that thermal conduction can assume a considerably more complicated form in a dilute plasma. We assume that we are treating the plasma on large enough length scales that the plasma is electrically neutral in its rest frame. I.e., all local charge imbalances are rapidly neutralized. We also assume that we wish to study the plasma on large enough time scales so that the displacement current, the $\partial\mathbf{D}/\partial t$ term in eqn. (1.86) is negligible. Together these two assumptions yield the *MHD approximation*. We will see that the MHD approximation implicitly results in assuming that in the limit of infinite conductivity the electric field is effectively zero *in the plasma's rest frame*. Because magnetic fields are strongly coupled to the fluid, which can indeed move, there will be a motional EMF. Consequently, the momentum equation will also be susceptible to body

forces stemming from the Lorentz force $\left(\mathbf{J}\times\mathbf{B}\right)/c$. Here $\mathbf{J}$ is the current density and "*c*" is the speed of light. Modifying eqn. (1.29) to include the Lorentz force then gives us the momentum equation in the MHD approximation as

$$\rho\frac{D\,\mathbf{v}}{D\,t} = -\nabla\,\mathrm{P} + \frac{1}{c}\left(\mathbf{J}\times\mathbf{B}\right) + \vec{\nabla}\pi \tag{1.90}$$

Here the $i^{\text{th}}$ component of $\vec{\nabla}\pi$ is given by $\partial_j\pi_{ij}$ . We will see shortly that there is a more convenient form for the above equation once the MHD approximation is utilized.

We also need an evolutionary equation for the magnetic field. To that end, we modify Maxwell's equations consistent with our previous description of the MHD approximation to get

$$\begin{aligned}&\frac{\partial\mathbf{B}}{\partial t} + c\,\nabla\times\mathbf{E} = 0\\ &\mathbf{J} = \frac{c}{4\,\pi}\,\nabla\times\mathbf{B}\end{aligned} \tag{1.91}$$

All we need to close the system formed by eqns. (1.90) and (1.91) is a constitutive relation for the current $\mathbf{J}$ . In the fluid's rest frame, such a relation is provided by Ohm's law which says that $\mathbf{J}^{/} = \sigma\,\mathbf{E}^{/}$. Here the primed quantities are the current density and electric field in the fluid's rest frame. The non-relativistic transformation of the current density $\mathbf{J}^{/}$ and electric field $\mathbf{E}^{/}$ from the fluid's rest frame to a frame where the fluid moves with a velocity $\mathbf{v}$ can then be written as

$$\mathbf{J}^{/} = \mathbf{J} \quad ; \quad \mathbf{E}^{/} = \mathbf{E} + \frac{1}{c}\left(\mathbf{v}\times\mathbf{B}\right) \tag{1.92}$$

Ohm's law, written in terms of the variables in an Eulerian frame of reference, then gives

$$\mathbf{J}' = \sigma\, \mathbf{E}' \quad \Rightarrow \quad \mathbf{J} = \sigma \left( \mathbf{E} + \frac{1}{c}\, \mathbf{v}\times\mathbf{B} \right) \quad \Rightarrow \quad \mathbf{E} = -\frac{1}{c}\, \mathbf{v}\times\mathbf{B} + \frac{c}{4\pi\sigma}\, \nabla\times\mathbf{B} \qquad (1.93)$$

where the second equation from eqn. (1.91) was used to obtain the last equation in (1.93). In the ideal limit, where the conductivity is infinite, we see that the electric field is just the motional term $-\left(\mathbf{v}\times\mathbf{B}\right)/c$ . Consequently, in that same limit, the electric field in the plasma's rest frame is exactly zero. Substituting the above electric field into Faraday's law , the first equation in eqn. (1.91), then yields

$$\frac{\partial \mathbf{B}}{\partial t} = \nabla\times\left(\mathbf{v}\times\mathbf{B}\right) + \frac{c^2}{4\pi\sigma}\, \nabla^2\mathbf{B} \qquad (1.94)$$

which is the evolutionary equation for the magnetic field in a resistive plasma.

Now that the equations associated with the MHD approximation have been built up, we can obtain a further simplification of the momentum equation, eqn. (1.90). This is achieved by simplifying the Lorentz force term as follows

$$\frac{1}{c}\left(\mathbf{J}\times\mathbf{B}\right) = -\frac{1}{4\pi}\, \mathbf{B}\times\left(\nabla\times\mathbf{B}\right) = -\nabla\left(\frac{\mathbf{B}^2}{8\pi}\right) + \frac{1}{4\pi}\, \left(\mathbf{B}\bullet\nabla\right)\mathbf{B} \qquad (1.95)$$

The momentum equation then yields

$$\rho \frac{D\,\mathbf{v}}{D\,t} = -\nabla\left( \mathrm{P} + \frac{\mathbf{B}^2}{8\pi} \right) + \frac{1}{4\pi}\, \left(\mathbf{B}\bullet\nabla\right)\mathbf{B} + \vec{\nabla}\pi \qquad (1.96)$$

The above equation shows us that the magnetic energy density, $\mathbf{B}^2/8\pi$ , also contributes as a pressure term. However, the term $\left(\mathbf{B}\bullet\nabla\right)\mathbf{B}/4\pi$ has the structure of a tensional term. Thus the magnetic fields can also exert tension forces along their length, quite the way a taut rubber band can. Fig. 1.14 illustrates how magnetic fields in a plasma can

provide pressure and tensional forces. Just as transverse waves can be set up in a taut rubber band, we can show that transverse waves, known as *Alfven waves*, can be set up in a magnetized plasma. A problem at the end of this chapter gives a mechanistic way of deriving the tension in the magnetic field and, from it, the speed of Alfven waves. In due time we will show that the Alfven speed can also be derived from rigorous characteristic analysis.

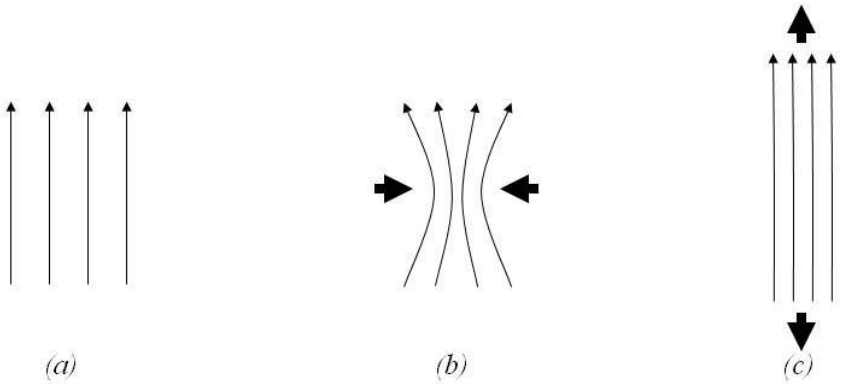


*Fig. 1.14a shows the original configuration of the magnetic field. Fig. 1.14b illustrates how the magnetic pressure might be built up in response to compression while Fig. 1.14c shows how magnetic tension is produced.*

Eqns. (1.22), (1.96), (1.36) and (1.94) constitute the full set of MHD equations in primitive form. Without the viscous and resistive terms they form the equations of ideal MHD. The ideal MHD equations can be written as

$$
\begin{aligned}
&\frac{\partial \rho}{\partial t} + \frac{\partial}{\partial x_i}\left(\rho\, \mathrm{v}_i\right) = 0 \\
&\frac{\partial}{\partial t}\left(\rho \mathrm{v}_i\right) + \frac{\partial}{\partial x_j}\left(\rho \mathrm{v}_i \mathrm{v}_j + \left(\mathrm{P} + \mathbf{B}^2/8\pi\right)\,\delta_{ij} - \mathrm{B}_i\,\mathrm{B}_j/4\pi\right) = 0 \\
&\frac{\partial\, \mathcal{E}}{\partial t} + \frac{\partial}{\partial x_i}\left(\left(\mathcal{E} + \mathrm{P} + \mathbf{B}^2/8\pi\right)\,\mathrm{v}_i - \mathrm{B}_i\left(\mathbf{v}\cdot\mathbf{B}\right)/4\pi\right) = 0 \\
&\frac{\partial \mathbf{B}}{\partial t} = \nabla\times\left(\mathbf{v}\times\mathbf{B}\right)
\end{aligned}
\qquad (1.97)
$$

The above equations can be cast into a form that looks very much like a conservation law. Here $\mathcal{E}$ is the total energy density and "P" is the pressure. For gas with a polytropic index $\Gamma$ we get

$$\mathcal{E} = \mathrm{e} + \frac{1}{2}\rho\,\mathbf{v}^2 + \frac{\mathbf{B}^2}{8\pi} \quad \text{with} \quad \mathrm{e} \equiv \frac{\mathrm{P}}{(\Gamma - 1)} \tag{1.98}$$

which shows that the magnetic energy density also contributes to the total energy density. The divergence-free constraint, $\nabla \bullet \mathbf{B} = 0$, also holds and Faraday's law, i.e. the last equation in eqn. (1.97) ensures that if it holds initially, it will hold forever.

The ideal MHD system can be shown to be hyperbolic. Its *x*-directional restriction yields seven waves: a left-going fast magnetosonic wave, a left-going Alfven wave, a left-going slow magnetosonic wave, an entropy wave, a right-going slow magnetosonic wave, a right-going Alfven wave and a right-going fast magnetosonic wave. The magnetosonic waves are longitudinal waves and cause compressions and rarefactions in the plasma. The Alfven waves are transverse waves and propagate without causing any change in the plasma density. The divergence-free constraint, $\nabla \bullet \mathbf{B} = 0$, ensures that the *x*-component of the magnetic field does not evolve when variations are restricted to the *x*-direction. We, therefore, see that the presence of a constraint reduces the number of waves in both Maxwell's equations and the MHD equations.

One can also find eigenvectors associated with the eigenvalues of the MHD system. The eigenvectors prove to be very valuable for numerical work. However, it is worth pointing out that under certain conditions the eigenvalues can become degenerate. In such situations the eigenvectors provided in Jefferey and Taniuti (1964) are known to become singular, diminishing their value in numerical work. With an appropriate normalization, Roe and Balsara (1996) have shown that the eigenvector degeneracy can be rectified. As a result, powerful numerical methods have been developed for numerical MHD.

### 1.10) Flux Limited Diffusion Radiation Hydrodynamics

There have been attempts to treat the radiation field that interacts with matter as a fluid that is made up of photons, leading to *radiation hydrodynamics*, see texts by

Mihalas and Wiebel-Mihalas (1999) and Castor (2004). The challenges inherent in formulating radiation hydrodynamics stem from the fact that in most systems of interest the photons can have a substantially longer mean free path than the atoms. In the radiation hydrodynamic equations, the radiation pressure tensor is obtained by taking the second moment of the radiation field, just as the gas pressure is obtained by taking the second moment of the distribution of material particles. For gases the small mean free path makes it easy to assume that the gas pressure is isotropic and to relate it to the other thermodynamic variables, leading to a closure in the Euler equations. Because the photons often do not have a small mean free path, the radiation pressure tensor ceases to be isotropic and it becomes difficult to relate the radiation pressure tensor to the other radiation variables. In other words, there is a difficulty in obtaining closure for the radiation hydrodynamics equations.

The *flux limited diffusion approximation* does not solve the above-mentioned problem. However, it does make the equations simpler and more tractable. As its name suggests, it works best when the photons diffuse through the material particles, i.e. when the photon mean free path is small compared to the system being studied. This limit is referred to as the *optically thick regime* and usually obtains when the matter density is large enough to obstruct the free streaming of the radiation. However, in many systems of interest, such as the atmosphere of a star, the matter density can transition over several orders of magnitude. Consequently, the photons begin to stream freely when the matter is not dense enough to hold them down. This limit, where the mean free path of the photons becomes comparable to or larger than the size of the system being studied, is called the *optically thin regime*. The flux limited diffusion approximation is certainly not valid in the optically thin regime. However, there are several systems where there is a great interest in understanding the diffusion of radiation in regions that are optically thick. In such systems the only requirement one might make for situations where the matter becomes optically thin is that the representation of the radiation field should graciously break down without doing any damage to the denser regions that are indeed of scientific interest. The flux limited diffusion approximation is designed to help us out in such situations. The utility of the approximation stems from the fact that there exist several

systems where the point of scientific interest conforms to its limitations. A modern derivation of the flux limited diffusion radiation hydrodynamics has been provided in Krumholz *et al.* (2007) and we will not repeat it here. We simply state the equations with explanations.

The flux limited diffusion approximation consists of asserting that the radiation energy density, defined by "E", is the primary quantity of interest. To define an equation that governs the dynamics of the radiation field one would, of course, need to define a radiation flux, labeled "**F**", as well as a radiation pressure tensor, represented by "**P**". The philosophy underlying the flux limited diffusion approximation is that the radiation flux in a fluid's rest frame can be written as a gradient of the radiation energy density. However, photons that are trapped by a dense parcel of gas can also be advected along by the gas velocity $\mathbf{v}$, providing another component to the radiation flux when it is measured in a frame that is not comoving with the fluid. Thus the flux vector is written as

$$\mathbf{F} = -\frac{c\lambda}{\kappa_{0R}} \nabla \mathrm{E} + \mathbf{v}\,\mathrm{E} + \mathbf{v} \bullet \mathbf{P} \tag{1.99}$$

Here "*c*" is the speed of light and $\kappa_{0R}$ is the Rosseland mean opacity and scales as the reciprocal of a mean free path for the photons. The pressure tensor **P** and the dimensionless quantity specified by the flux-limiter $\lambda$ have yet to be explained. Obtaining the symmetric, 3×3, radiation pressure tensor **P** from a scalar quantity associated with the radiation energy density E is a precarious business because it consists of extracting six pieces of information from one piece of information. The flux limiter $\lambda$ tries to codify our best hunches for making this transcription. Thus for an optically thick medium we wish to have $\lambda \to 1/3$ whereas for an optically thin medium we want $\lambda \to 1$. The Levermore and Pomraning (1981) flux limiter achieves this by setting

$$\lambda = \frac{1}{\mathrm{R}}\left(\coth\,\mathrm{R} - \frac{1}{\mathrm{R}}\right) \quad ; \quad \mathrm{R} = \frac{|\nabla\,\mathrm{E}|}{\kappa_{0R}\,\mathrm{E}} \tag{1.100}$$

The only way to build a second rank radiation pressure tensor from a scalar is to use the gradient of the radiation energy density and assemble a physically suitable expression. This was done by Levermore (1984) to get

$$\mathbf{P} = \frac{\mathrm{E}}{2}\left[\left(1-\mathrm{R}_2\right)\mathbf{I} + \left(3\,\mathrm{R}_2 - 1\right)\mathbf{n}\otimes\mathbf{n}\right] \;\; ; \;\; \mathrm{R}_2 = \lambda + \lambda^2\,\mathrm{R}^2 \;\; ; \;\; \mathbf{n} = -\frac{\nabla \mathrm{E}}{\left|\nabla \mathrm{E}\right|} \qquad (1.101)$$

Eqns. (1.99) to (1.101) lay out the approximations that are inherent in the flux limited diffusion approximation.

Now that we have expressions for the radiation flux and pressure tensor in terms of the radiation energy density, we are in a position to write out the evolution equations for the hydrodynamic variables as well as the radiation energy density. Thus we have

$$\begin{aligned}
&\frac{\partial \rho}{\partial t} + \frac{\partial}{\partial x_i}\left(\rho\, \mathrm{v}_i\right) = 0 \\
&\frac{\partial}{\partial t}\left(\rho \mathrm{v}_i\right) + \frac{\partial}{\partial x_j}\left(\rho \mathrm{v}_i \mathrm{v}_j + \mathrm{P}\,\delta_{ij}\right) = -\,\lambda\,\frac{\partial \mathrm{E}}{\partial x_i} \\
&\frac{\partial \mathcal{E}}{\partial t} + \frac{\partial}{\partial x_i}\left(\left(\mathcal{E} + \mathrm{P}\right)\mathrm{v}_i\right) = -\,\kappa_{0P}\left(4\pi\,\mathrm{B} - c\,\mathrm{E}\right) + \lambda\left(2\frac{\kappa_{0P}}{\kappa_{0R}} - 1\right)\mathbf{v}\bullet\nabla \mathrm{E} - \frac{3-\mathrm{R}_2}{2}\,\kappa_{0P}\,\frac{\mathbf{v}^2}{c}\,\mathrm{E} \\
&\frac{\partial \mathrm{E}}{\partial t} + \frac{\partial}{\partial x_i}\left(\frac{3-\mathrm{R}_2}{2}\,\mathrm{E}\,\mathrm{v}_i\right) = \nabla\bullet\left(\frac{c\lambda}{\kappa_{0R}}\,\nabla\,\mathrm{E}\right) \\
&\qquad\qquad + \kappa_{0P}\left(4\pi\,\mathrm{B} - c\,\mathrm{E}\right) - \lambda\left(2\frac{\kappa_{0P}}{\kappa_{0R}} - 1\right)\mathbf{v}\bullet\nabla \mathrm{E} + \frac{3-\mathrm{R}_2}{2}\,\kappa_{0P}\,\frac{\mathbf{v}^2}{c}\,\mathrm{E}
\end{aligned} \qquad (1.102)$$

Here $\kappa_{0P}$ is the Planck mean opacity and scales as the reciprocal of a mean free path for the photons and $\mathrm{B} = c\,\mathrm{a}_R\,\mathrm{T}^4/\left(4\pi\right)$ is the frequency-integrated Planck function. The $\lambda\,\nabla \mathrm{E}$ source term in the momentum equation specifies the force imparted to the fluid by the radiation. The term $\left(3-\mathrm{R}_2\right)\mathrm{E}\,\mathrm{v}_i/2$ on the left hand side of the radiation energy equation represents the advective flux of radiation energy. The first term on the right

hand side of the radiation energy equation is a divergence of $c\lambda \nabla \mathrm{E}/\kappa_{0R}$. As a result, $c\lambda \nabla \mathrm{E}/\kappa_{0R}$ is the diffusive flux of radiation energy and its divergence gives us the diffusion of radiant energy through a material medium. The source term $\kappa_{0P}\left(4\pi \mathrm{B} - c\,\mathrm{E}\right)$ in the two energy equations shows how the temperature of the radiation field and matter come into equilibrium. The source term $\lambda\left(2\kappa_{0P}/\kappa_{0R} - 1\right)\mathbf{v} \bullet \nabla \mathrm{E}$ in the two energy equations specifies the work done by the radiation as it diffuses through the gas. The term proportional to $\kappa_{0P}\mathrm{E}/c$ in the two energy equations represents a relativistic work term and pertains to the boosting of the flux from the comoving frame to the frame in which the dynamics is viewed. As one can see, the source terms in the two energy equations are equal and opposite, ensuring that the total energy is conserved. Except for the source terms we also see that the evolutionary equation for the radiation energy density is in a flux conservative form, which is very useful for its numerical solution.

### 1.11) The Radiative Transfer Equation

The previous section has shown that it is possible to come up with an adequate treatment for radiation when photons diffuse through a medium. But there are several areas of science when flux limited diffusion might become a particularly inadequate approach for treating radiation. Examples include combustion physics, controlled thermonuclear fusion and astrophysics. In such problems the photons can have long path lengths in some parts of the matter. If the matter is tenuous, the radiation can propagate unimpeded over long, straight lines. The medium in which the photons propagate may not be homogenous or isotropic with the result that the direction of propagation of individual rays at any point does become important. Furthermore, photons can be absorbed by the medium, resulting in an absorption opacity. The medium can also emit photons, especially if it is sufficiently hot. Photons can also scatter off the atoms that make up the medium. Thus the physics of absorption, emission and scattering has to be adequately represented in our governing equations. The text by Modest (2003) shows that there is not a single method for treating the radiation field that is superior to all others, i.e.

each method for *radiative transfer* has its advantages as well as its drawbacks. We will not catalogue alternative methods here. Instead we will catalogue the *discrete ordinates method* which was first formulated by Chandrasekhar (1950) for describing radiative transfer. It was later developed by Lathrop and Carlson (1965, 1966) within the context of *neutron transfer* problems and the numerical solution of the Boltzmann equation, thus demonstrating its versatility. We will describe the discrete ordinates method here as it pertains to radiative transfer.

The radiative transfer equations in moving media have been written out in their most general form by Mihalas and Klein (1982). We specialize them to a static medium for simplicity. At any given location "**x**" we are interested in the amount of radiation that propagates in an angular direction $\mathbf{\Omega}$ , which we refer to as an ordinate direction. The ordinate direction is a unit vector. We are actually interested in the radiant energy that propagates in an infinitesimally small solid angle $d\mathbf{\Omega}$ that is centered around the direction $\mathbf{\Omega}$. Radiation is usually emitted or absorbed over a spectrum of frequencies $\nu$ so we say that we are interested in an infinitesimal range of frequencies $d\nu$ around the frequency $\nu$. We then say that the amount of radiant energy propagating per unit time through an infinitesimal area $dA$ that is orthogonal to $\mathbf{\Omega}$ (and in the previously specified range of frequencies) is given by $I(\mathbf{x},\mathbf{\Omega},\nu,t)\, d\mathbf{\Omega}\, dA\, d\nu$. The function $I(\mathbf{x},\mathbf{\Omega},\nu,t)$ is called the *radiation intensity*. Fig. 1.15 illustrates a vertically stratified atmosphere, shown by a grayscale that is varying in the vertical direction. The atmosphere could correspond to that of a star or a planet. Radiation usually propagates through such atmospheres. The arrows schematically depict the different ordinates that contribute to the radiation intensity at any point of interest. Because the magnitude of a photon's momentum is proportional to its frequency, and also because its direction is specified by $\mathbf{\Omega}$, we see that the radiation intensity is analogous to a distribution function except that it applies to photons instead of particles. The evolution equation for the radiation intensity is often referred to as the *radiative transfer equation*. It is entirely analogous to the Boltzmann equation and is given by

$$\frac{1}{c}\frac{\partial}{\partial t} I\left(\mathbf{x},\boldsymbol{\Omega},\nu,t\right) + \boldsymbol{\Omega} \bullet \nabla\, I\left(\mathbf{x},\boldsymbol{\Omega},\nu,t\right) = \kappa\left(\mathbf{x},\nu,t\right)\, I_b\left(\mathrm{T}\left(\mathbf{x},t\right),\nu\right)$$
$$-\left(\kappa\left(\mathbf{x},\nu,t\right)+\sigma\left(\mathbf{x},\nu,t\right)\right) I\left(\mathbf{x},\boldsymbol{\Omega},\nu,t\right)$$
$$+\ \frac{\sigma\left(\mathbf{x},\nu,t\right)}{4\pi} \int \Phi\left(\boldsymbol{\Omega},\boldsymbol{\Omega}'\right)\, I\left(\mathbf{x},\boldsymbol{\Omega}',\nu,t\right)\, d\boldsymbol{\Omega}' \tag{1.103}$$

Here "*c*" is the speed of light, $\kappa\left(\mathbf{x},\nu,t\right)$ is the *absorption opacity*, $\sigma\left(\mathbf{x},\nu,t\right)$ is the *scattering opacity* , $\Phi\left(\boldsymbol{\Omega},\boldsymbol{\Omega}'\right)$ is the *scattering phase function* and $I_b\left(\mathrm{T}\left(\mathbf{x},t\right),\nu\right)$ is the *blackbody intensity* and depends on the temperature $\mathrm{T}\left(\mathbf{x},t\right)$. Eqn. (1.103) holds for *each* ordinate of interest and for *each* range of frequencies that are relevant to the scientific problem. The left hand side of the above equation is a Lagrangian derivative and clearly shows the hyperbolic character of the radiative transfer equation. The terms on the right hand side of eqn. (1.103) can be thought of as source terms with interesting physical interpretations. A medium at a finite temperature emits photons and the blackbody intensity characterizes the tendency of the medium to emit photons. The absorption opacity is a measure of the tendency of the material medium to absorb photons while the scattering opacity relates to the rate at which photons get scattered by the medium. Just as photons get scattered out of the ordinate $\boldsymbol{\Omega}$ of interest in eqn. (1.103), there are other photons that get scattered into this ordinate from several different directions. The integral on the right hand side of eqn. (1.103) is a measure of that process. In that integral, the scattering phase function $\Phi\left(\boldsymbol{\Omega},\boldsymbol{\Omega}'\right)$ quantifies the tendency of the medium to take a photon that is propagating in the direction $\boldsymbol{\Omega}'$ and scatter it into the direction of interest, given by $\boldsymbol{\Omega}$. Notice that the temperature of the medium depends on the nature of the radiation field that it experiences. Likewise, the absorption and scattering opacities can depend on the medium's chemical or atomic composition, its temperature as well as the radiation field. As a result, the radiative transfer equation is highly non-linear and extremely difficult to solve in its entirety. Judicious simplifications are, therefore, highly desirable.

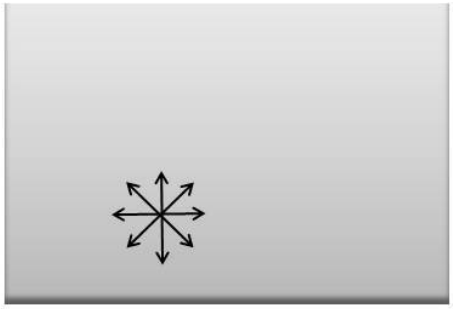

*Fig. 1.15 illustrates a vertically stratified atmosphere, shown by a grayscale that is varying in the vertical direction. The arrows schematically depict the different ordinates that contribute to the radiation intensity at any point of interest.*

One possible simplification consists of realizing that the speed of light is much faster than the speed at which material objects move. Thus photons can propagate through the object several times and establish radiative equilibrium. Consequently, we will only be interested in the steady state version of eqn. (1.103), i.e. the time dependence can be dropped. The radiation field can also span a large range of frequencies. However, radiation that interacts strongly with matter can be shown to take on a frequency distribution that is given by the Planck function with a temperature that is characteristic of the matter it interacts with. We cannot always guarantee that the radiation interacts strongly with the matter but, as a working ansatz, we can integrate eqn. (1.103) over a small number of bins in frequency space. A more extreme assumption consists of integrating eqn. (1.103) over the entire range of frequencies. This assumption is called the *gray approximation* and is indeed used quite frequently. Since photons can propagate in any direction, there are an infinite number of ordinates in eqn. (1.103). The discrete ordinates method consists of picking a special, finite set of favored directions for the ordinates. The ordinates are usually chosen so that several of the lower moments of the radiative transfer equation are exactly represented. Fiveland (1991) and Balsara (2001) provide several useful quadrature sets. A quadratre set is usually labeled by an integer "*N*" which yields a set of $N\left(N+2\right)$ ordinates $\left\{\mathbf{\Omega}_i \mid i=1,...,N\left(N+2\right)\right\}$. The method of discrete ordinates methods is, therefore, also known as the $S_N$ *method*. Along with the quadrature set, one is supplied a set of weights $\left\{w_i \mid i=1,...,N\left(N+2\right)\right\}$ so that integrals appearing on the right hand side of eqn. (1.103) can be performed by using the weights. The radiative transfer equation is then discretized as

$$\boldsymbol{\Omega}_i \bullet \nabla I\left(\mathbf{x},\boldsymbol{\Omega}_i,\nu\right) = \kappa\left(\mathbf{x},\nu\right) I_b\left(\mathrm{T}\left(\mathbf{x}\right),\nu\right) - \left(\kappa\left(\mathbf{x},\nu\right)+\sigma\left(\mathbf{x},\nu\right)\right) I\left(\mathbf{x},\boldsymbol{\Omega}_i,\nu\right) + \frac{\sigma\left(\mathbf{x},\nu\right)}{4\pi} \sum_{j=1}^{N(N+2)} w_j \, \Phi\left(\boldsymbol{\Omega}_i,\boldsymbol{\Omega}_j\right) I\left(\mathbf{x},\boldsymbol{\Omega}_j,\nu\right) \tag{1.104}$$

Notice that eqn. (1.104) represents a set of $N\left(N+2\right)$ equations for each frequency bin centered around $\nu$. The above equations are solved with boundary conditions that are tailored to the physical properties of the material boundary. We will learn more about solution techniques for the $S_N$ method later in this book.

**1.12) The Equations of Linear Elasticity**

The easiest way to get introduced to the equations of linear elasticity is to hold one end of a reasonably rigid spring and set it in oscillation. By stretching the spring along its long axis and releasing it abruptly, we see that we can set up longitudinal oscillations in the spring. In an idealized, infinite spring, these oscillatory waves can be made to propagate to the left or to the right. When the spring is stretched, Hooke's law tells us that the restoring force is proportional to the extent by which the spring is stretched. As the spring is stretched, quite literally, the bonds between the atoms in the spring are also deformed. As long as the bonds remain intact, i.e. the spring does not break (or fracture), we will obtain a restoring force, suggestively called the stress, which is proportional to the deformation, suggestively referred to as the strain. The amount by which the atoms in a solid are stretched or compressed relative to one another has a technical name called the *strain*. Fig. 1.16b shows a solid lattice where the atoms are undergoing compression; the initial lattice is shown in Fig. 1.16a for comparison purposes. Hooke's law simply asserts that this strain sets up a restoring force between the atoms, and this restoring force also has a technical name; it is called the *stress*.

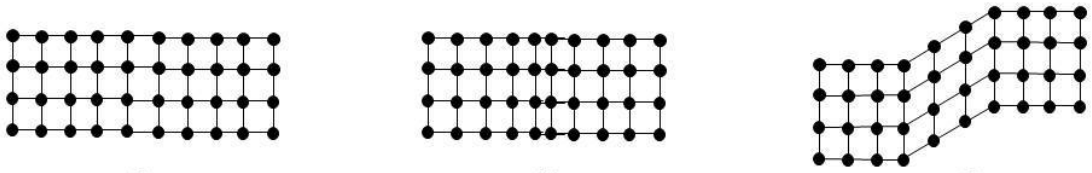

(a) (b) (c)

*Fig. 1.16a shows an idealized lattice of atoms, shown as dots, with atomic bonds between them, shown as lines. In Fig. 1.16a the lattice is undeformed. Fig. 1.16b shows the same lattice where the atoms are undergoing compressional strain. Fig. 1.16c shows the same lattice where the atoms are undergoing shear strain.*

Notice that the spring in our example also has two directions that are transverse to its long axis. By plucking the spring in either of these two transverse directions, we can also set up wavelike oscillations in the spring. Keeping Fig. 1.8 in mind, realize that these are transverse oscillations. In an idealized, infinite spring, these transversely oscillating waves can be made to propagate to the left or to the right. Because we have two transverse directions, we realize that we have four transversely polarized waves. The amount of restoring force provided by the spring in response to a transverse deformation is proportional to the amount of the deformation. As before, the bonds between the atoms that make up a solid can also resist bending, just like the spring. Fig. 1.16c shows a solid lattice where the atoms are undergoing a transverse deformation. The amount of restoring force they can provide in the transverse direction, also called the stress, is proportional to the transverse deflection itself, also called the strain.

We see that depending on the direction of the original deformation, the strain can be of two types. Consider holding a solid at two points and applying deformations to it. If the deformation that we impart to the solid is along the line joining the two points, the strain can be referred to as *extensional strain*. If the deformation that we provide is transverse to the line joining the two points, the strain is called *shear strain*. Note though that rigid body rotations of the solid do not count as shear strains because they do not cause any relative motion between the atoms in the solid nor do they cause any deformation of the atomic bonds. The concept of strain can now be formalized as follows. Let $\mathbf{x} = (x, y, z)$ be the original location of an atom in a solid and let $\mathbf{X} = (\mathrm{X}(x, y, z, t), \mathrm{Y}(x, y, z, t), \mathrm{Z}(x, y, z, t))$ be its location when it is deformed at a time

"*t*". (Note that we are using the "atoms" as a proxy for point particles in a solid, without considering their thermal oscillations.) The displacement vector is then given by $\boldsymbol{\delta} \equiv \mathbf{X} - \mathbf{x}$ . Fig. 1.17 illustrates a small part of a two-dimensional solid lattice. The undeformed structure is shown by the black square with black dots at its vertices. The displacement vectors $\boldsymbol{\delta}$ are shown by the dashed black arrows. The deformed structure is shown in gray. Note that these displacements can include overall translations and rotations of the solid, i.e. translations and rotations that have it moving as a rigid body. Such displacements do not contribute to the deformation of the atomic bonds in the solid and, therefore, do not contribute to the strain in the solid. To get a measure of the deformation, let us therefore consider the 3×3 tensor $\partial\boldsymbol{\delta}/\partial\mathbf{x}$. It is clearly insensitive to overall translations of the solid. It does not, however, eliminate overall rotations of the solid. Realize that a rotation is an anti-symmetric tensor, i.e. the rigid body rotation of the solid is proportional to $\left[\left(\partial\boldsymbol{\delta}/\partial\mathbf{x}\right)-\left(\partial\boldsymbol{\delta}/\partial\mathbf{x}\right)^{T}\right]/2$. The strain should, therefore, be proportional to the symmetric part of the above 3×3 tensor. Defining the strain tensor as $\boldsymbol{\varepsilon}$ we can define it as $\left[\left(\partial\boldsymbol{\delta}/\partial\mathbf{x}\right)+\left(\partial\boldsymbol{\delta}/\partial\mathbf{x}\right)^{T}\right]/2$. This definition excludes solid body rotations.

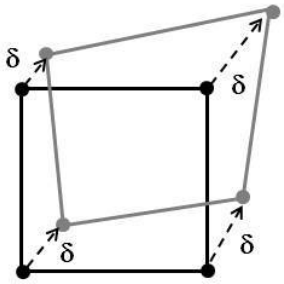


*Fig. 1.17 shows a small part of a two-dimensional solid lattice. The undeformed structure is shown by the black square with black dots at its vertices. The displacement vectors* $\boldsymbol{\delta}$ *are shown by the dashed black arrows. The deformed structure is shown in gray.*

We can now think about the elastic waves that are induced in a solid even before we lay out a mathematical theory for them. Our analogy to a spring is in fact quite a good one because we can set up exactly six families of propagating waves in a spring, two with longitudinal oscillations and four with transverse oscillations. At a microscopic level, the atomic bonds mimic the same kinds of tensional and shear forces that the spring provides at a macroscopic level. We will therefore see that when studying one-dimensional wave propagation in a solid, there are six families of propagating waves. Two of those waves are referred to as *P-waves*, because of their analogy with the longitudinally oriented

sound waves in a fluid. (The sound waves can also be loosely thought of as "pressure" waves.) The other four waves are referred to as *S-waves* because they are transverse waves arising from shearing deformations in the solid. S-waves have no analogous wave structure in fluid dynamics because atoms in two shearing streams in a fluid do not form bonds and, hence, cannot set up restoring forces. However, note that electromagnetic waves arising from Maxwell's equations as well as Alfven waves in magnetohydrodynamics provide us with examples of transverse waves that arise in other systems.

As long as the atoms undergo small displacements relative to their original locations, the atomic bonds will only be stretched/sheared by a small fraction of their original length. The relative displacements between the atoms should be small enough that the atomic bonds do not break. In such situations a linear *stress-strain relation* remains a good assumption; recall Hooke's law for a spring. The stress-strain relation depends on the properties of the material being considered and can be viewed as a constitutive relationship that allows the equations of elasticity to form a closed set. Note that the linear relation between strain and stress that was assumed in the above discussion is just a simplifying assumption. It only holds as long as the atomic bonds are not broken. For large displacements the bonds could break permanently resulting in a *fracture* in the material. Alternatively, the atomic bonds could break and reform, as in *plastic deformation*. When the deformations become quite large, it is also possible to have a non-linear relationship between strain and stress, giving rise to the possibility of shocks forming in the system, see Trangenstein and Pember (1991,1992). We restrict our considerations to the simpler, linear systems.

Several texts provide very good introductions to the equations of elastodynamics, see Landau and Lifshitz (1975) or Antman (1995). The text by Davis and Selvadurai (1996) provides an introduction that is well-suited for hyperbolic systems. The stress and strain tensors in the solid are denoted by $\boldsymbol{\sigma}$ and $\boldsymbol{\varepsilon}$ respectively. In response to the stresses the solid will respond with a velocity $\mathbf{v} \equiv \left(\mathrm{v_x}, \mathrm{v_y}, \mathrm{v_z}\right) = \left(\partial \mathrm{X}/\partial t, \partial \mathrm{Y}/\partial t, \partial \mathrm{Z}/\partial t\right)$. Let the solid have a constant density $\rho$. As per Newton's second law, the stresses will cause

accelerations in the solid. Note though that our definition of the velocities and our definition of the strain tensor imply that there are consistency relationships between them. Thus we have

$$\partial_t \varepsilon_{11} = \frac{\partial}{\partial t}\left( \frac{\partial \mathrm{X}(x,y,z,t)}{\partial x} - 1 \right) = \frac{\partial}{\partial x}\left( \frac{\partial \mathrm{X}(x,y,z,t)}{\partial t} \right) = \partial_x \mathrm{v_x}$$
$$\partial_t \varepsilon_{12} = \frac{1}{2}\frac{\partial}{\partial t}\left( \frac{\partial \mathrm{X}(x,y,z,t)}{\partial y} + \frac{\partial \mathrm{Y}(x,y,z,t)}{\partial x} \right) = \frac{1}{2}\left( \frac{\partial}{\partial y}\left( \frac{\partial \mathrm{X}(x,y,z,t)}{\partial t} \right) + \frac{\partial}{\partial x}\left( \frac{\partial \mathrm{Y}(x,y,z,t)}{\partial t} \right) \right) = \frac{1}{2}\left( \partial_y \mathrm{v_x} + \partial_x \mathrm{v_y} \right)$$

(1.105)

The dynamical equations for linear elasticity are given by

$$\partial_t \varepsilon_{11} - \partial_x \mathrm{v_x} = 0 \quad ; \quad \partial_t \varepsilon_{22} - \partial_y \mathrm{v_y} = 0 \quad ; \quad \partial_t \varepsilon_{33} - \partial_z \mathrm{v_z} = 0 \quad ;$$
$$\partial_t \varepsilon_{12} - \frac{1}{2}\left( \partial_y \mathrm{v_x} + \partial_x \mathrm{v_y} \right) = 0 \quad ; \quad \partial_t \varepsilon_{23} - \frac{1}{2}\left( \partial_z \mathrm{v_y} + \partial_z \mathrm{v_y} \right) = 0 \quad ; \quad \partial_t \varepsilon_{13} - \frac{1}{2}\left( \partial_z \mathrm{v_x} + \partial_x \mathrm{v_z} \right) = 0 \quad ;$$
$$\rho\, \partial_t \mathrm{v_x} - \partial_x \sigma_{11} - \partial_y \sigma_{12} - \partial_z \sigma_{13} = 0 \quad ;$$
$$\rho\, \partial_t \mathrm{v_y} - \partial_x \sigma_{12} - \partial_y \sigma_{22} - \partial_z \sigma_{23} = 0 \quad ;$$
$$\rho\, \partial_t \mathrm{v_z} - \partial_x \sigma_{13} - \partial_y \sigma_{23} - \partial_z \sigma_{33} = 0 \quad ;$$

(1.106)

Notice from eqn. (1.105) that the first six of the above equations represent consistency conditions between the velocity and the strain. The last three, in turn, express Newton's second law.

As given, eqn. (1.106) cannot be solved because there are more unknowns than there are evolution equations. The stress $\boldsymbol{\sigma}$ can be related to the strain $\boldsymbol{\varepsilon}$ via the following tensorial, constitutive relationship

$$\begin{bmatrix} \sigma_{11} \\ \sigma_{22} \\ \sigma_{33} \\ \sigma_{12} \\ \sigma_{23} \\ \sigma_{13} \end{bmatrix} = \begin{bmatrix} \Lambda + 2\mu & \Lambda & \Lambda & 0 & 0 & 0 \\ \Lambda & \Lambda + 2\mu & \Lambda & 0 & 0 & 0 \\ \Lambda & \Lambda & \Lambda + 2\mu & 0 & 0 & 0 \\ 0 & 0 & 0 & 2\mu & 0 & 0 \\ 0 & 0 & 0 & 0 & 2\mu & 0 \\ 0 & 0 & 0 & 0 & 0 & 2\mu \end{bmatrix} \begin{bmatrix} \varepsilon_{11} \\ \varepsilon_{22} \\ \varepsilon_{33} \\ \varepsilon_{12} \\ \varepsilon_{23} \\ \varepsilon_{13} \end{bmatrix} \tag{1.107}$$

Where $\Lambda$ and $\mu$ are the *Lamé parameters* and can be related to the *Young's modulus* "*E*" and the *Poisson ratio* "$\nu$" of the solid via the following relationships

$$E = \frac{\mu\left(3\Lambda + 2\mu\right)}{\Lambda + \mu} \quad ; \quad \nu = \frac{\Lambda}{2\left(\Lambda + \mu\right)} \tag{1.108}$$

After drawing on the constitutive relations provided by eqn. (1.107) the equations of linear elasticity can be written in their final form as

$$\begin{aligned}
&\partial_t \sigma_{11} - \left(\Lambda + 2\mu\right)\partial_x \mathrm{v_x} - \Lambda\, \partial_y \mathrm{v_y} - \Lambda\, \partial_z \mathrm{v_z} = 0 \\
&\partial_t \sigma_{22} - \Lambda\, \partial_x \mathrm{v_x} - \left(\Lambda + 2\mu\right)\partial_y \mathrm{v_y} - \Lambda\, \partial_z \mathrm{v_z} = 0 \\
&\partial_t \sigma_{33} - \Lambda\, \partial_x \mathrm{v_x} - \Lambda\, \partial_y \mathrm{v_y} - \left(\Lambda + 2\mu\right)\partial_z \mathrm{v_z} = 0 \\
&\partial_t \sigma_{12} - \mu\left(\partial_y \mathrm{v_x} + \partial_x \mathrm{v_y}\right) = 0 \\
&\partial_t \sigma_{23} - \mu\left(\partial_z \mathrm{v_y} + \partial_x \mathrm{v_y}\right) = 0 \\
&\partial_t \sigma_{13} - \mu\left(\partial_z \mathrm{v_x} + \partial_x \mathrm{v_z}\right) = 0 \\
&\rho\, \partial_t \mathrm{v_x} - \partial_x \sigma_{11} - \partial_y \sigma_{12} - \partial_z \sigma_{13} = 0 \\
&\rho\, \partial_t \mathrm{v_y} - \partial_x \sigma_{12} - \partial_y \sigma_{22} - \partial_z \sigma_{23} = 0 \\
&\rho\, \partial_t \mathrm{v_z} - \partial_x \sigma_{13} - \partial_y \sigma_{23} - \partial_z \sigma_{33} = 0
\end{aligned} \tag{1.109}$$

In the above form, the equations of elasticity can indeed be solved. Notice that all the coefficients in the above equations are constants and, as a result, the above equations are linear.

The above equations can be written in the form given by eqn. (1.69) and in that form they can be shown to be hyperbolic. Restricting attention to the x-direction we see that the characteristic matrix admits an ordered sequence of ten eigenvalues given by

$$\lambda^1 = -c_P \; ; \; \lambda^2 = \lambda^3 = -c_S \; ; \; \lambda^4 = \lambda^5 = \lambda^6 = 0 \; ; \; \lambda^7 = \lambda^8 = c_S \; ; \; \lambda^9 = c_P \tag{1.05}$$

where $c_P$ is the propagation speed of the *P*-wave and $c_S$ is the propagation speed of the *S*-wave. These wave speeds are given by

$$c_P = \sqrt{\frac{\Lambda + 2\mu}{\rho}} \;\; ; \;\; c_S = \sqrt{\frac{\mu}{\rho}} \tag{1.06}$$

The above two equations show that the *P*-waves always propagate faster than the *S*-waves. A problem at the end of this chapter helps us with the derivation of the above eigenvalues. It is important to note that while the characteristic matrices resulting from eqn. (1.109) seem very large, they are mostly sparse. The problem of obtaining eigenvalues and eigenvectors of a 9×9 matrix, while daunting at first blush, can actually be handed off to a symbolic manipulation package.

**1.13) Relativistic Hydrodynamics and Magnetohydrodynamics**

The equations of relativistic hydrodynamics and MHD are used to model high speed flows. While some nuclear collisions have been modeled by the equations of relativistic hydrodynamics, most of the applications derive from high energy astrophysics. These equations are primarily used to model phenomena that take place at speeds approaching the speed of light. Such speeds are reached in astrophysical settings, especially when considering flows around neutron stars and black holes. As a result, special and sometimes general relativistic effects have to be considered. For all other situations, the regular Euler and MHD equations prove to be very serviceable. Thus this section is primarily targeted towards astronomers. In studying this topic it is quite advantageous to arrive at it in gradual stages. For that reason, in this section we introduce the special relativistic form of the hydrodynamic and MHD equations. General relativistic effects, which incorporate the effects of a curved space-time, can be considered later.

The special relativistic hydrodynamic equations have been very nicely discussed in the text by Synge (1957) and the physics of relativistic shock waves arising from those equations have been nicely presented in Taub (1948). The first thing to realize about a

parcel of fluid that is moving with a velocity $\mathbf{v}$ that is close to the speed of light "*c*" is that the parcel will experience length contraction when viewed in the frame of reference of a stationary observer, i.e. the *lab frame*. Thus in the lab frame, one considers the Lorentz contraction which is given by the *Lorentz factor* $\gamma \equiv 1/\sqrt{1-\mathbf{v}^2/c^2}$ . If the fluid has a density $\rho$ in its own rest frame, the rest frame density increases to a value of $\rho\,\gamma$ in the lab frame. The continuity equation is, therefore, an expression of the conservation of the total number of atoms and is given by

$$\frac{\partial}{\partial t}(\rho\,\gamma)+\frac{\partial}{\partial x_i}(\rho\,\gamma\,\mathrm{v}_i)=0 \tag{1.112}$$

Fluids that are flowing at relativistic speeds can only be accelerated to these speeds by very energetic processes. As a result, they often have unusually large amounts of internal energy and pressure. That internal energy and pressure can also contribute to the fluid's inertia. As a result, we define the specific enthalpy as $h \equiv 1+\Gamma\,\mathrm{P}/c^2(\Gamma-1)$ which provides a further multiplicative contribution from the fluid's internal energy to the rest mass. Here $\Gamma$ is the polytropic index of the gas, which is assumed to be ideal for the sake of simplicity. As a result, the fluid has $\rho\,h\,\gamma$ amount of mass density when viewed from the lab frame. The specific momentum of the fluid is given by $\gamma\,\mathbf{v}$ . The momentum density of the fluid is then given by $\rho\,h\,\gamma^2\,\mathbf{v}$ and the equation that describes its evolution can be written as

$$\frac{\partial}{\partial t}\left(\rho\,h\,\gamma^2\,\mathrm{v}_i\right)+\frac{\partial}{\partial x_j}\left(\rho\,h\,\gamma^2\,\mathrm{v}_i\,\mathrm{v}_j+\mathrm{P}\,\gamma\,\delta_{ij}\right)=0 \tag{1.113}$$

The energy density of the fluid includes just the contribution of the internal energy to the fluid's inertia and is therefore given by $\rho\,h\,\gamma^2-\mathrm{P}/c^2$ . The equation for the energy density is then given by

$$\frac{\partial}{\partial t}\left(\rho\, h\, \gamma^2 - \mathrm{P}/c^2\right) + \frac{\partial}{\partial x_i}\left(\rho\, h\, \gamma^2\, \mathrm{v}_i\right) = 0 \qquad (1.114)$$

Synge (1957) provides an extensive derivation of the relativistic continuity equation as well as the relativistic momentum and energy equations. Pons *et al.* (1998) have shown a very interesting connection between general and special relativistic hydrodynamics based on analyzing locally flat space-times. Aloy *et al.* (1999) have provided an extensive review of numerical methods for special and general relativistic hydrodynamics.

The parallels between eqns. (1.112) to (1.114) and the Euler equations are then easy to spot. Setting $\gamma = h = 1$ for the non-relativistic limit in eqns. (1.112) and (1.113) then gives back the continuity and momentum equations in eqn. (1.42). Reducing eqn. (1.114) to yield the last equation in eqn. (1.42) is a little more subtle, because the rest mass of a particle contributes to the energy density when considering relativistic flows whereas that energy can be cleanly subtracted away for non-relativistic flows. The relativistic flow equations also form a hyperbolic set of equations and have the same foliation of waves as the Euler equations. While there are many parallels between the Euler equations and their relativistic extensions, there are two prominent points of difference. First, while it is quite easy to obtain the primitive variables from the conserved variables for Euler flow, doing so for relativistic flow involves solving a transcendental equation. Second, carrying out the eigenmodal analysis for relativistic flow is a lot harder. These two attributes, which make the relativistic flow equations harder to work with, also carry over to relativistic MHD.

The text by Anile (1989) provides an excellent introduction to relativistic MHD. Several excellent formulations for general relativistic MHD have recently been presented in the literature, see Komissarov (2004), McKinney (2006) and DelZanna *et al.* (2007). General relativists usually use a set of geometrized units where $\mathrm{G}=c=1$ and we use those units here in describing the equations of relativistic MHD. Here G is Newton's constant and $c$ is the speed of light. The factor of $4\pi$ that we met in classical MHD is also absorbed via a redefinition of the magnetic field. We do not provide a detailed derivation

of the relativistic MHD equations, but we do give some information in order to build intuitive familiarity with the equations. All the same considerations that we made for relativistic hydrodynamics also have to be made here, with the result that the continuity equation is identical to eqn. (1.112). The introduction of a magnetic field $\mathbf{B}$ also introduces a motional emf, thus resulting in an electric field in the plasma which is given by $\mathbf{E} = -\mathbf{v}\times\mathbf{B}$ even in the relativistic limit. The *Poynting flux* $\mathbf{E}\times\mathbf{B}$ is a measure of the momentum flux density of the electromagnetic field and so it's time evolution has also to be factored in when accounting for the total momentum density. The energy density of the electric and magnetic fields can also make a significant contribution to the magnetofluid's pressure. Thus the momentum equation becomes

$$\begin{aligned}&\frac{\partial}{\partial t}\left(\rho\, h\, \gamma^2\, \mathrm{v}_i + \left(\mathbf{E}\times\mathbf{B}\right)_i\right) \\ &\quad + \frac{\partial}{\partial x_j}\left(\rho\, h\, \gamma^2\, \mathrm{v}_i\, \mathrm{v}_j - \mathrm{E}_i\, \mathrm{E}_j - \mathrm{B}_i\, \mathrm{B}_j + \left(\mathrm{P} + \frac{1}{2}\left(\mathbf{E}^2 + \mathbf{B}^2\right)\right)\gamma\, \delta_{ij}\right) = 0\end{aligned} \tag{1.115}$$

Just as the magnetic energy contributed to the energy density for classical MHD, the electric and magnetic energy densities now contribute to the energy density of a magnetofluid. In electromagnetism, the Poynting flux also represents the flux of energy. Consequently, it makes a further contribution to the energy flux. The energy equation is therefore given by

$$\frac{\partial}{\partial t}\left(\rho\, h\, \gamma^2 - \mathrm{P} + \frac{1}{2}\left(\mathbf{E}^2 + \mathbf{B}^2\right)\right) + \frac{\partial}{\partial x_i}\left(\rho\, h\, \gamma^2\, \mathrm{v}_i + \left(\mathbf{E}\times\mathbf{B}\right)_i\right) = 0 \tag{1.116}$$

Faraday's law is already relativistically invariant. As a result, the evolution equation for the relativistic magnetic field is still given by

$$\frac{\partial \mathbf{B}}{\partial t} = \nabla\times\left(\mathbf{v}\times\mathbf{B}\right) \tag{1.117}$$

The magnetic field is still divergence-free, i.e. $\nabla\bullet\mathbf{B}=0$ . This completes our description of the special relativistic MHD equations.

The above equations for relativistic MHD can be compared to the equations of classical MHD in eqn. (1.97). The parallels are easy to spot. The relativistic flow equations also form a hyperbolic set of equations and have the same foliation of waves as the classical MHD equations. The same eigenvector degeneracies that plague classical MHD also plague relativistic MHD. The degeneracies have been catalogued in Anile (1989) and a set of eigenvectors that are suitable for computational work has been catalogued in Komissarov (1999), Balsara (2001) and Anton et al. (2010).

## 1.14) The Importance of Scientific Visualization, Symbolic Manipulation and Parallel Programming

The solution methods for the PDEs discussed in this book can yield some very appealing results. The results can be as scientifically illuminating as they can be visually stunning. There are few things as satisfying to a computationalist as solving a computational problem, visualizing the results and verifying that they conform with expectation. It is, therefore, important to have at least a small amount of working familiarity with scientific visualization. Several big software packages come with their in-built visualization capabilities and copious documentation for the same. There are also a few software packages that are devoted almost exclusively to scientific visualization. IDL is one of them, and scientific visualization using IDL is extensively discussed in Fanning (2000). MATLAB, which is widely used by mathematicians and engineers, also has visualization capabilities (Chapman 2007, Gander and Hřebíček 2004). At a very minimum, it is advantageous to have graphical capabilities for visualizing one-dimensional and two-dimensional data using a commercially available, basic, graphical package. To that end, the computational exercises at the end of this chapter provide a few simple IDL scripts that give the reader ready-made access to a simple visualization capability.

Several modern numerical methods require rather detailed analysis before they can be implemented. Symbolic manipulation packages, such as Mathematica and Maple,

have become very proficient at carrying out such tasks for us. Web-based tutorials and videos have become available that can provide a gradual introduction to these packages. Both the packages can also be made to write Fortran or C++ code, with the result that after using them to design parts of a numerical scheme, they can also be made to write the associated code. They also come with a modicum of visualization capability that is pre-programmed. Freeware packages like VisIt are also gaining popularity.

Most big applications codes run on parallel computers these days. The Message Passing Interface (MPI) and the OpenMP API provide industry-standard methods for using parallel machines. Several texts, like those of Karniadakis and Kirby (2003) or Gropp, Lusk and Skjellum (1999), provide introductions to MPI. An easy introduction to OpenMP is provided in the text by Chapman, Jost and van der Pass (2008). For structured mesh applications there exist frameworked approaches that abstract away the details of MPI programming, see Colella *et al.* (2007) for the CHOMBO framework; MacNeice and Olson (2008) for the PARAMESH framework and Henshaw and Schwendeman (2008) for the OVERTURE framework. Several tools are also available for unstructured mesh applications, and several of them have been nicely encapsulated in the ZOLTAN framework from Sandia labs, see Boman *et al.* (2010). We therefore see that there is plenty of support on all fronts to make it easy for new people to enter this field. Welcome!

**References**

Aloy, M.A., Ibanez, J.-M., Marti, J.-M. and Muller, E., GENESIS: A High-Resolution Code for Three-dimensional Relativistic Hydrodynamics, Astrophysical Journal Supplement, 122 (1999) 151-166

Anile, A.M., *Relativistic Fluids and Magneto-Fluids*, Cambridge Univ. Press, Cambridge, UK, 1989

Antman, S.S., *Nonlinear Problems of Elasticity*, Springer-Verlag: New York (1995)

Anton, L. *et al.* , Relativistic magnetohydrodynamics: renormalized eigenvectors and full wave decomposition Riemann solver, Astrophysical Journal Supplement, 188 (2010) 1-31

Aris, R., *Vectors, Tensors, and the Basic Equations of Fluid Mechanics*, Dover (1989)

Balsara, D.S., *Fast and accurate discrete ordinates methods for multidimensional radiative transfer, Part I, basic methods*, J. Quant. Spec. and Rad. Trans., 69 (2001) 671

Balsara, D.S., *Total variation diminishing scheme for relativistic MHD*, Astrophys. J. 132 (2001) 1

Batchelor, G.K., *Introduction to Fluid Dynamics*, Cambridge University Press (2000)

Boman, E. et al. (2010) Zoltan User Guide v3.5
http://www.cs.sandia.gov/Zoltan/ug_html/ug.html

Born, M. and Green, H.S., *A General Kinetic Theory of Liquids I. The Molecular Distribution Functions*, Proc. Roy. Soc. A, 188 (1946) 10–18

Bogoliubov, N.N., *Kinetic Equations*, Journal of Physics USSR 10 (3), (1946) 265–274

Castor, J.I., *Radiation Hydrodynamics*, Cambridge University Press (2004)

Chandrasekhar, S., *Radiative Transfer*, Oxford: Clarendon Press (1950)

Chapman, S.J., *MATLAB Programming for Engineers*, (2007)

Chapman, B., Jost, G. and van der Pass, R. *Using OpenMP*, Scientific and Engineering Computation, MIT Press, (2008)

Chapman, S. and Cowling, T.G., *The Mathematical Theory of Nonuniform Gases*, Cambridge University Press (1961)

Clarke, J.F. and McChesney, M., *Dynamics of Relaxing Gases*, Butterworths (1976)

Colella. P. *et al. Performance and Scaling of Locally-Structured Grid methods for partial differential equations*, SciDAC Annual Meeting (2007)

Courant, R. & Friedrichs, K.O., *Supersonic Flow and Shock Waves*, Interscience Publishers Inc., New York (1948)

DelZanna, L. *et al. ECHO: a Eulerian conservative high-order scheme for general relativistic MHD*, Astronomy & Astrophysics, 473 (2007) 11.

Davis, R.O. and Selvadurai, A.P.S., *Elasticity and Geomechanics*, Cambridge Univ. Press (1996)

Faber, T. E., *Fluid Dynamics for Physicists*, Cambridge University Press, (1995)

Fanning, D.W. *IDL Programming Techniques*, Fanning Software Consulting (2000)

Fiveland, W., *The selection of discrete ordinate quadrature sets for anisotropic scattering*, Fundamentals of Radiation Heat Transfer, ASME, HDT, 160 (1991) 89

Gander, W. and Hřebíček, J., *Solving Problems in Scientific Computing Using Maple and Matlab*, Springer Verlag, (2004)

Gropp, W.D. Lusk, E. and Skjellum, A., *Using MPI*, Scientific and Engineering Computation, MIT Press, (1999)

Henshaw, W.D. and D. W. Schwendeman, *Parallel Computation of Three-Dimensional Flows using Overlapping Grids with Adaptive Mesh Refinement*, J. Comp. Phys., 227 (2008)

Hesthaven, J.S. and Warburton, T., *Nodal High-Order Methods on Unstructured Grids I. Time-Domain Solution of Maxwell's Equations*, Journal of Computational Physics, 181 (2002) 186

Huang, K., *Statistical Mechanics*, Wiley (1963)

Jackson, J.D., *Classical Electrodynamics*, New York:Academic Press (1998)

Jefferey, A. & Taniuti, A. , *Nonlinear Wave Propagation*, Academic Press, New York (1964)

Karniadakis, G.E. and Kirby, R.M., *Parallel Scientific Computing in C++ and MPI : A Seamless Approach to Parallel Algorithms and their Implementation*, Cambridge University Press (2003)

Kirkwood, J.G., *The Statistical Mechanical Theory of Transport Processes II. Transport in Gases*, The Journal of Chemical Physics, 15 (1) (1947) 72

Komissarov, S.S., *A Godunov scheme for relativistic magnetohydrodynamics*, Monthly Notices of the Royal Astronimical Society, 303 (1999) 343

Komissarov, S.S., General relativistic magnetohydrodynamic simulations of monopole magnetospheres of black holes, Monthly Notices of the Royal Astronimical Society, 350 (2004) 1431

Krumholz, M.R., Klein, R.I., McKee, C.F. and Bolstad, J., *Equations and algorithms for mixed-frame flux-limited diffusion radiation hydrodynamics*, Astrophysical Journal, 667 (2007) 626

Landau, L.D. and Lifshitz, E.M., *Fluid Mechanics*, Butterworth-Heinemann (2000)

Landau, L.D. and Lifshitz, E.M., *Theory of Elasticity*, Pergamon Press (1975)

Lathrop, K.D. and Carlson, B.G., *Discrete ordinates angular quadrature of the neutron transport equation*, Los Alamos Scientific Laboratory Report, 3186 (1965)

Lathrop, K.D. and Carlson, B.G., *Numerical solution of the Boltzmann transport equation*, Journal of Computational Physics, (1966) 173

Levermore, C.D., *Relating Eddington factors to flux limiters*, Journal of Quantitative Spectroscopy and Radiative Transfer, 31 (1984) 149

Levermore, C.D. and Pomraning, G.C., *A flux-limited diffusion theory*, Astrophys. J., 248 (1981) 321

MacNeice, P. and Olson, K. PARAMESH V4.1 Parallel Adaptive Mesh Refinement, March (2008), http://www.physics.drexel.edu/~olson/paramesh-doc/User_manual/amr.html

McKinney, J.C, Monthly Notices of the Royal Astronimical Society, 367 (2006) 1797

Mihalas, D. & Weibel-Mihalas, B., *Foundations of Radiation Hydrodynamics*, New York:Dover (1999)

Modest, M., *Radiative Heat Transfer*, 2nd edition, Academic Press (2003)

Montgomery, D.C. and Tidman, D.A., *Plasma Kinetic Theory*, McGraw Hill (1964)

Munz, C.-D., Omnes, P. Schneider, R., Sonnendrücker, E. and Voß, U., *Divergence correction techniques for Maxwell solvers based on a hyperbolic model*, Journal of Computational Physics, 161 (2000) 484

Pons, J.A. *et al.* , General relativistic hydrodynamics with special relativistic Riemann solvers, Astronomy and Astrophysics, 339 (1998) 638-642

Reif, F., *Fundamentals of Statistical and Thermal Physics*, John Wiley, (2008)

Roe, P. L. and Balsara, D. S., *Notes on the eigensystem of magnetohydrodynamics*, SIAM Journal of applied Mathematics 56 (1996), 57

Spitzer, L., *Physical Processes in the Interstellar Medium*, Interscience (1978)

Shu, F.H., *The Physics of Astrophysics, Volume II: Gas Dynamics*, University Science Books (1992)

Synge, J.L, *The Relativistic Gas,* North Holland, Amsterdam (1957)

Taub, A.H., *Phys. Rev.* 74, 3 (1948)

Trangenstein, J.A. and Pember, R.B., *The Riemann problem for longitudinal motion in an elastic-plastic bar*, SIAM Journal of Scientific Computation, 12 (1991) 180

Trangenstein, J.A. and Pember, R.B., *Numerical algorithms for strong discontinuities in elastic-plastic solids*, Journal of Computational Physics, 103 (1992) 63

Uhlenbeck, G.E. and Ford, G.W., *Statistical Mechanics*, American Mathematical Society (1963)

Van Dyke, M., *An Album of Fluid Motion*, Parabolic Press (1982)

Yee, K.S., *Numerical Solution of Initial Boundary Value Problems Involving Maxwell Equation in an Isotropic Media*, IEEE Trans. Antenna Propagation 14 (1966) 302

Yvon, J. Theorie Statistique des Fluides et l'Equation et l'Equation d'Etat, Actes Sientifique et Industrie, # 203. Paris (1935) Hermann

**Problem Set**

**1.1)** Substitute eqn. (1.6) in eqns. (1.3) and (1.4) to verify that they are true. Use eqn. (1.6) along with the definitions in eqn. (1.8) to derive eqn. (1.7) for a monoatomic, ideal gas. Use $\Gamma = 5/3$ . Hint: Make a change of variables given by $\mathbf{q} = \left(\mathbf{p} - m\,\mathbf{v}(\mathbf{x},t)\right)\Big/\sqrt{2\,m\,k\,\mathrm{T}(\mathbf{x},t)}$ .

**1.2)** Show that the collision terms on the right hand side of eqn. (1.18) average to zero when $\psi(\mathbf{p})$ is given by eqn. (1.17). Do this using the following steps. First write the right hand side of eqn. (1.18) explicitly. Use eqn. (1.16) to help you do that. Realize, therefore, that $\mathbf{p}$ and $\mathbf{p}_1$ are dummy variables in the integral and may be interchanged. This allows us to make the transcription $\psi(\mathbf{p}) \to \frac{1}{2}\left(\psi(\mathbf{p}) + \psi(\mathbf{p}_1)\right)$. Using time-reversibility and the conservation of phase space, see eqns. (1.14) and (1.15), show that the right hand side of eqn. (1.18) can be written with the substitution $\psi(\mathbf{p}) \to \frac{1}{4}\left(\psi(\mathbf{p}) + \psi(\mathbf{p}_1) - \psi(\mathbf{p}') - \psi(\mathbf{p}_1')\right)$ . Because of conservation, eqn. (1.11), and the structure of $\psi(\mathbf{p})$, it can now be shown that the right hand side of eqn. (1.18) averages to zero.

**1.3)** The Lorentz force gives us the force on a charged particle that moves in a magnetic field. Thus we have $\mathbf{F} = q\,\mathbf{v}\times\mathbf{B}$ where $q$ is the charge, $\mathbf{v}$ is the velocity and $\mathbf{B}$ is the magnetic field. Show that despite the Lorentz force being a velocity-dependent force, the second line of eqn. (1.20) may be legitimately obtained.

**1.4)** The following problem explains why the stream of water in a waterfall becomes more tapered as it descends. Realize that water is almost incompressible. Imagine the stream of water starting with an initial downward speed $v_0$ and an initial cross section $A_0$ . Say the water descends a distance "d". Write an expression for the velocity "v" of the water at the distance "d". In steady state, what is conserved across an imaginary,

horizontal surface that intersects the stream of water? Hence, write an expression for the area of the stream of water as a function of the distance "d".

**1.5)** Past a certain radius, the solar wind moves at an almost constant velocity. Assuming that velocity to be a constant for the purposes of this simple problem, write an expression for the density of the solar wind as a function of its radius.

**1.6)** This problem is designed to develop the reader's familiarity in manipulating the equations of fluid dynamics. Use eqns. (1.22) and (1.28) to derive eqn. (1.29). Also use (1.22) and (1.28) to derive eqns. (1.35) and (1.36). Then use eqn. (1.36) along with (1.22) to derive eqns. (1.37) and (1.38).

**1.7)** Notice from eqn. (1.45) that $D_{ij}$ is a traceless, symmetric tensor. Consequently, show that such a structure for $D_{ij}$ is sufficient to ensure that the viscous terms, when they are present, always cause the internal energy and entropy to increase in eqns. (1.36) and (1.38).

**1.8)** In a fashion that is analogous to Figs. 1.5 and 1.6, draw a figure showing a gas kinetic model of a hot slab of gas abutting a cold slab of gas. Realize that there should be a temperature gradient between the two slabs. Just as we did for viscosity, substitute eqn. (1.47) into eqn. (1.44) and draw on eqns. (1.1) and (1.2) to obtain a dimensional scaling for $\kappa$. Now show that $\kappa \sim C_V \mu$, where $C_V$ is the specific heat at constant volume for the gas.

**1.9)** Figs. 1.9 and 1.10 show the range of influence and domain of dependence for subsonic flow. Draw analogous figures for supersonic flow.

**1.10)** By examining the matrices in eqn. (1.85) show that the *x*-directional variations in the shallow water equations form a hyperbolic system. Take the source terms to be zero.

**1.11)** In some situations a fluid's temperature can equilibrate to a constant value. This usually happens when a fluid has an external source of heat which is balanced by radiative cooling of the fluid. The fluid's temperature can then remain constant to a good approximation, leading to the isothermal equations. Because the temperature remains constant, the energy equation can be dispensed with. For variations that are restricted to the x-direction, show that the continuity and momentum equation for the Euler system then yields

$$\frac{\partial}{\partial t}\begin{bmatrix} \rho \\ \rho\, \mathrm{v_x} \end{bmatrix} + \frac{\partial}{\partial x}\begin{bmatrix} \rho\, \mathrm{v_x} \\ \rho\, \mathrm{v_x^2} + \mathrm{c_0^2}\, \rho \end{bmatrix} = 0$$

Here $\mathrm{c_0}$ is the constant, isothermal sound speed. The primitive variables may be taken to be $\left[\rho,\ \mathrm{v_x}\right]^T$. Obtain the characteristic matrices in primitive and conserved form. Show that one obtains the same eigenvalues in either form. Derive the orthonormalized right and left eigenvectors in primitive and conserved form.

**1.12)** Consider the two-dimensional flow field for a fluid vortex. In the time-steady case, start with the velocities

$$\begin{bmatrix} \mathrm{v_x}(x,y) \\ \mathrm{v_y}(x,y) \\ \mathrm{v_z}(x,y) \end{bmatrix} = \frac{\kappa}{2\pi}\, \mathrm{e}^{0.5\left(1-r^2\right)} \begin{bmatrix} -y \\ x \\ 0 \end{bmatrix} \quad ; \quad r \equiv \sqrt{x^2+y^2}$$

How are the streamlines oriented? Draw them. Assume that the density is constant at a value of $\rho_0$. Also assume that the pressure at $r \to \infty$ is given by a constant value $\mathrm{P_0}$. By substituting the velocity field in the momentum equation, find the variation in the pressure as a function of radius "*r*". Plot out the pressure as a function of radius and realize that the pressure gradient provides the centripetal force for the fluid's rotation. This problem is most easily done by writing the Euler equations in cylindrical geometry. However, it can also be done very easily by realizing that it is cylindrically symmetric and, therefore, focusing on the variations along the x-axis.

**1.13)** This problem is a variant on the previous one. Assume the same velocity field as in the previous problem. However, this time, we drop the constant density assumption. Instead assume that the entropy of the flow is constant all over. Thus as $r \to \infty$ assume that the density and pressure tend to constant values given by $\rho_0$ and $\mathrm{P}_0$ respectively. However, at a general location, both the density and pressure terms can have fluctuations given by $\delta\rho(x,y)$ and $\delta\mathrm{P}(x,y)$ respectively. Because of cylindrical symmetry, these variations only vary as a function of radius "*r*". Consistent with the isentropic assumption, we have

$$\frac{\left(\mathrm{P}_0 + \delta\mathrm{P}(r)\right)}{\left(\rho_0 + \delta\rho(r)\right)^{\Gamma}} = \frac{\mathrm{P}_0}{\rho_0^{\Gamma}}$$

Use the thermal energy along with the momentum equation to obtain the variation of density and pressure as a function of radius "*r*".

**1.14)** This problem provides an intuitive derivation of the Alfven speed. It does so by first reminding us that a string or rubber band with a force of tension "*T*" and mass per unit length $\mu$ carries transverse oscillations with a speed $\sqrt{T/\mu}$. Plasmas that are threaded by magnetic fields also experience a tension force. Of course, any compression of the plasma also causes a change in its pressure which will contribute as an extra force. Since we only want the tension force, we will make sure that we do not make any volumetric changes to the fluid that we consider in this problem. Thus consider the cylinder of magnetized fluid in the associated figure. Initially it has a cross-sectional area "*A*" and a length "*l*". Let the cylinder be threaded by a longitudinal magnetic field with an initial value "B" as shown. Let the cylinder be squeezed in a volume-preserving fashion so that its cross-sectional area becomes "$A - \Delta A$" and its length becomes "$l + \Delta l$". Because magnetic flux is conserved, the magnetic field increases to "$\mathrm{B}+\Delta\mathrm{B}$". Assert volume conservation as well as flux conservation to show that $\Delta\mathrm{B}/\mathrm{B} = \Delta l/l$. The change in the magnetic energy density is given by $\Delta u_m = \left[\left(\mathrm{B}+\Delta\mathrm{B}\right)^2 - \mathrm{B}^2\right] \Big/ \left(8\pi\right)$. Let the tensional force provided by the magnetic field along the cylinder's axis be denoted by "*T*". The work-energy theorem then asserts that the total change in magnetic energy

$\Delta u_m (Al)$ is equal to the work done by the tensional force provided by the magnetic field, $T\ \Delta l$ . As a result, show that $T = \mathrm{B}^2 A/(4\pi)$. If the plasma has density "$\rho$", the linear mass density of the cylinder is given by $\mu = \rho A$ . Now, given the tensional force and the linear mass density, show that the Alfven wave speed in the plasma is given by $\mathrm{v_A} = \mathrm{B}/\sqrt{4\pi\rho}$ . Unlike sound waves or their analogues, the magnetosonic waves, Alfven waves can propagate through a plasma without introducing any compression or rarefaction.

*Figure for Problem 1.14 showing the volume-preserving change in the cylinder and the corresponding increase in the magnetic field.*

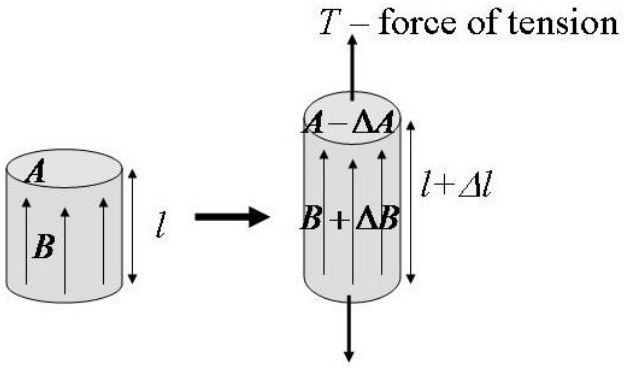


**1.15)** This problem describes a magnetized version of the vortex that was first presented in problem 1.12. Assume the same velocity field as in problem 1.12. However, also consider a magnetic field given by

$$\begin{bmatrix} \mathrm{B_x}(x,y) \\ \mathrm{B_y}(x,y) \\ \mathrm{B_z}(x,y) \end{bmatrix} = \frac{\mu}{2\pi}\, \mathrm{e}^{0.5(1-r^2)} \begin{bmatrix} -y \\ x \\ 0 \end{bmatrix} \quad ; \quad r \equiv \sqrt{x^2+y^2}$$

Assume that the vortex as a constant density $\rho_0$. Also assume that the pressure asymptotically tends to $\mathrm{P_0}$ as $r \to \infty$. Using the momentum equation, find the variation of the pressure as a function of radius. Notice that the presence of magnetic tension contributes to the pressure. Which way does it contribute and why?

**1.16)** Write out the x-directional variations of eqn. (1.109) in the form $\mathrm{u}_t + \mathrm{A}\,\mathrm{u}_x = 0$ . Realize that the matrix "A" is very sparse. Symbolic manipulation packages, such as Maple and Mathematica, have become very proficient at extracting eigenvalues and

eigenvectors of a given matrix. Each of those packages has extensive on-line documentation. Consequently, use a symbolic package to obtain the eigenvalues in eqns. (1.110) and (1.111). The problem illustrates that tasks that would have seemed daunting are now easily performed using the software tools that are available to us.

**Computational Exercises**

**1.1)** The CD-ROM associated with this book has an IDL script for making one-dimensional plots along with some one-dimensional data. Obtain the plots using the script.

**1.2)** The CD-ROM also has an IDL script for making two-dimensional plots along with some two-dimensional data. Visualize the data.

**1.3)** Choose reasonable values for the constant state in eqn. (1.78). Then numerically solve for the eigenvalues and eigenvectors for some representative values of the wave number. Verify some of the statements that are made in the text that follows eqn. (1.79).